Molecular Phylogenetics and Evolution 125 (2018) 100–115

Contents lists available at ScienceDirect

Molecular Phylogenetics and Evolution

journal homepage: www.elsevier.com/locate/ympev

Resolving complex phylogeographic patterns in the Balkan Peninsula using closely related wall-lizard species as a model system

Nikolaos Psonis[a,b,*], Aglaia Antoniou[c], Emmanouela Karameta[d], Adam D. Leaché[e], Panayiota Kotsakiozi[f], Diego Darriba[g], Alexey Kozlov[g], Alexandros Stamatakis[g,h], Dimitris Poursanidis[i], Oleg Kukushkin[j,k], Daniel Jablonski[l], Jelka Crnobrnja–Isailović[m,n], Iulian Gherghel[o,p], Petros Lymberakis[a], Nikos Poulakakis[a,b]

[a] Natural History Museum of Crete, School of Sciences and Engineering, University of Crete, Knosos Avenue, Irakleio GR71409, Greece
[b] Department of Biology, School of Sciences and Engineering, University of Crete, Vassilika Vouton, Irakleio GR70013, Greece
[c] Institute of Marine Biology, Biotechnology and Aquaculture, Hellenic Centre for Marine Research, Gournes Pediados, P.O. Box 2214, Irakleio GR71003, Greece
[d] Section of Zoology and Marine Biology, Department of Biology, National and Kapodistrian University of Athens, Panepistimioupolis, Athens 157-84, Greece
[e] Department of Biology and Burke Museum of Natural History and Culture, University of Washington, Seattle, WA, USA
[f] Department of Ecology and Evolutionary Biology, Yale University, 21 Sachem Street, New Haven, CT 06520-8105, USA
[g] The Exelixis Lab, Scientific Computing Group, Heidelberg Institute for Theoretical Studies, Schloss-Wolfsbrunnenweg 35, 69118 Heidelberg, Germany
[h] Karlsruhe Institute of Technology, Institute for Theoretical Informatics, Postfach 6980, 76128 Karlsruhe, Germany
[i] Foundation for Research and Technology – Hellas (FORTH), Institute of Applied and Computational Mathematics, N. Plastira 100, Vassilika Vouton, Iraklion GR70013, Greece
[j] Department of Biodiversity Studies and Ecological Monitoring, T.I. Vyazemski Karadag Research Station – Nature Reserve of Russian Academy of Sciences, Nauki Str. 24, stm. Kurortnoe, Theodosia 298188, Republic of the Crimea, Russia
[k] Department of Herpetology, Institute of Zoology of Russian Academy of Sciences, Universitetskaya Emb. 1, Saint Petersburg 199034, Russia
[l] Department of Zoology, Comenius University in Bratislava, Mlynská dolina, Ilkovičova 6, 842 15 Bratislava, Slovakia
[m] Department of Biology and Ecology, Faculty of Sciences and Mathematics, University of Niš, Višegradska 33, Niš 18000, Serbia
[n] Department of Evolutionary Biology, Institute for Biological Research "Siniša Stanković", University of Belgrade, Despota Stefana 142, Beograd 11000, Serbia
[o] Department of Biology, Case Western Reserve University, 2080 Adelbert Road, Cleveland, OH 44106, USA
[p] Faculty of Geography and Geology, Alexandru Ioan Cuza University of Iasi, Carol I Bvd, no 20A, Iasi, Romania

ARTICLE INFO

Keywords:
ddRADseq
MessinianSalinity Crisis
Quaternary climatic refugia
Phylogenomics
Podarcis tauricus species subgroup
Population structure

ABSTRACT

The Balkan Peninsula constitutes a biodiversity hotspot with high levels of species richness and endemism. The complex geological history of the Balkans in conjunction with the climate evolution are hypothesized as the main drivers generating this biodiversity. We investigated the phylogeography, historical demography, and population structure of closely related wall-lizard species from the Balkan Peninsula and southeastern Europe to better understand diversification processes of species with limited dispersal ability, from Late Miocene to the Holocene. We used several analytical methods integrating genome-wide SNPs (ddRADseq), microsatellites, mitochondrial and nuclear DNA data, as well as species distribution modelling. Phylogenomic analysis resulted in a completely resolved species level phylogeny, population level analyses confirmed the existence of at least two cryptic evolutionary lineages and extensive within species genetic structuring. Divergence time estimations indicated that the Messinian Salinity Crisis played a key role in shaping patterns of species divergence, whereas intraspecific genetic structuring was mainly driven by Pliocene tectonic events and Quaternary climatic oscillations. The present work highlights the effectiveness of utilizing multiple methods and data types coupled with extensive geographic sampling to uncover the evolutionary processes that shaped the species over space and time.

1. Introduction

Located at the crossroads of three continents, the Mediterranean Basin combines different cultural, geological and biological features of Europe, Asia and Africa, and represents one of the richest and most complex regions on Earth (Blondel et al., 2010). Species richness and genetic diversity are notably higher in the southern European peninsulas extending into the Mediterranean Sea (Iberian, Italian, and the

* Corresponding author at: Department of Biology, School of Sciences and Engineering, University of Crete, Vassilika Vouton, Irakleio GR70013, Greece.
E-mail address: nikos.psonis@gmail.com (N. Psonis).

https://doi.org/10.1016/j.ympev.2018.03.021
Received 17 July 2017; Received in revised form 8 March 2018; Accepted 14 March 2018
Available online 21 March 2018
1055-7903/

Balkans), compared to higher latitudes (Hewitt, 2011), rendering them as biodiversity hotspots (Blondel and Aronson, 1999; Myers et al., 2000). The Balkan peninsula has played a key role as a source of postglacial colonization of central and northern Europe (Griffiths et al., 2004) and generally hosts higher species richness in comparison to the Iberian and the Italian ones, yet still remains phylogeographically understudied (Hewitt, 2011). This comes as no surprise considering the complex geological history of this area. The Eocene orogeny was followed by successive connections or land mass submergence, that were more pronounced in the Miocene and the Pliocene (22–2.56 Mya), e.g. the progressive fragmentation of the Aegean landmass (comprising the Balkans and western Turkey) by the formation of the Mid Aegean Trench (MAT) (Creutzburg, 1963; Dermitzakis and Papanikolaou, 1981). These events provided many opportunities for dispersal and vicariance throughout this period and might be responsible for the high species diversity observed today. Indeed, phylogeographic studies on various taxa of this region have revealed extensive intra- and interspecific divergence in this period (Poulakakis et al., 2014).

The southwestern part of the Balkans, defined by the Dinarides and External Hellenides of continental Greece and southern Albania mountain ranges (Pindos Mts., Fig. 1A) and their adjacent areas, represent one of the richest areas of Europe in reptile species (Džukić and Kalezić, 2004; Sillero et al., 2014). These mountain ranges have acted as important biogeographic barriers for numerous species (Lymberakis and Poulakakis, 2010) including lizards (Gvoždík et al., 2010; Marzahn et al., 2016; Sagonas et al., 2014; Valakos et al., 2008), snakes (Ferchaud et al., 2012; Guicking et al., 2009; Mizsei et al., 2017; Musilová et al., 2010; Ursenbacher et al., 2008), frogs (Džukić and Kalezić, 2004; Valakos et al., 2008)], insects (Allegrucci et al., 2009)], spiders (Kornilios et al., 2016)], and land snails (Kotsakiozi et al., 2012; Psonis et al., 2015; Welter-Schultes, 2012). Furthermore, the aforementioned mountain ranges have also affected the fauna of the Peloponnese (Fig. 1A) as indicated by the fact that several closely related taxa (see above studies) are only distributed in the western part of Pindos Mts. and in the Peloponnese. This fact, in conjunction with the complex geological history of the Peloponnese (Creutzburg, 1963) and the climatic changes since the Tertiary (Zachos et al., 2001), has given rise to a plethora of Peloponnesian endemic species that exhibit high levels of genetic diversity [e.g. *Algyroides moreoticus, Hellenolacerta graeca*, *P. peloponnesiacus*, and *Anguis cephallonica* (Valakos et al., 2008)].

During the Pleistocene, glacial refugia were highly important for the maintenance and promotion of biodiversity, especially for the species (endemics or not) that shifted their ranges (Barbosa et al., 2017). Therefore, numerous phylogeographic studies have focused on the expansion of widespread temperate species from 'glacial refugia' (Hewitt, 2000 and references therein). However, geographic, habitat and climatic heterogeneity within the glacial refugia may have often subdivided populations resulting in 'refugia within refugia' (Abellán and Svenning, 2014; Gomez and Lunt, 2007). Describing the genetic patterns within refugia is paramount to the interpretation of the structure of both widespread species that have expanded their ranges far beyond the refugia, and species that are currently restricted therein, i.e., 'refugial endemics' (Bilton et al., 1998; Kryštufek et al., 2007).

The wall lizards of the genus *Podarcis* have been assigned to several species groups (Harris and Arnold, 1999; Oliverio et al., 2000) with the focal taxa of this study falling into the Balkan species group and the *Podarcis tauricus* species subgroup (Poulakakis et al., 2005a, 2005b; Psonis et al., 2017). The species subgroup includes at least five species that inhabit southeastern Europe. These include *P. gaigeae* (Werner, 1930) and *P. milensis* (Werner, 1930), which are Aegean endemics of the Skyros and Milos island groups, respectively, *P. melisellensis* (Braun, 1877) along the Dalmatian coasts, with high intraspecific genetic differentiation (Podnar et al., 2004), and two putative species within *P. tauricus* species complex, hereafter named *P. ionicus* (exhibiting high genetic diversification with five distinct subclades *a-e*) and *P. tauricus*, as proposed by Psonis et al. (2017). The two latter putative species have evolved allopatrically in the western and the eastern parts of the

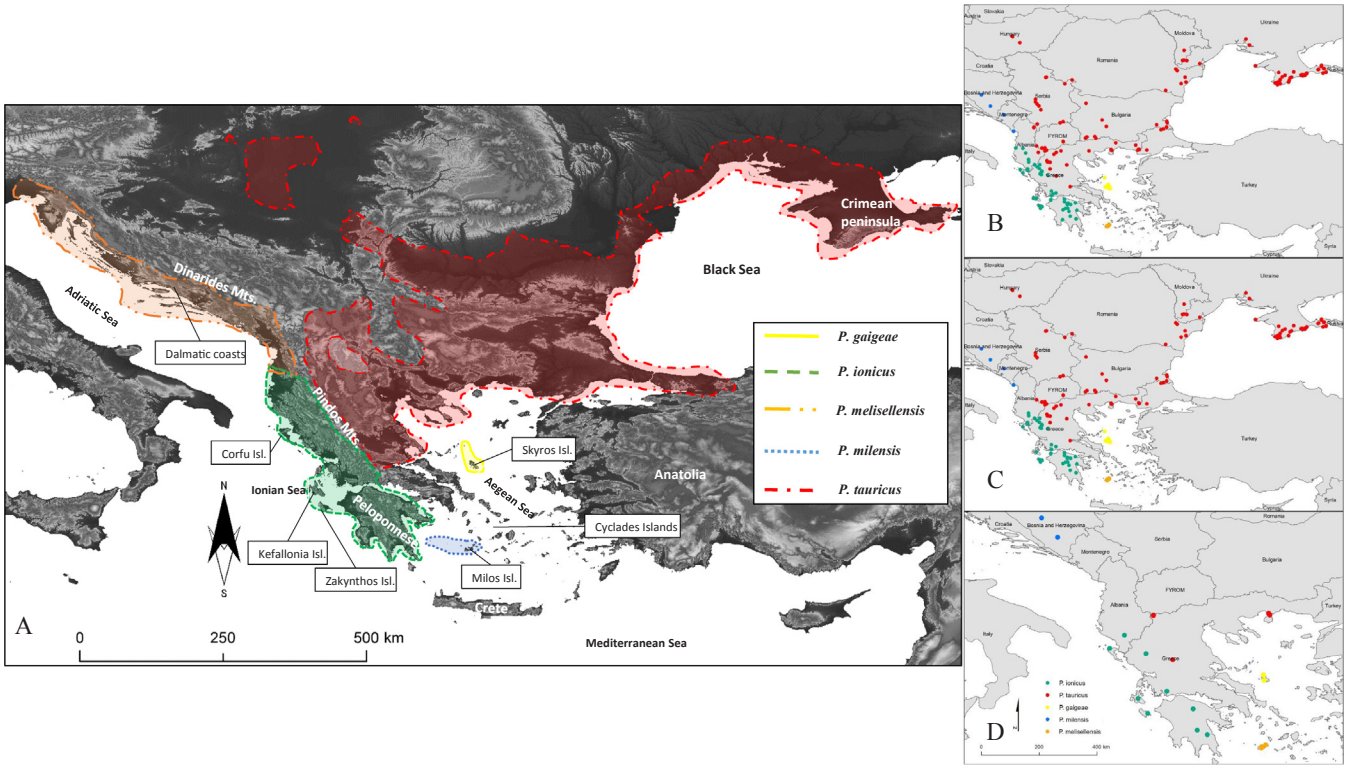

Fig. 1. (A) Species distribution of *Podarcis tauricus* species subgroup in Southern Europe according to IUCN. (B) The geographic localities of all specimens used in the present study). (C) and (D) indicate the geographic localities of the specimens used in the analyses with microsatellites data and phylogenomic analyses with ddRADseq data. Multiple samples may have been collected in some sites.

Table 1
Species and subspecies of the *Podarcis tauricus* species subgroup according to the literature, clades/subclades identified by Podnar et al. (2004) and Psonis et al. (2017), the classification system followed in the present study based on suggestions of the these studies, and the taxa/clades distribution.

Recognized species	Recognized subspecies	Identified clades/ subclades	Classification system followed in the present study	Distribution
Podarcis gaigeae	*P. g. gaigeae*	*P. gaigeae*	*P. gaigeae* (no subspecies)	Skyros Isl. and satellite islets, Greece
	P. g. weigandi			Piperi islet (Northern Sporades Islands), Greece
Podarcis melisellensis	*P. m. melisellensis*	*P. m. melisellensis*	*P. m. melisellensis* (Samples not included)	Jabuka Isl., Brusnik Isl., Biševo Isl. and Vis Isl. and satellite islets, Croatia
	P. m. fiumanus	*P. m. fiumanus*	*P. m. fiumanus*	Italy (near Trieste), Croatian coast including many offshore islands and islets, Bosnia-Herzegovina, Montenegro and northwestern Albania
	P. m. ssp. (Lastovo)	Lastovo subclade	Lastovo subclade (Samples not included)	Lastovo Isl. and satellite islets, Croatia
Podarcis milensis	*P. m. milensis*	*P. m. milensis*	*P. m. milensis*	Milos Isl., Kimolos Isl., Polyaigos Isl. and Antimilos Isl. and their satellite islets, Greece
	P. m. gerakuniae[*]	Not included in the studies	*P. m. gerakuniae* (Samples not included)	Falkonera islet and Velopoula islet, (W of Milos Isl.), Greece
	P. m. adolfjordansi[*]	Not included in the studies	*P. m. adolfjordansi* (Samples not included)	Ananes islet (SW of Milos Isl.), Greece
Podarcis tauricus	*P. t. tauricus*	*P. tauricus*	*P. tauricus* (no subspecies)	From Crimean peninsula and southern Ukraine, through southern Moldova, and eastern and southern Romania (excluding the Danube Delta), to Bulgaria, F.Y.R.O.M., eastern and southern Serbia, Albania, mainland Greece (east side of Pindos Mt. excluding central Greece and Evvoia Isl.), northwestern Turkey, and Hungary.
	P. t. thasopulae			Thasopoula islet (N of Thasos Isl.), Greece
	P. t. ionicus	Subclade *a*	*P. ionicus* subclade *a*	Ithaca Isl., Kefallonia Isl., Zakynthos Isl, Strofades islets (south of Zakynthos Isl.), Greece
		Subclade *b*	*P. ionicus* subclade *b*	Southwestern central Greece
		Subclade *c*	*P. ionicus* subclade *c*	Northeastern Peloponnese, Greece
		Subclade *d*	*P. ionicus* subclade *d*	Central and southeastern Peloponnese, Greece
		Subclade *e*	*P. ionicus* subclade *e*	West Peloponnese and northwestern mainland Greece including Corfu Isl. and southwestern Albania

[*] *P. m. gerakuniae* and *P. m. adolfjordansi* have never been analyzed genetically.

External Hellenides (Pindos Mts.), respectively (Fig. 1A and Table 1). A thorough understanding of the evolutionary and adaptive history of the *P. tauricus* species subgroup has been hampered by the lack of genome-wide data, as traditional mitochondrial (mtDNA) and nuclear (nDNA) markers have failed to resolve key phylogenetic relationships within this subgroup (Psonis et al., 2017 and references therein). The main issue is the existence of polytomies both among and within the five species of the subgroup. These polytomies were attributed to rapid diversification (Psonis et al., 2017), a phenomenon quite common in Lacertidae (Pavlicev and Mayer, 2009) and especially in *Podarcis* (Oliverio et al., 2000), rendering the use of numerous and more appropriate molecular markers indispensable (Psonis et al., 2017).

Double-digest Restriction site associated DNA sequencing (ddRADseq) is emerging as one of the most useful reduced-representation genome sequencing methods for phylogenetic and population-level studies (Peterson et al., 2012), providing thousands of SNPs suitable for estimating high-resolution phylogenetic trees (DaCosta and Sorenson, 2016; Leaché et al., 2015; Nieto-Montes de Oca et al., 2017). These genome-wide approaches coupled with Species Distribution Modelling (SDM) methods may provide deeper insights into the historical biogeography of the species subgroup (Blois, 2012; Psonis et al., 2016; Senczuk et al., 2017; Svenning et al., 2011; Wielstra et al., 2013) and can also be used to test niche similarity and overlap between extant species and niche evolution across phylogenies (Ahmadzadeh et al., 2016, 2013; Rato et al., 2015).

The main scope of the present study is to improve our understanding of the processes that produced the high genetic and species diversity found in the Balkan Peninsula, using the *P. tauricus* species subgroup as a case study, as it is distributed along the entire focal area with high levels of genetic diversity (Psonis et al., 2017). In order to address these questione, we employed a multi-level approach, studying the evolutionary history of the entire subgroup, considering processes that impacted multiple taxonomic levels from populations to species, using a sampling scheme that covers the distribution of the subgroup and estimated its diversification over time from the Late Miocene to the Holocene. To improve our inferences we used multiple analytical methods incorporating genome-wide SNPs (ddRADseq), nuclear (nDNA) and mitochondrial (mtDNA) DNA sequences, as well as microsatellites. We used these methods and data to investigate (a) phylogenomic relationships, (b) phylogeography, (c) population structure, (d) historical demography, and (e) contemporary distribution and niche overlap of all taxa and populations belonging to the focal species subgroup.

2. Material and methods

Overall, we used a total of 420 specimens of the *P. tauricus* species subgroup was used in our analyses, including 65 specimens of *P. gaigeae*, 86 of *P. ionicus*, 10 of *P. melisellensis*, 58 of *P. milensis*, and 201 of *P. tauricus* (Fig. 1B and Table S1). However, not the same individuals were analyzed at all genetic markers (see below). Total genomic DNA was extracted from muscle tissue or blood using a typical ammonium acetate protocol (Bruford et al., 1998) or the DNeasy Blood & Tissue Extraction kit (Qiagen®, Hilden, Germany). DNA quality and quantity was evaluated using agarose gel electrophoresis (TAE 1.5%) and the Qubit® 2.0 Fluorometer (Invitrogen®, Carlsbad, California, USA), respectively.

2.1. Phylogenomics (ddRADseq) on Podarcis tauricus species subgroup

2.1.1. ddRADseq - Taxon sampling

We collected genome-wide SNPs via the ddRADseq method from 36 specimens (Fig. 1D) representing each major clade and subclade of the *P. tauricus* species subgroup, (Podnar et al., 2004; Poulakakis et al., 2005a, 2005b; Psonis et al., 2017). In particular, we included five specimens of *P. gaigeae*, 11 of *P. ionicus*, two of *P. melisellensis*, six of *P. milensis*, and 12 of *P. tauricus* (Table S1). We also included 10 specimens from five closely related species as outgroups (two each for *P. cretensis*, *P. erhardii, P. levendis*, *P. muralis,* and *P. peloponnesiacus*).

2.1.2. ddRADseq - Data collection

The ddRADseq library was prepared using 500 ng of genomic DNA and two restriction enzymes (SbfI and MspI; New England Biolabs) based on the protocol described by Peterson et al. (2012). The sequencing of the library was performed on an Illumina HiSeq 2000 lane (Illumina Inc., San Diego, California, USA) (100-bp, single end reads) at the QB3 facility at the University of California, Berkeley (California, USA). The detailed procedure followed can be found in the Supporting Text S1. Raw Illumina reads were processed with pyRAD (v3.0.6; Eaton, 2014) using three different clustering threshold values (Wclust equal to 0.85, 0.90, and 0.95), as this parameter has been shown to affect phylogenetic relationships (Leaché et al., 2015). To assess the impact of missing data on phylogenetic inference and to determine the minimum amount of data that carry sufficient phylogenetic signal for resolving the topology, we constructed a set of supermatrices by selecting subsets of loci according to the minimum number of unique sequences per locus (min_taxa). The subsets were selected such that they most closely contain 100% (min_taxa = 4), 50% (min_taxa = 7), 25% (min_taxa = 9), and 12.5% (min_taxa = 11) of the loci, respectively. Overall, 12 datasets were assembled (three clustering thresholds × four min_taxa filters). Details on the bioinformatics pipeline followed for ddRADseq data filtering and dataset generation are presented in the Supporting Text S2.

2.1.3. ddRADseq - Phylogenomic analyses (concatenated loci tree)

To evaluate the stability of the phylogenetic signal for each assempled dataset we first performed a Maximum Likelihood tree inference using ExaML (v.3.0.17; Kozlov et al., 2015) with 100 random starting trees (random seed numbers). Then, we used the 100 resulting topologies to calculate the average Robinson Foulds distance (RF distance; Robinson and Foulds, 1981) in each of the 12 datasets. Based on these distances, we selected the most stable dataset for further analyses. Using the selected dataset, we calculated bootstrap values in RAxML (v.8.2.9; Stamatakis, 2014). Bootstrap support was reported onto the best-scoring tree of the selected dataset. We also constructed a Bayesian Inference tree in ExaBayes (v.1.5; Aberer et al., 2014). Details on the evaluation of the phylogenetic signal and on the Maximum Likelihood and Bayesian Inference phylogenetic analyses using the selected concatenated dataset are given in the Supporting Text S3.

2.1.4. ddRADseq - Phylogenomic analyses (species tree)

To fully exploit the power of the ddRADseq data (i.e., both sequences and genotypes), we obtained a SNP based species tree using the multispecies coalescent method SVDQuartets (Chifman and Kubatko, 2014) as implemented in PAUP (v.4.0a152; Swofford, 2002). This method infers the topology among randomly sampled quartets of predefined species, and then a quartet method is used to assemble the sampled quartets into a species tree. An exhaustive search of quartet sampling was selected and the uncertainty in relationships was measured using non-parametric bootstrapping with 100 replicates.

2.1.5. ddRADseq - Reconstruction of the ancestral geographical distribution

We used a combination of phylogenetic and distributional information to infer the genus evolution in southeastern Europe. The ancestral area reconstruction method employed was the Dispersal-Extinction-Cladogenesis analysis (DEC) implemented in LAGRANGE (Ree and Smith, 2008) using the Reconstruct Ancestral States in Phylogenies (RASP; Yu et al., 2013) software. For this biogeographic analysis we used the ddRADseq phylogenomic tree from the BI analysis. We assigned all taxa (species/subspecies/populations) to eight geographic areas: (i) northwestern Balkans (including all specimens of *P. melisellensis*), (ii) eastern Balkans and Southern Europe (i.e, Moldavia, Ukraine, and Crimean peninsula) including all specimens of *P. tauricus*,

(iii) Skyros Island group (including all specimens of *P. gaigeae*), (iv) Milos Island group (including all specimens of *P. milensis*), (v) the Peloponnese (including all specimens of *P. ionicus* distributed in the area), (vi) south Ionian islands (including all specimens of *P. ionicus* distributed on Kefalonia and Zakynthos Islands), (vii) west central continental Greece (including all specimens of *P. ionicus* distributed in the area around the lake Trichonida), and finally (viii) northwestern continental Greece and southwestern Albania [including all specimens of *P. ionicus* distributed in this range, including on the Ionian island of Corfu (Kerkyra), as this island was isolated from the mainland during the Holocene (Perissoratis and Conispoliatis, 2003)]. The geographic locations mentioned can be found on the maps of Fig. 1A and S10.

2.1.6. ddRADseq – SNPs based population structure analysis

We inferres population structure using the Bayesian clustering method implemented in STRUCTURE (v.2.3.4, Pritchard et al., 2000) and the dataset of Wclust = 0.85. The correlated allele frequency with admixture model (F-model) was applied. Given the number of *K* clusters, this model pursues solutions that are, as far as possible, in Hardy-Weinberg and linkage equilibrium. In this study, five replicate runs were performed for each *K* that ranged from 1 to 10. Each run comprised 200,000 generation as burn-in period, followed by 800,000 MCMC iterations from which the results were collected. Using longer MCMC runs did not modify the results. The inference of *K* was evaluated by the ΔK method (Evanno et al., 2005) using the software STRUCTURE HARVESTER (Earl and vonHoldt, 2012). The program CLUMPP v1.1.2 (Jakobsson and Rosenberg, 2007) was used to define run modes (if more than one), to generate consensus solutions allowing for label switching, to test for convergence from the five independent STRUCTURE runs, and to provide the Q values based on which a population or an individual can be assigned to a specific cluster above a given value (here Q = 0.90). The results were plotted using DISTRUCT v.1.1 (Rosenberg, 2004). To complement this analysis we used a multivariate approach that does not seek to maximize HW equilibrium as the previous one. We used Discriminant Analysis of Principal Components (DAPC) (Jombart et al., 2010) implemented in the R package adegenet (v.1.3.1, Jombart and Ahmed, 2011). We assumed nine predefined populations corresponding to the nine major clades and subclades of the *P. tauricus* species subgroup suggested by Psonis et al. (2017). To prevent overfitting of the DAPC, the number (five) of retained principal components (PCs) was chosen according to the optimal *α*-score.

2.2. Microsatellites data - Population genetics on Podarcis tauricus species subgroup

Since the cost of NGS methods prevents the analysis of large numbers of individuals, we also screened a subset of the 420 individuals for microsatellites loci variation to complement to SNPs based analyses (e.g. Antoniou et al., 2017).

2.2.1. Microsatellites data – Taxon sampling and genotyping

Seventeen microsatellite loci designed/developed for the genera of *Podarcis* and *Lacerta* were amplified in multiplex PCRs (see Table S2). The microsatellite dataset consisted of 60 specimens of *P. gaigeae*, 10 of *P. melisellensis*, 56 of *P. milensis*, 197 of *P. tauricus*, and 84 of *P. ionicus* (Fig. 1**C**). Table S1 shows the individuals analyzed and if they were scored at other markers.

PCR products were combined in five multi-loading schemes (Table S2) and genotyped on an ABI 3730 (Applied Biosystems) using GS-500 Liz (Applied Biosystems) as an internal size standard in each capillary. Genotypes were determined using the STRand software (v.2.4.0.59, Toonen and Hughes, 2001) (http://www.vgl.ucdavis.edu/STRand). To minimize the negative consequences of poor allele calling, binning was accomplished with Flexibin 2 (v.2, Amos et al., 2007) the output of which was manually evaluated.

2.2.2. Microsatellites data – Summary statistics

The software MICRO-CHECKER (v.2.2.3, van Oosterhout et al., 2004) was used to check for per-locus heterozygote deficit, the presence of null alleles, large allele dropout, and possible scoring errors. GENEPOP (v.3.4, Raymond and Rousset, 1995) was used to estimate measures of genetic diversity [number of alleles per locus (*A*), F_{IS} index (Weir and Cockerham, 1984), expected (H*e*) and observed (H*o*) heterozygosity per locus] and to test for Hardy–Weinberg (HW) equilibrium. The above parameters were estimated in several different datasets, including the entire dataset (all samples) and clusters revealed by the population STRUCTURE analyses (nine sub-datasets; see below). We used GENETIX (Belkhir et al., 2001) to estimate pairwise F*st* values (Weir and Cockerham, 1984) with statistical significance evaluated over 1000 permutations.

Following Gariboldi et al. (2016), we used ML-RELATE (Kalinowski et al., 2006) to identify potential parent–offspring and full sibling pairs, as relatedness could impact downstream results interpretation. After determining the most likely pairwise relationship (first order, second order, or unrelated) within each species, we performed the relatedness specific hypothesis test with 1×10^5 simulations of random genotype pairs in order to determine whether the putative relationship (parent–offspring or full sibling) has a better fit to the data compared to the alternative relationship (full sibling or half sibling, respectively) (p-value = 0.001).

2.2.3. Microsatellites data – Population structure

The underlying population structure based on microsatellites was inferred by methods implemented in STRUCTURE and DAPC (50 PCs) as described in Section 2.1.6. We used hierarchical STRUCTURE analysis (Vähä et al., 2007) to recursively infer clustering patterns in each major cluster, as suggested by Evanno et al. (2005). Each reiteration was carried out using only individuals with high membership value to a given cluster (here Q ≥ 0.90).

2.2.4. Microsatellites data – Historical demographic inference and recent migration detection

Since the SNP dataset, given its small number of individuals and populations, could not be used to detect signatures of demographic events, we carried out historical demographic analyses using the microsatellites dataset on each of the nine clusters revealed by the hierarchical STRUCTURE analysis.

To evaluate demographic size changes we used BOTTLENECK (v.1.2.02; Cornuet and Luikart, 1996; Piry et al., 1999) under a two-phase model (TPM) constraining the model by defining 90% of mutations as conforming to a stepwise mutation model and 10% as multistep. We also carried out two demographic expansion tests, the k intralocus variability statistic (or kurtosis test; k-test) and the g interlocus variability statistic (g-test) as described by Reich et al. (1999), using the macro program kgtests (Bilgin, 2007) implemented in Microsoft Excel ®.

Recent migration rate (*m*) among the nine clusters identified by the hierarchical structuring analysis was estimated using BayesAss (v. 3.0.4; Wilson and Rannala, 2003). The program uses genotypes to estimate rates of recent migration among populations, without requiring HWE within populations (Wilson and Rannala, 2003). Two independent runs of 5×10^7 generations (sampling every 2000) with 3×10^7 generations omitted as burn-in were performed. After performing initial test runs we used the proposed step size for the different parameters (delta values) was adjusted to: $m = 0.2$, $a = 0.4$, and $f = 0.2$, as more reliable results are obtained when the acceptance rates of proposed changes for allele frequencies (*a*), inbreeding coefficient (*f*), and migration rate (*m*) are between 40 and 60% of the total chain length (http://rannala.org/docs/BayesAss.1.3.pdf).

2.3. Sanger sequencing data

2.3.1. Mitochondrial DNA data - Historical demographic inference

To complement and compare the results of the previous analyses we also performed historical demographic analyses [mismatch distributions, Bayesian Skyline Plots (BSP), and haplotype networks] and estimated demographic and diversity indices using previously published mtDNA data (Podnar et al., 2004; Poulakakis et al., 2005a, 2005b; Psonis et al., 2017). In total, 324 sequences (298 of them belonging to the same specimens as those used in microsatellites analyses) were used, including 18 of *P. gaigeae*, 15 of *P. melisellensis*, 30 of *P. milensis*, 175 of *P. tauricus* and 86 of *P. ionicus* (see Table S1 for sample information) for each main clade and subclade identified in Psonis et al. (2017). More details about mtDNA analyses can be found in the Supporting Text S4).

2.3.2. Mitochondrial and nuclear DNA data – Estimation of divergence times within the Podarcis tauricus species subgroup

To estimate divergence times among the major clades of the *P. tauricus* species subgroup we used previously collected sequence data from two mtDNA (16S rRNA and cyt *b*) and three nDNA (MC1R, Pod15b, and Pod55) genes for three specimens of *P. gaigeae*, two of *P. melisellensis*, four of *P. milensis*, 10 of *P. tauricus*, and 15 of *P. ionicus*. This sample selection includes all distinct clades and subclades of the *P. tauricus* species subgroup (Table S1) (Podnar et al., 2014, 2004; Psonis et al., 2017). These data were combined with sequences from 26 specimens of other *Podarcis* species and 12 specimens of other lacertids (*Lacerta, Timon,* and *Gallotia*). These data were included to set age constraints (Table S1). We selected six age constraints using a normal prior distribution, and mean and standard deviation (SD) values as follows: (a) colonization of El Hierro Island (Canary Islands) by the endemic *Gallotia caesaris caesaris* from the neighboring La Gomera Island at 1.12 Mya (Cox et al., 2010; Guillou et al., 1996); mean: 1.05 and SD: 0.20, (b) the divergence time of *P. peloponnesiacus* from *P. cretensis* and *P. levendis* at 5–5.5 Mya (Poulakakis et al., 2005a) corresponding to the separation of Crete from the Peloponnese (Meulenkamp, 1985; Schule, 1993); mean: 5.30 and SD: 0.10, (c) the divergence of *P. lilfordi* from *P. pityusensis* at ~5 Mya (Brown et al., 2008) when their respective island groups split (Terrasa et al., 2004); mean: 5.25 and SD: 0.03, (d) the divergence between the genera *Lacerta* and *Timon* (Čerňanský, 2010) in Lower Miocene (18.1–17.2 Mya); mean: 17.50 and SD: 0.30, (e) the divergence of European *Timon* from the North African lineages at 5.3 Mya (Estes, 1983); mean: 5.30 and SD: 0.7, and (f) the differentiation of the *L. viridis* species group into its constituent species (Venczel, 2006) during the Upper Miocene (9.0–5.3 Mya); mean: 8.70 and SD: 0.50. Sequence alignment was performed as described in Psonis et al. (2017), using MAFFT (v.7; Katoh and Standley, 2013). Divergence times were calculated using the StarBEAST2 (v.0.13.5; Ogilvie et al., 2017) template of BEAST 2 (v.2.4.5; Bouckaert et al., 2014) with the input file being formatted in the BEAUti v.2.4.5 utility included in the same software. The species tree prior category was set to birth-death model, and the uncorrelated lognormal model was used to describe the relaxed clock. Model parameters were unlinked across partitions (tree models for mtDNA genes were linked). Site Models for each partition were calculated using jModelTest2 (Darriba et al., 2012) as follows: 16S rRNA and cyt *b* - GTR + G, MC1R and Pod55 – HKY + I, and Pod15b – HKY + G (four Gamma categories were selected, as well as estimated proportion of invariable sites where applicable). The analysis was run for 5×10^8 generations with a 5000-step thinning. Results were analyzed in Tracer to assess convergence and ESSs values for all parameters (acceptable values > 200). The –*ln*L was stabilized prior to 5×10^8, and the first 10% of the 100,000 sampled generations were discarded. The final tree with divergence time estimates was computed in TreeAnnotator v.2.4.5 and visualized using FigTree v.2.4.5 (both in BEAST 2).

2.4. Species distribution modelling and niche overlap

A SDM analysis was utilized in order to test a suite of general hypotheses about the factors contributing to the diversity of the of *P. tauricus* subgroup in the Balkans. The analysis was performed for all species of the *P. tauricus* subgroup based on maximum entropy modelling of their geographical distributions. This method combines presence only data with environmental parameters' layers to predict relative probabilities of species' presence in the defined geographic space (Phillips et al., 2006). Occurrence records were obtained from the database of the Natural History Museum of Crete (NHMC). Additional data for *P. melisellensis* were collected from the literature (Podnar et al., 2014, 2004). In total, 427 occurrences were retrieved, from which we retained only one presence point per pixel, so that the final analysis was based on 339 occurrences, 22 of which belonged to *P. gaigeae*, 81 to *P. melisellensis*, 12 to *P. milensis*, 165 to *P. tauricus* and 59 to *P. ionicus*.

To build a species distribution model, environmental layers of climate variables for the present, the last glacial maximum (LGM) (~21 kya) and the last interglacial (LIG) (~120–140 kya) at a 2.5 arc-minutes resolution were downloaded from the WorldClim database website (http://www.worldclim.org/) (Hijmans et al., 2005). Species distributions were estimated using MAXENT (v3.3.3 k; Phillips et al., 2006) based on 10 cross-validation steps. Effectiveness of the model was evaluated using the AUC statistic (Araújo and Guisan, 2006) and the area under the receiver operator curve (ROC) (Phillips et al., 2004). Seven bioclimatic factors from the WorldClim database (bio1,5,6,7,12,14,15) were selected to describe habitat variability and species preferences (Kaliontzopoulou et al., 2008). Niche overlap between species within the subgroup was compared using the relevant indices for niche overlap, *D* and *I*, based on Schoener's *D* (Schoener, 1968) and modified Hellinger *I* (van der Vaart, 1998) distances, respectively, as proposed by Warren et al. (2008), using the ENMtools (Warren et al., 2010).

3. Results

3.1. Phylogenomic (ddRADseq) relationships and biogeographic analysis

The Illumina sequencing of ddRADseq library including 46 samples resulted in an average of 925,185 good quality reads per sample (after applying a Phred quality filtering threshold of 20) ranging from 43,897 to 3,016,940 reads per sample. The average number of loci per sample for each dataset based on the three different Wclust values (equal to 0.85, 0.90, and 0.95) was 28,304 (range = 11,857–80,468), 30,620 (range = 12,062–84,484), and 44,897 (range = 13,134–133,676) loci, respectively. The number of SNPs present in at least four samples (MinCov = 4, paralogs removed) increased with higher orthology thresholds (20,318, 21,617, and 24,687, respectively for each dataset). However, as we needed to have at least four unique sequences per locus (min_taxa = 4) for phylogenetic purposes, SNP numbers were reduced to 12,560, 12,761, and 11,853 loci, respectively, resulting also in a slightly increase of the percentage of missing data (66.72%, 67.82%, and 71.08%, respectively) when using a higher orthology threshold. By subsampling the datasets and retaining 50% (min_taxa = 7), 25% (min_taxa = 9), and 12.5% (min_taxa = 11) of the initial amount of loci, the amount of gaps/undetermined characters was reduced as expected (56.58%, 56.59%, and 58.40%, respectively for min_taxa = 7, to 50.25%, 50.02%, and 51.25%, respectively for min_taxa = 9, and to 44.85%, 44.45%, and 45.20%, respectively for min_taxa = 11). Summary statistics for all ddRADseq datasets are given in Table 2, whereas various parameters (i.e., sample representation, the percentage of samples per locus, gappyness, and percentage of variable sites per locus) for each Wclust-based dataset and its subsets assembled using the different selected min_taxa filter, are plotted in Figs. S1 and S2.

The mean relative RF distances (a proxy of phylogenetic signal stability) among the 100 ExaML trees produced by each dataset, are

Table 2
Summary statistics for the ddRADseq datasets of the *P. tauricus* species subgroup used. Loci and SNPs statistics are in italics and bold, respectively.

Statistic	Bioinformatics Pipeline step	Wclust = 0.85	Wclust = 0.90	Wclust = 0.95
Retained reads that passed quality filtering - NQual (avg ± sd)[a]	pyRAD step 2 (filtering)	830,692 ± 620,159	803,121 ± 601,359	764,506 ± 576,221
Mean depth of clusters with depth greater than NQual (avg ± sd)	pyRAD step 3 (within-sample clustering)	55.7 ± 26.5	56.3 ± 26.4	58.1 ± 27.7
Number of loci per sample (avg ± sd)	pyRAD step 5 (consensus sequences)	*28,304 ± 11,648*	*30,620 ± 12,671*	*44,987 ± 21,211*
Number of loci per sample with depth greater than NQual (avg ± sd)	pyRAD step 5 (consensus sequences)	*9,539 ± 3,361*	*9,974 ± 3,596*	*10,370 ± 3,786*
Number of loci per sample with depth greater than NQual and paralogs removed (avg ± sd)	pyRAD step 5 (consensus sequences)	*8,580 ± 2,999*	*9,062 ± 3,253*	*9,857 ± 3,580*
Number of sites across loci per sample with depth greater than NQual and paralogs removed (avg ± sd)	pyRAD step 5 (consensus sequences)	761,718 ± 266,456	804,845 ± 289,044	875,893 ± 318,193
Number of polymorphic sites across loci per sample with depth greater than NQual and paralogs removed (avg ± sd)	pyRAD step 5 (consensus sequences)	2,258 ± 1,302	2,431 ± 1,389	2,577 ± 1398
Number of loci with at least MinCov samples containing data[b]	pyRAD step 6 (across-sample clustering)	*21,906*	*23,173*	*25,895*
Number of loci with at least MinCov samples containing data and paralogs removed	pyRAD step 7 (alignment and paralog filtering)	*20,318*	*21,617*	*24,687*
Total variable sites	pyRAD step 7 (alignment and paralog filtering)	133,930	124,539	95,575
Sampled unlinked SNPs	pyRAD step 7 (alignment and paralog filtering)	**18,391**	**19,361**	**21,412**
Sampled unlinked bi-allelic SNPs	pyRAD step 7 (alignment and paralog filtering)	**13,214**	**13,789**	**14.065**
Number of loci after Min_taxa = 4 filtering	Subset selection	*12,560*	*12,761*	*11,853*
Number of loci after Min_taxa = 7 filtering	Subset selection	*7,531*	*7,126*	*5,062*
Number of loci after Min_taxa = 9 filtering	Subset selection	*5,100*	*4,626*	*2,683*
Number of loci after Min_taxa = 11 filtering	Subset selection	*3,289*	*2,862*	*1,240*

[a] NQual equals to 14, 9, and 5 for the 0.85, 0.90, and 0.95 Wclust filtered datasets, respectively.
[b] MinCov equals to 4 for all three Wclust filtered datasets.

shown in Table S3. The corresponding pairwise mean relative RF distances between the best scoring ExaML trees inferred from the 12 different datasets are given in Table S4. It is worth noting that only four distinct best-scoring ExaML trees were obtained from these 12 datasets, with one of them (Fig. 2A) being the most consistent across most of the datasets (i.e. in 8 datasets: 0.85 and 0.90 clustering thresholds and all min_taxa filters). The remaining three topologies are presented in Fig. S3. We chose the dataset with Wclust = 0.85 for downstream analyses based on phylogenetic signal stability and amount of missing data for min_taxa = 4 (since all subsets of Wclust = 0.85 had the same RF distance). This dataset was used to reconstruct phylogenies with the ML and the BI methods. The ML analysis completed after 150 bootstrap pseudo-replicates, controlled by the bootstopping option of autoMRE (Pattengale et al., 2010). The BI analysis that converged after 2,000,000 generations according to the sdsfConvergence option, resulted in high effective sample sizes (ESS > 631) and *ln*L = −2,350,840.74. The extended Majority Rule Consensus tree computed from the final 8000 trees is in agreement with the ML tree, and is presented in Fig. 2A. According to the consensus between the ML and BI methods inferred phylogeny, five major clades were revealed, each corresponding to one of the five species of the *P. tauricus* species subgroup. The relationships among them are fully resolved, with *P. melisellensis* being the sister taxon to all the rest. Two subsequent cladogenetic events led to *P. milensis* and *P. gaigeae,* whereas *P. tauricus* and *P. ionicus* were the last clades that diverged, and have a sister group relationship. Within the clade of *P. ionicus* four subclades were recognized, with one (subclade *a*) originating from the south Ionian Sea (Zakynthos and Kefalonia Islands), one (subclade *e*) from the western part of Pindos Mt., one (subclades *b* and *d*) from southeastern Peloponnese and west central Greece, and a final one (subclade *c*) from northeastern Peloponnese (see Fig. 1 for locations mentioned).

The exhaustive quartet search of SVDQuartets method resulted in 163,185 quartets, which were used to infer the SNP based species tree, whose topology matches the one inferred from the concatenated dataset (Fig. 2A).

Biogeographic reconstructions for 17 major nodes are presented in Fig. 2A. All reconstructed areas and detected biogeographic events had 100% statistical support. This analysis suggests that the ancestral form of the *P. tauricus* species subgroup was distributed across the southern Balkans and its biogeographic history was the result of several recurring vicariance and dispersal events (six and two, respectively). The divergence events leading to the splits among the *P. melisellensis*, *P. milensis*, *P. gaigeae*, *P. tauricus*, and *P. ionicus* were likely due to vicariance, as the splits leading to the differentiation of the *P. ionicus* subclades *a* and *e*. In contrast, separation of the three *P. ionicus* subclades *b*, *c*, and *d* were likely due to dispersal.

The STRUCTURE analysis based on the ddRADseq dataset resulted in seven clusters with two equally likely solutions/modes (bimodality), as shown in Fig. 2B. In both cases, five of the clusters include samples from previously recognized taxonomic groups (*P. gaigeae, P. milensis, P. melisellensis*, *P. tauricus*, and subclade *c* of *P. ionicus*, respectively; Fig. 2A). The bimodality pertains to the remaining two subclades of *P. ionicus*. The members of the *P. tauricus* species subgroup were partially discriminated at the species level according to the DAPC analysis, using five discriminant factors (Fig. S6).

3.2. Population genetics using microsatellites data

Three loci (Pb47, Pod3, and Pod8) were discarded from the microsatellites dataset either due to unsuccessful genotyping or to being monomorphic. Furthermore, 48 specimens were discarded (Table S1) from subsequent analyses due to missing data (i.e., less than half of the loci were genotyped). Thus, the final analyses were performed using 361 specimens (52*P. gaigeae*, eight *P. melisellensis*, 53*P. milensis*, 177*P. tauricus*, and 71*P. ionicus*) and 14 microsatellite polymorphic loci. None of the microsatellite loci showed negative F_{IS} values. Large allele

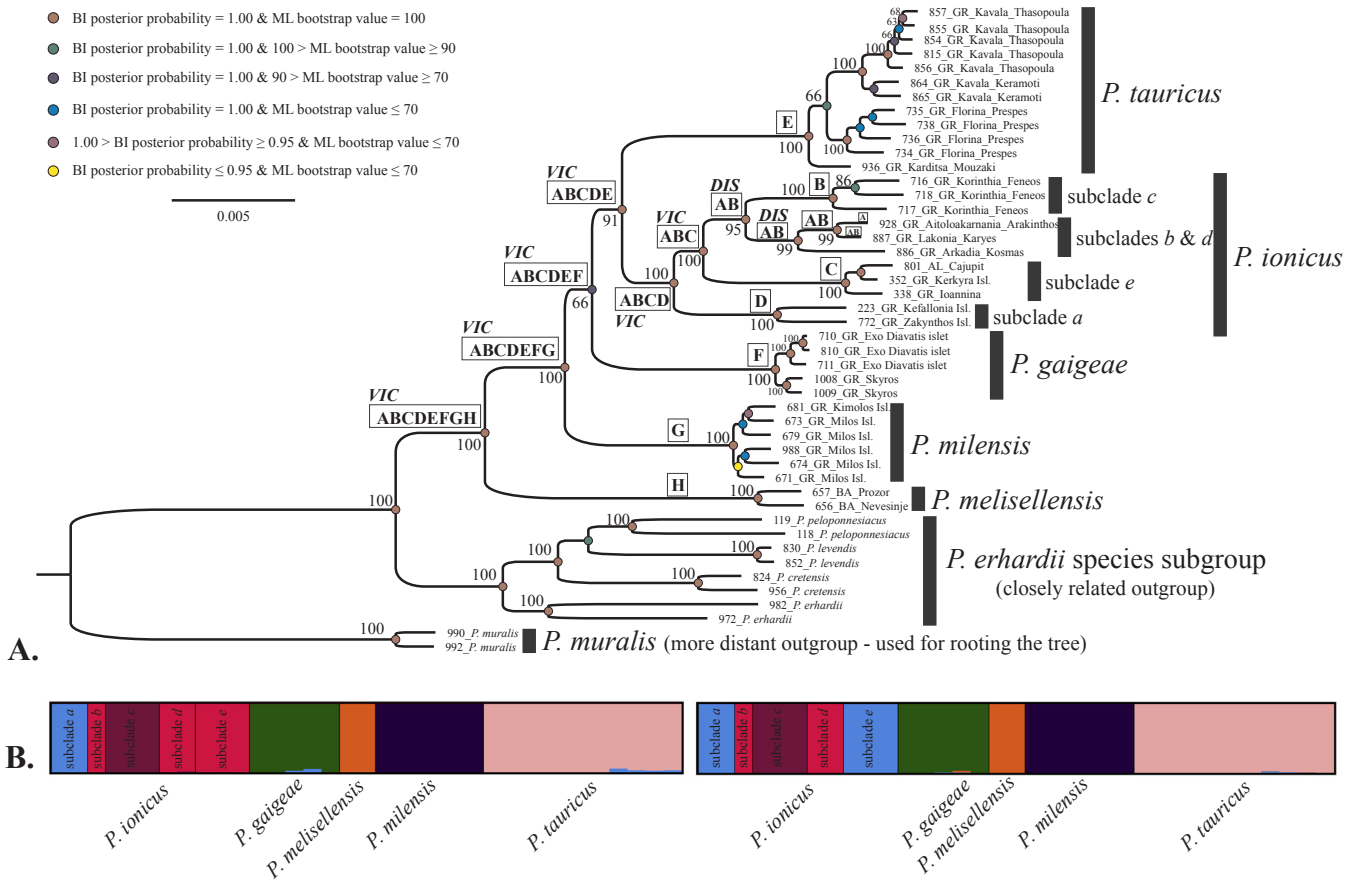

Fig. 2. (A) Bayesian Inference phylogenomic tree of the *P. tauricus* species subgroup based on ddRADseq data using the clustering threshold of 0.85 and min_taxa filter of 4. The colors of the nodes correspond to different combinations of posterior probabilities (BI method) and bootstrap values (ML method) as indicated in the inlaid table at the upper left corner. Numbers near the nodes correspond to the statistical support (bootstrap values) of the SNP based species tree inferred using the SVDQuartets method, which resulted in the same topology. The names of subclades (*a* to *e*) match with the corresponding subclades revealed in chronophylogenetic analysis (see Fig. 3) and in Psonis et al. (2017). The capital letters within the squares next to the nodes correspond to reconstructed ancestral distributions inferred by the DEC biogeographic analysis, as follows: A – west central continental Greece, B – Peloponnese, C – northwestern continental Greece and southwestern Albania, D – south Ionian islands, E – Eastern Balkans and eastern Europe (Moldavia, Ukraine, and Crimea), F – Skyros Island group, G – Milos Island group, H – Northwestern Balkans. The capital italicized letters indicate vicariance (VIC) and dispersal (DIS) events detected by the DEC analysis. All reconstructed areas and biogeographic events had 100% statistical support. (B) The estimated population structure (two possible modes) of the *P. tauricus* species subgroup using the ddRADseq dataset. The Q value corresponds to the percentage of estimated assignment of the individual to each one of the *K* clusters.

Table 3
Population genetics descriptive statistics for all data and for each species of the *P. tauricus* subgroup (excluding *P. melisellensis* due to small number of samples) based on microsatellites data.

Loci	N_A[a]	All data			P. tauricus			P. ionicus			P. gaigeae			P. milensis		
		H_o[b]	H_e[c]	F_{IS}[d]	H_o	H_e	F_{IS}	H_o	H_e	F_{IS}	H_o	H_e	F_{IS}	H_o	H_e	F_{IS}
B6	28	0.722	0.921	0.217	0.661	0.837	0.211	0.729	0.947	0.232	0.730	0.914	0.204	0.906	0.909	0.004
C9	31	0.417	0.763	0.454	0.263	0.410	0.359	0.426	0.930	0.544	0.490	0.739	0.339	0.885	0.893	0.001
Lv3-19	22	0.732	0.919	0.204	0.728	0.889	0.181	0.618	0.848	0.273	0.773	0.923	0.164	0.846	0.911	0.072
Lv4-72	26	0.629	0.883	0.291	0.529	0.719	0.2641	0.642	0.923	0.306	0.727	0.924	0.215	0.823	0.895	0.081
Pb10	36	0.655	0.938	0.302	0.715	0.922	0.225	0.191	0.384	0.504	0.686	0.854	0.198	0.708	0.941	0.250
Pb50	15	0.329	0.683	0.609	0.174	0.386	0.549	0.157	0.674	0.768	0.520	0.735	0.295	0.189	0.595	0.685
Pli4	34	0.726	0.949	0.235	0.748	0.931	0.197	0.672	0.942	0.288	0.750	0.947	0.211	0.729	0.898	0.189
Pm16	24	0.776	0.904	0.151	0.819	0.857	0.045	0.717	0.876	0.183	0.704	0.854	0.177	0.769	0.889	0.136
Pm27	36	0.616	0.918	0.329	0.716	0.860	0.168	0.449	0.927	0.517	0.680	0.882	0.231	0.461	0.886	0.481
Pmeli02	45	0.588	0.941	0.375	0.609	0.922	0.340	0.364	0.955	0.623	0.600	0.921	0.352	0.721	0.947	0.241
Pmeli19	45	0.781	0.965	0.191	0.741	0.918	0.193	0.735	0.949	0.227	0.844	0.902	0.065	0.923	0.948	0.027
Pod1A	20	0.136	0.493	0.724	0.045	0.320	0.860	0.191	0.384	0.504	0.038	0.146	0.7381	0.417	0.597	0.304
Pod1B	23	0.329	0.683	0.518	0.214	0.310	0.310	0.380	0.784	0.517	0.333	0.533	0.378	0.674	0.943	0.287
Pod2	32	0.495	0.819	0.395	0.378	0.494	0.235	0.596	0.923	0.356	0.762	0.869	0.126	0.706	0.915	0.230
Average across all loci		0.566	0.841		0.524	0.698		0.491	0.923		0.617	0.796		0.697	0.869	

[a] For all data.
[b] H_o: observed heterozygosity.
[c] H_e: estimated expected heterozygosity (Nei, 1987).
[d] F_{IS}: Inbreeding index ofWeir and Cockerham (1984).

dropout was not observed in any of the 14 loci. Average number of alleles equals to 29.8, ranging from 15 (Pb50) to 45 (Pmeli02 & Pmeli09; Table 3).

Relatedness analyses suggested that the proportion of putative first-order related individuals found was < 1%. No parent–offspring relationship was statistically supported and only eight full siblings were present (results not shown).

The first step of the hierarchical analysis with STRUCTURE led to $K = 2$, with one cluster containing samples of *P. tauricus* and the second containing the remaining species. The second step led to $K = 3$ for the first cluster and $K = 4$ for the second one. In the first case, the three clusters correspond to: (i) western range of *P. tauricus* that incudes Albania, Bulgaria, FYROM, Greece, Hungary, Romania, Serbia and Turkey (final cluster 'tauricus 1'), (ii) eastern range of *P. tauricus* that consists of the Crimean Peninsula, Ukraine and Moldova (final cluster 'tauricus 2'), and (iii) Thasopoula islet (final cluster 'tauricus 3'). In the second case, the four clusters correspond to: (i) *P. ionicus* subclade *e* (final cluster 'ionicus 1'), (ii) *P. ionicus* subclades *c* and *d* (final cluster 'ionicus 1'), (iii) *P. melisellensis* and *P. milensis* ('melisellensis-milensis'), and (iv) *P. gaigeae* ('gaigeae'). The third hierarchical STRUCTURE analysis step was applied only to clusters with > 20 samples, so that there is sufficient information for the detection of population structure signs (if any). All led to $K = 1$, except for three cases ('ionicus 2', 'melisellensis-milensis', and 'gaigeae') that showed population substructure with $K = 3$ (bimodality issues), $K = 2$ (final clusters 'melisellensis' and 'milensis'), and $K = 2$ (final clusters 'gaigeae 1' and 'gaigeae 2'), respectively. Finally, the fourth STRUCTURE step that was conducted only for one of the clusters ('milensis') resulted in $K = 1$. The results of the hierarchical STRUCTURE analysis are given in Fig. 3B and Fig. S4A. A detailed description of these results is provided in the Supporting Information (Supporting Figures PDF, Comment S1A). The Ho, He, and F_{IS} values for each hierarchical STRUCTURE cluster are given in Tables S5 and S6. For the majority of the resulting clusters the F_{IS} values were positive. Departures from HW equilibrium were observed for most of the loci in each cluster ($P < 0.00001$ after Bonferroni correction). The number of loci with null alleles ranged from two to nine, whereas large allele dropout was not observed for any locus in any cluster. The pairwise F*st* values between the final clusters are listed in Table S7. Migration analyses suggests low migration rates ($m < 0.025$) between clusters, except for those of 'tauricus 1' to 'tauricus 2' ($m = 0.17$), and of 'milensis' to 'melisellensis' ($m = 0.21$), where unidirectional migration was identified. The results between the two separate runs were consistent (Table S8).

Eight discriminant functions (DFs) better reflected the observed differences among clusters while minimizing variation within clusters according to the DAPC analysis (Fig. S5). The members of the *P. tauricus* species subgroup were discriminated at the species level.

The infinite allele model (IAM), TPM and stepwise mutation model (SMM) were used to test for population bottlenecks. Populations exhibiting a significant heterozygosity excess are considered to have gone through a genetic bottleneck. Based on the Wilcoxon test (which is considered to be more reliable than the sign test and standardized differences test), the SMM and TPM models did not show significant results for population bottleneck in any cluster ($p > 0.05$), except for those of 'ionicus 1' (under SMM), 'tauricus 1' (under SMM), and 'tauricus 2' (under both TPM and SMM) (Table S9). The same test showed a significant excess of heterozygosity in 'tauricus_3', 'milensis', and 'gaigeae 2' clusters under the IAM ($p < 0.05$) model. However, this is not necessarily indicative of true heterozygosity excess, as the IAM is considered less appropriate for microsatellites than the SMM (Shriver et al., 1993).

Demographic expansions were detected by the intralocus k-test on the 14 microsatellite loci for three final hierarchical STRUCTURE clusters (i.e., 'gaigeae 2', 'ionicus 1', and 'tauricus 2'; Table S10). By contrast, the interlocus g-test was not significant in any case, as the observed g statistic was higher than the five-percentile cut-off value. However, g-tests are sensitive to variation in mutation rates among loci (King et al., 2000). This could explain the non-significance of the g-tests herein, given the extensive variability in allele size range and allele numbers among the different microsatellite loci (Table 3).

3.3. mtDNA haplotype networks and historical demographics

The mtDNA haplotype networks for each major phylogenetic clade and subclade of the *P. tauricus* species subgroup are shown in Figs. S7–S12. In the case of *P. melisellensis,* we show the haplotype network from Podnar et al. (2004) due to the limited number of samples in our study compared to the one used therein. The highest genetic diversity is observed within *P. ionicus* and *P. melisellensis* (Table S11), whereas the lowest within *P. tauricus* and *P. gaigeae*. The mtDNA demographic analyses resulted in a variety of patterns (Table S12, Figs. S13 and S14). In some cases, there was a clear indication of demographic expansion during the past (i.e., *P. tauricus* and subclade *e* of *P. ionicus*), or of demographic equilibrium (i.e., subclades *a* and *b* of *P. ionicus*). According to the Bayesian Skyline Plots (Fig. S13), during the past, *Ne* for *P. gaigeae* and *P. melisellensis* remained quite stable, experienced a small increase for *P. milensis* and progressively increased for *P. tauricus* . In contrast, a recent sudden *Ne* reduction, followed by a sudden expansion, was detected in *P. ionicus* and in subclade *e* of the same species.

3.4. Divergence time estimation

The chronophylogenetic analysis on the five gene dataset resulted in high posterior ESS values (> 209) for all parameters, and convergence was reached prior to 5×10^8 generations ($lnL = -11{,}827.66$). According to the inferred dates (Fig. 3), the *P. tauricus* species subgroup started to diversify in the Messinian (Late Miocene) around 5.55 Mya Mya with the divergence of *P. melisellensis*. The other three major cladogenetic events occurred in the early Pliocene (4.71–3.88 Mya).

3.5. Species distribution modelling and niche similarity

The model yielded AUC scores > 0.92, indicating a good model performance (Fig. S15). The overall estimated distribution patterns of the focal species were consistent with their actual distribution. The most important climatic parameter was the annual range of temperature for *P. gaigeae*, *P. milensis*, and *P. tauricus*, the minimum temperature of the coldest month for *P. melisellensis,* and precipitation seasonality for *P. ionicus* (Table S13). However, the projection of the models over the LGM (Fig. S16) produced a predicted distribution different from their current one (Fig. 4). Significant range contractions of all species were observed during the LGM compared to the present, except for *P. milensis*. For *P. ionicus*, the potential distribution was smaller in LGM, whereas during the LIG it was limited mostly to regions of low elevation and to coastal areas.

The niche similarity analyses (Schoener's *D*) showed that there is no niche overlap between any pair of the focal taxa, except for a low overlap for the *P. gaigeae* – *P. milensis* niche. For more details see Table S14. The Hellinger's *I* suggested low niche overlap between *P. tauricus* – *P. ionicus* and *P. ionicus* – *P. melisellensis*, and moderate overlap between *P. gaigeae* – *P. milensis*.

4. Discussion

4.1. Phylogenomic relationships within the P. tauricus species subgroup

Although previous phylogenetic studies, based either on nuclear and/or mitochondrial genes, supported the monophyly of the species, phylogenetic relationships among them remained ambiguous (Poulakakis et al., 2005a, 2005b; Psonis et al., 2017). The ddRADseq data clarified these relationships within the *P. tauricus* species subgroup and produced a completely resolved phylogeny at the species level

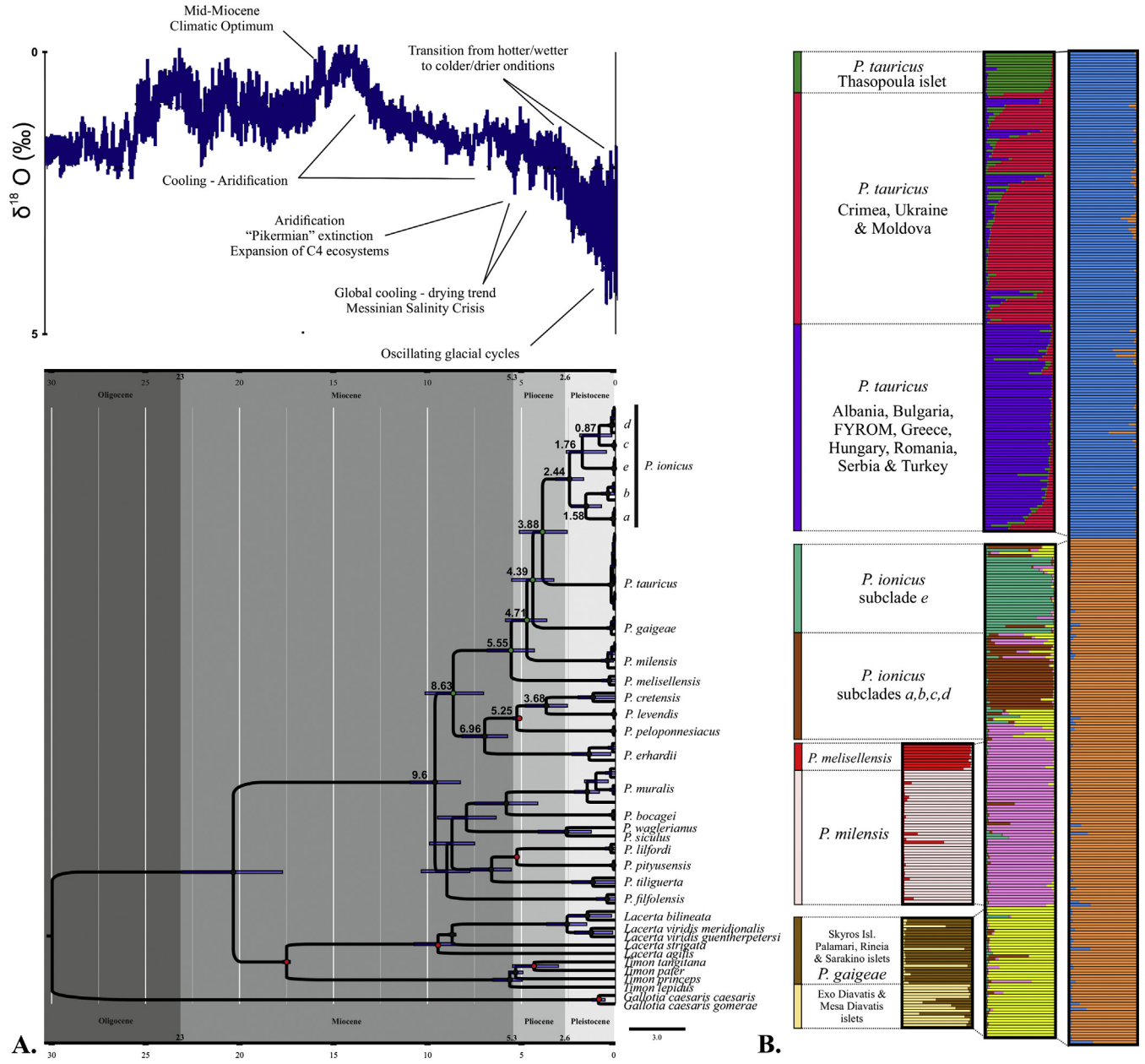

Fig. 3. (A) The calibrated starBEAST2 species tree of the *P. tauricus* species subgroup distributed in the Southern Europe, from the chronophylogenetic analysis based on three nuclear (Pod55, Pod15b, and *MC1R*) and two mitochondrial gene fragments (16S rRNA and cyt *b*). The black and grey circles on the nodes correspond to absolute (posterior probability = 1.00) and very good (0.95 < posterior probability < 1.00) statistical support, whereas the absence of a circle indicate low statistical support. With red colors are the nodes used as calibration points. The numbers on clades of interest constitute the divergence times in Mya, whereas the horizontal bars show the uncertainty (95% HPD) in molecular dating. The bar at the bottom measures Mya. At the top of the Figure, a graphical representation of temperature fluctuations during the past ~35 My, as depicted from deep-sea oxygen isotope records (redrawn after Zachos et al., 2001). (B) The estimated population structure of the *P. tauricus* species subgroup after four steps of the hierarchical STRUCTURE analysis using microsatellites data. Every individual is represented by a thin horizontal line that consists of *K* numbers of colors. The Q value corresponds to the percentage of estimated assignment of the individual to each one of the *K* clusters.

(Fig. 2). Within this subgroup, *P. melisellensis* branches off first, *P. milensis* diverged next, and *P. gaigeae* is the sister taxon to *P. tauricus* and *P. ionicus*.

The genomic data also revealed a well-supported within species structure for *P. tauricus* and *P. ionicus* (Fig. 2). Within the former, although three lineages were observed, the low representation of each species in the ddRADseq dataset prevents to assess the validity of this grouping. For *P. ionicus* this study suggests the occurrence of four subclades, a finding that partially agree with that of a previous study (Psonis et al., 2017). According to the later *P. ionicus* includes five subclades (Figs. S10–S12). These include subclade *a* from south Ionian Islands, subclade *b* from western central Greece (Trichonida lake), subclade *c* from northeastern Peloponnese, subclade *d* from central and southeastern Peloponnese, and subclade *e* from western Peloponnese and northwestern Greece – southwestern Albania. However, subclade *b* and *d* are not distinct in the genomic tree of the present study, in contrast to Psonis et al. (2017) where subclade *b* appears as a separate subclade with a sister group relationship with subclade *a*.

4.2. Population structure and demographic events

The hierarchical structuring analyses on microsatellites dataset

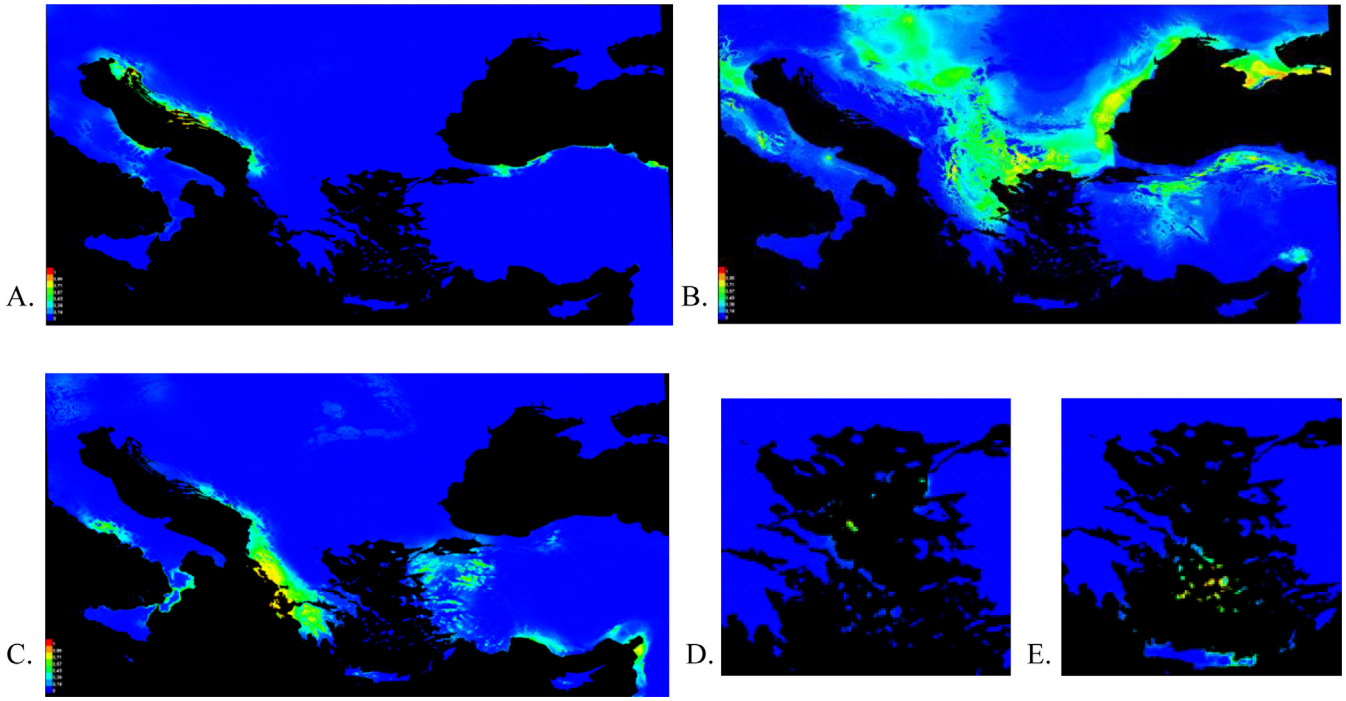

Fig. 4. Species Distribution Modelling using the MaxEnt model for the focal species (A: *P. melisellensis*, B: *P. tauricus*, C: *P. ionicus*, D: *P. gaigeae*, E: *P. milensis*). The SDM projection correspond to the current time period.

revealed nine clusters, which were approximately geographically consistent. One of them ('ionicus 2'; *P. ionicus* subclades *a-d*) was further subdivided although with bimodality issues. These final clusters support the differentiation of *P. tauricus* species subgroup into five species and reveal further sub-structuring within them. The pattern of population structure based on the SNPs is in accordance with the above findings, albeit no further sub-structuring within species was observed, except for *P. ionicus* that, again, showed bimodality issues. Sudden expansion was detected in the microsatellites clusters of 'ionicus 1' (*P. ionicus* subclade *e*), 'tauricus 1' (*P. tauricus* from Thasopoula islet, North Aegean, Greece), and 'tauricus 2' (*P. tauricus* from the Crimean Peninsula, Moldova, and Ukraine), with the first and the third showing signs of sudden expansion during the recent past, possibly following a bottleneck. The above findings are also concordant with the demographic analyses based on mtDNA data. Moderate unidirectional migration was observed from 'melisellensis' (in the present study, only from Montenegro and Bosnia-Herzegovina) to 'tauricus 1'. However, the large geographical distance between the two coupled with the fact that these are different species makes this scenario implausible, suggesting that shared ancient allele polymorphisms rather than current migration might be a better explanation for the observed pattern. In contrast, unidirectional migration from 'gaigeae 1′ (Skyros Isl.; main island of the archipelago) to the nearby located 'gaigeae 2' (Mesa Diavatis and Exo Diavatis satellite islets) is highly plausible, given the proximity of the two and the size difference among the respective islands.

4.3. Phylogeographic hypothesis for P. tauricus species subgroup

Ecological competition among the Balkan *Podarcis* species has been proposed as one of the main drivers of their evolutionary history (Oliverio et al., 2000; Poulakakis et al., 2005a, 2005b). Either the ancestral form of *P. erhardii* species subgroup was the first to colonize the Balkan Peninsula and the ancestor of *P. tauricus* subgroup arrived later (Oliverio et al., 2000) or the reverse (Poulakakis et al., 2005a, 2005b). These two species subgroups are ecologically differentiated, with *P. erhardii* inhabiting more rocky habitats and *P. tauricus* usually found in areas with low vegetation (Valakos et al., 2008). Nevertheless, both scenarios have several shortcomings. According to the first, while the ancestral form of *P. tauricus* dispersed in the Aegean it would have colonized only two island groups (Skyros and Milos) leading to the modern *P. gaigeae* and *P. milensis*, respectively. According to the second, the two species subgroups that today are ecologically distinct, would have been competitors so that the ancestor of *P. erhardii* would have displaced the ancestor of *P. tauricus*. However, given that the spatial and temporal patterns of ecological diversification among those species groups remain ambiguous, it is not safe to consider competition between the ancestral forms as the main force of *Podarcis'* differentiation in the Balkan Peninsula. Since a proper phylogeographic scenario should take into account several possible drivers of differentiation, we present and discuss below a revised phylogeographic scenario from the Late Miocene to the present, taking into account a series of historical and ecological factors. The scenario is shown in a series of maps in Fig. 5.

4.4. Species divergence in the Late Miocene and Early Pliocene

The differentiation of *Podarcis* started in the Upper Miocene (~9.60 Mya) following the tectonic collision of the Adriatic-Apulian mass with Eurasia at ~14–15 Mya (Steininger and Rögl, 1984). The intense orogenetic activity during this period was likely the main factor driving the genetic differentiation within *Podarcis*, which colonized the Balkan Peninsula from the western parts of Europe (Oliverio et al., 2000). The differentiation of the Balkan species group started at 8.63 Mya, which is two million years earlier than previously estimated (10.6 Mya; Poulakakis et al., 2005a, 2005b), which were was inferred using a concatenated mtDNA dataset and not a multilocus species tree, as in the present study. The new divergence time coincides with the formation of the Mid-Aegean Trench (MAT; Creutzburg, 1963; Dermitzakis and Papanikolaou, 1981). The absence of *Podarcis* from Anatolia and the east Aegean islands could be an indication that the colonization of the southern Balkans occurred after the formation of MAT. This period coincides with global cooling and aridification (Fig. 3A), a major expansion of dry zones, and replacement of forests by woodland and

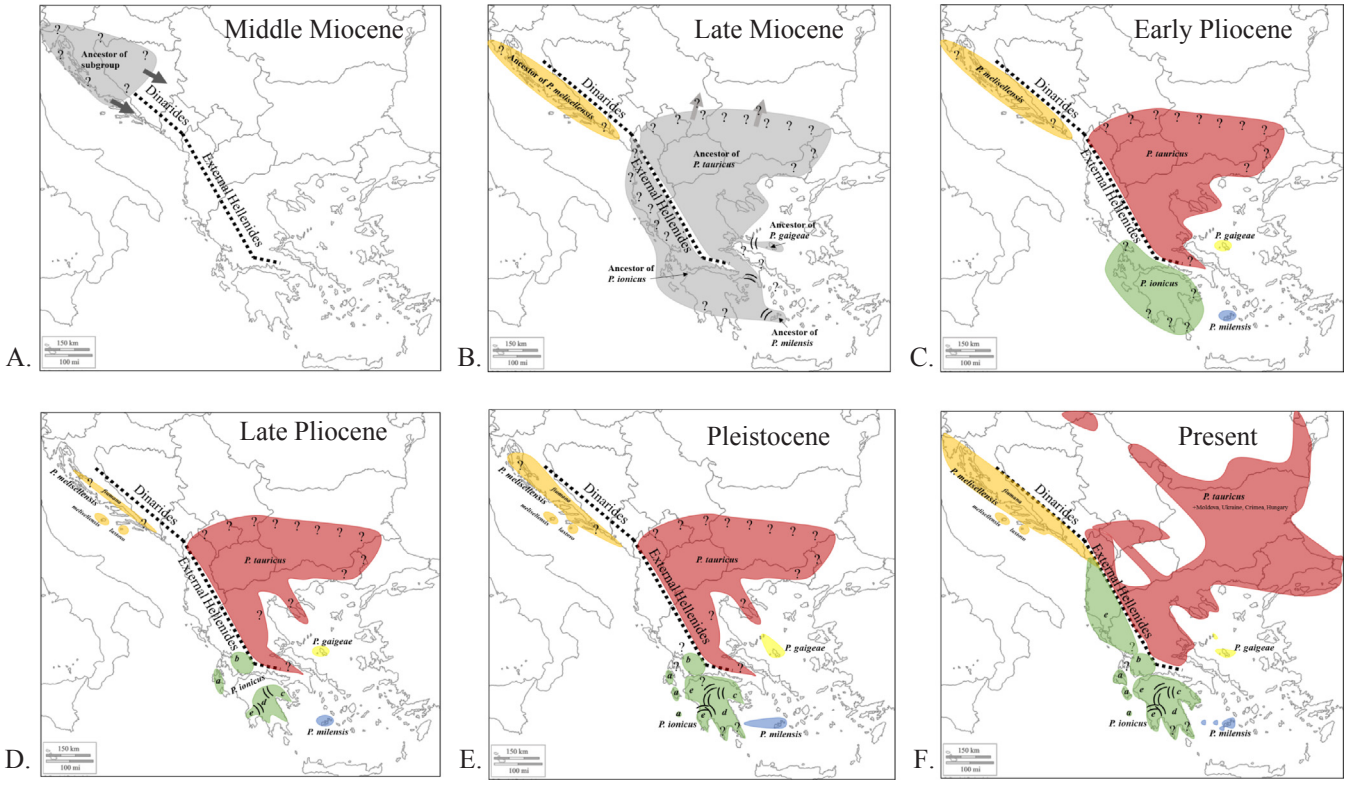

Fig. 5. The proposed phylogeographic scenario of the *P. tauricus* species subgroup distributed in the Southern Europe described in a series of six maps from the Late Miocene to the present.

grasslands (Middle and Late Miocene), particularly in mid-latitudes (Crowley and North, 1991; Potts and Behrensmeyer, 1992). The exact colonization route (from the east, the west or from both sides of the Dinarides and Pindos Mts.) followed by the *P. tauricus* species subgroup is difficult to infer. The Pindos mountain range (Fig. 1A), could have had an important filtering effect for the species' dispersal to the south, as observed in other amphibians and reptiles [*Lacerta viridis* and Adriatic lineage of *L. billineata* (Marzahn et al., 2016; Mayer and Beyerlein, 2001; Sagonas et al., 2014), *Natrix natrix* (Kindler et al., 2013), *N. tessellata* (Guicking et al., 2009), *Pelophylax epeiroticus* (Akın et al., 2010; Lymberakis et al., 2007), and *Vipera ammodytes* (Ursenbacher et al., 2008)]. During the Messinian Salinity Crisis (MSC = 5.96–5.33 Mya, Late Miocene) (Hsü, 1972; Jolivet et al., 2006; Kenneth et al., 1977; Krijgsman et al., 1999) the Mediterranean islands became mountains surrounded by steppes or saline deserts, enabling over land dispersal for several organisms (Poulakakis et al., 2014 and references therein). Irrespective of the time when the ecological differentiation of *P. tauricus* and *P. erhardii* subgroups took place, both subgroups started to diverge in the Messinian. The diversification of the *P. tauricus* species subgroup coincides with the end of MSC (at ~5.55 Mya), when *P. melisellensis* split (Fig. 3A). Its exclusive presence in the Dalmatic coasts, in combination with the vicariance event inferred from this study's biogeographic analysis (Fig. 2), suggests that its divergence could have occurred in that area. The uplift of the Dinarides mountain range, which was initiated in the Middle Miocene (Kuhlemann, 2007) at ~8 Mya, in conjunction with the remarkable alterations in the Dalmatian coasts during the MSC (Popov et al., 2004), could have caused a vicariance event that lead to the isolation of the ancestral *P. melisellensis* population. Subsequent events that might have further promoted the divergence of the subgroup at the species level occurred in the early Pliocene (4.71–4.39 Mya) (Fig. 3A). During the late Miocene, southern Greece consisted of two small peninsulas forming a fork (Creutzburg, 1963; Dermitzakis and Papanikolaou, 1981); one in the southwest, corresponding to the present area of the Peloponnese and Crete, and another in the southeast, corresponding to the east central Greece and the Cyclades of today (Fig. 1A). The reopening of the Mediterranean Sea after the end of the MSC, leading to the refilling of the basin, caused the permanent isolation of Crete from Anatolia, the Peloponnese, and the Cyclades, a fact also supported by additional evidence regarding faunal evolution on the island (Dermitzakis, 1990). The exact ancestral distribution of the *P. tauricus* species subgroup at that time is difficult to determine. One of the most parsimonious hypotheses is that the ancestral form of this subgroup was distributed in the areas that are now occupied by the present species (*P. gaigeae, P. milensis, P. tauricus,* and *P. ionicus*). Then this area became permanently subdivided into four isolated areas in the early Pliocene (Fig. 5), including areas that presently correspond to (a) the island group of Skyros, (b) the island group of Milos, (c) the (at that time united) areas of Peloponnese, western central Greece, and the Ionian Islands, and (d) the area east of Pindos Mt. (see Fig. 1A for current geographic locations). According to the biogeographic analysis, vicariance events were the main drivers of diversification. However, several factors could have contributed to this particular distribution pattern, including historical and ecological constraints acting independently or synergistically. Historical factors (vicariance) include the isolation of the areas inhabited by the ancestors of the species *P. ionicus*, *P. gaigeae*, *P. milensis*, and *P. tauricus* during the MSC. High temperatures and lack of suitable habitats for taxa preferring low vegetation could be considered as important ecological constraints. In any case, competition between the focal subgroup and the *P. erhardii* subgroup, today adapted to more xeric environments, should not be excluded.

Overall, it seems that the first phase (differentiation among species) of the evolutionary history of the *P. tauricus* species subgroup was shaped by several geomorphological alterations and climatic oscillations that happened at the end of late Miocene. These events, at the end of the MSC, have been considered as the major differentiation drivers enhancing allopatric speciation also for other insular populations of Aegean species, such as the lizards *Ablepharus kitaibelii* (Skourtanioti

et al., 2016), *P. erhardii* (Poulakakis et al., 2005b), and *Lacerta trilineata* (Sagonas et al., 2014).

4.5. Within species differentiation during the Pliocene and Early Pleistocene

During the Pliocene, most of the Cyclades islands, including Milos island group, as well as the Skyros archipelago (Fig. 1A) became permanently isolated from the Peloponnese and continental Greece, respectively (Dermitzakis, 1990, 1989). The mountain range of Pindos has probably been an important biogeographic barrier between western Greece / Peloponnese and eastern Greece. Based on our estimations, intra-specific differentiation occurred in the Pliocene for *P. ionicus* and in the Pleistocene for *P. milensis, P. gaigeae, P. tauricus*, and *P. melisellensis*. Several tectonic faults that were activated during the Pliocene in the Corinthian Gulf caused the isolation of the Peloponnese from continental Greece, whereas subsequent tectonic events separated Zakynthos and Kefalonia islands (Fig. 1A) from the Peloponnese (Creutzburg, 1963; Zelilidis et al., 1998). The isolation of the Peloponnese from continental Greece has been assumed to be the main cause of allopatric differentiation and speciation for several species, including the lizards *P. peloponnesiacus* (Poulakakis et al., 2005b) and *L. trilineata* (Sagonas et al., 2014), the mammal *Talpa stankovici* (Tryfonopoulos et al., 2010), the land snails *Codringtonia* (Kotsakiozi et al., 2012) and *Josephinella* (Psonis et al., 2015), and the beetle *Gnaptor boryi* (Gkontas et al., 2016). Intense tectonic rearrangements during the Pliocene caused an important size reduction of the Peloponnese, with the present mountainous areas being the only non-submerged land surfaces (Creutzburg, 1963). Thus, only mountain foots and plateaus were able to host suitable habitats, while mountains acted as biogeographic barriers that prevented gene flow among populations.

4.6. Pleistocene climatic oscillations, eustatic changes, and glacial refugia

During the Pleistocene, the glacial and interglacial periods caused eustatic changes that greatly affected the intraspecific genetic diversity and relationships of insular and coastal *Podarcis* populations. *Podarcis gaigeae* displayed low genetic diversity, shallow and unresolved relationships among individuals, a star-like mtDNA haplotype network, weak population structure, as well as demographic equilibrium (according to mtDNA) or partial population expansion (according to microsatellites). These results suggest a recent genetic differentiation, which is in agreement with Runemark et al. (2012) and the recent paleogeography of the Skyros island group. Indeed, the present form consisting of a main island and several satellite islets, is the result of Lower Pleistocene geographic fragmentation due to eustatic changes caused by climatic oscillations (Perissoratis and Conispoliatis, 2003; van Andel and Shackleton, 1982). Similarly, the current distribution of *P. milensis*, although with higher nucleotide diversity than *P. gaigeae*, is the result of very recent eustatic-driven island isolations (Lambeck, 1996). Geographic fragmentation due to sea level changes has been considered as the most important factor of differentiation also in the case of the Cyclades populations of *P. erhardii* (Hurston et al., 2009).

The divergence among the three phylogenetic subclades of *P. melisellensis* was estimated at 1.2–1.9 Mya by Podnar et al. (2004), hypothesizing that a gradual sea level rise during the Pleistocene (De Giuli et al., 1987) caused the split among its three subclades. Finally, the differentiation of *P. tauricus* population of Thasopoula islet in North Aegean revealed by the microsatellites dataset, might be attributed to a founder event.

The distributional pattern of *P. ionicus* lineages is quite interesting. On one side, there is a group of lineages (subclade *e*) that are widely distributed in the Peloponnese (Fig. S10) and in western Greece, and on the other there is a group of lineages (the four other subclades) with a very restricted distribution, mainly in the Peloponnese (Figs. S11 and S12). The first group showed low genetic diversity, indicating recent expansion. The demographic analyses, such as the mtDNA BSP, the microsatellite k-test and BOTTLENECK, suggested a post-bottleneck sudden expansion in the recent past. This concurs with the SDM projections for LGM and LIG of *P. ionicus* in western Greece and Albania, showing a considerable reduction of the potential distribution during the glacial/interglacial cycle compared to the present. The higher genetic diversity of *P. ionicus* subclades in the Peloponnese compared to western Greece and Albania, indicates that the direction of the spatial expansion is more likely to have happened from the Peloponnese to the north, a pattern also proposed for isopods and land snails (Klossa-Kilia et al., 2006; Kotsakiozi et al., 2012; Parmakelis et al., 2008; Psonis et al., 2015).

The effect of the Pleistocene glacial-interglacial periods on the diversification of other Balkan amphibians and reptiles [i.e. *Anguis* (Jablonski et al., 2016), *Triturus* (Wielstra et al., 2013), *Vipera ursinii* (Zinenko et al., 2015), *L. viridis* (Marzahn et al., 2016), *P. muralis* (Salvi et al., 2013), *Dalmatolacerta oxycephala* and *Dinarolacerta mosorensis* (Podnar et al., 2014)] led to the discovery of several climatic refugia in the southern Balkans. These local refugia gave rise to the hypothesis of 'refugia within refugia', according to which geographic (habitat richness) and climatic heterogeneity within the major glacial refugia may have provided discrete regions where populations diverged (Abellán and Svenning, 2014; Gomez and Lunt, 2007). Based on the dispersal ability of a species and the opportunities for post-glacial expansion to the north, a lineage or species can be characterized either as a 'post-glacial re-colonizer', which is the main biogeographic pattern leading to 'southern richness - northern purity' (Hewitt, 2000; Hewitt, 1999), or as a 'refugial endemic' with limited expansion potential (Bilton et al., 1998; Kryštufek et al., 2007).

According to the present study, the focal *P. tauricus* species subgroup includes both of these types, with *P. tauricus* being a prime example of a post-glacial colonizer. The mtDNA phylogenetic relationships within this taxon are unresolved, forming a characteristic comb-like shape with short branch lengths. The wide distribution range of this taxon, combined with the demographic analyses results, suggest a recent post-bottleneck spatial expansion of *P. tauricus.* This expansion happened from south to north during interglacial periods or after the end of the LGM that possibly caused the bottleneck, and from east to west, as indicated by the k-test on microsatellites that showed population expansion only of the eastern populations (Crimean Peninsula, Moldavia, and Ukraine). The SDM projections for the LGM and the LIG underpinned this hypothesis by showing a considerable reduction of the potential distribution in most of the taxon's range, with only a few spots exhibiting increased probability of potential presence in the southern Balkans and Eastern Europe (Fig. S16X). The southern Balkans could be considered as a local climatic refugium (Joger et al., 2007; Taberlet et al., 1998), also suggested by other phylogeographic studies on Balkan Lacertidae (Marzahn et al., 2016; Sagonas et al., 2014). The Crimean Peninsula (Fig. 1A) and the surrounding area could also be considered as another local refugium, hosting a distinct genetic population, as indicated by the microsatellite data (Fig. 3B). During glacial maxima, the regression of the Black Sea exposed a wide shelf connecting Crimea with the Balkans. The revealed mtDNA haplotype diversity in the Crimean Peninsula suggests that this territory acted as a diversity 'pocket', receiving colonization waves from south Balkans to the northeastern Europe. In this framework, the subclade *e* of *P. ionicus* is probably another post-glacial colonizer, whereas the rest of *P. ionicus* subclades are examples of glacial endemics that are confined by geographical barriers (e.g., mountains, islands).

5. Conclusions

Here we provide evidence that the integration of different types of molecular markers and the utilization of multiple methods is crucial in uncovering detailed processes that shape the evolutionary history of species groups throughout space and time. Previously unresolved phylogenetic relationships that appeared as polytomies by analysis of

traditional sequence data, were here resolved using genome-wide data, obtained by ddRADseq. Moreover, by genotyping microsatellites for hundredths of samples from the entire distribution of the *P. tauricus* species group we confirmed the existence of at least two cryptic evolutionary lineages and we revealed extensive population structuring. Our proposed phylogeographic scenario of the *P. tauricus* species subgroup identifies the Messinian Salinity Crisis as the main event causing species divergence, and Pliocene tectonic events and Quaternary climatic oscillations as the main drivers of the observed intraspecific patterns of genetic diversity. The current high-throughput sequencing approaches have the potential to address previously intractable questions in evolution of non-model organisms (Carstens et al., 2012; Goodwin et al., 2016; Lemmon and Lemmon, 2013), leading to the development of large-scale sequencing arrays based on reduced genome representations, which may provide thousands of markers densely covering the genome data at moderate to low costs (such as ddRADseq). However, the main drawback of these approaches concerns the performance and efficiency of software available for estimating divergence times, to handle large datasets, such as those obtained by ddRADseq. Advance in this field is expected to provide more robust estimates and reduce uncertainty.

Data accessibility

The datasets generated during this study are available (in PHILIP format) from the corresponding author upon request.

Acknowledgements

We wish to express our gratitude to (in alphabetical order): Roman Alekseev, Miguel A. Carretero, Igor Doronin, Arkadyi Dovzhenko, Daniel Gruľa, Václav Gvoždík, Tomáš Husák, Daniel Koleska, Spartak Litvinchuk, Andrey Matvyeyev, Edvárd Mizsei, Anton Nadolnyi, Panayiotis Pafilis, Boyan Petrov, Georgi Popgeorgiev, Konstantinos Sagonas, Leonid Sokolov, Konstantinos Sotiropoulos, Ivan Stolárik, Ilias Strachinis, Manos Stratakis, Helen Sviridenko, Vladimir Tsurcanu, Nikolay Tzankov, and Judit Vörös, for sending us several tissue samples or for their assistance in the field. We also thank the Municipal Port Fund of Keramoti and the fishing boat 'Parmenides' for helping us traveling to Thasopoula islet (North Aegean), and to Apostolos Trichas (NHMC) for the lizard's photograph used in the graphical abstract. Finally, we express our gratitude to Adalgisa Caccone (Yale University) for her help and advice on ddRADseq libraries' preparation.

This study was part of the EcoGenoDiv project funded by NSFR 2007-2013 programme for development, European Social Fund, Operational Programme, Education and Lifelong Learning investing in knowledge society, Ministry of Education and Religious Affairs, Managing Authority, Co-financed by Greece and the European Union. JCI was funded by Grant No. 173025 Ministry of Education, Science and Technological Development of Republic of Serbia. DJ was supported by the Slovak Research and Development Agency under the contract no. APVV-15-0147. Part of this work was funded by the Klaus Tschira Foundation.

Author Contributions

NP (Psonis) collected samples, performed laboratory work, analyzed data and wrote the manuscript. AA, EK, and PK performed laboratory work, analyzed the data and commented on the manuscript. DD, AK, AS, ADL advised on the phylogenetic analyses on ddRADseq data and commented on the manuscript. DP performed the SDM. OK, DJ, JCI, IG, PL collected or provided samples. NP (Poulakakis) designed and supervised the research and refined the manuscript. All authors read and improved the final manuscript.

Conflict of interest

The authors have no conflict of interest to declare.

Appendix A. Supplementary material

Supplementary data associated with this article can be found, in the online version, at https://doi.org/10.1016/j.ympev.2018.03.021.

References

Abellán, P., Svenning, J., 2014. Refugia within refugia – patterns in endemism and genetic divergence are linked to Late Quaternary climate stability in the Iberian Peninsula. Biol. J. Linnean Soc. 113, 13–28.
Aberer, A.J., Kobert, K., Stamatakis, A., 2014. ExaBayes: Massively Parallel Bayesian Tree Inference for the Whole-Genome Era. Mol. Biol. Evol. 31, 2553–2556.
Ahmadzadeh, F., Flecks, M., Carretero, M.A., Böhme, W., Ihlow, F., Kapli, P., Miraldo, A., Rödder, D., 2016. Separate histories in both sides of the Mediterranean: phylogeny and niche evolution of ocellated lizards. J. Biogeogr.
Ahmadzadeh, F., Flecks, M., Rödder, D., Böhme, W., Ilgaz, Ç., Harris, D.J., Engler, J.O., Üzüm, N., Carretero, M.A., 2013. Multiple dispersal out of Anatolia: biogeography and evolution of oriental green lizards. Biol. J. Linnean Soc. 110, 398–408.
Akın, Ç., Can Bilgin, C., Beerli, P., Westaway, R., Ohst, T., Litvinchuk, S.N., Uzzell, T., Bilgin, M., Hotz, H., Guex, G.D., Plötner, J., 2010. Phylogeographic patterns of genetic diversity in eastern Mediterranean water frogs were determined by geological processes and climate change in the Late Cenozoic. J. Biogeography 37, 2111–2124.
Allegrucci, G., Rampini, M., Gratton, P., Todisco, V., Sbordoni, V., 2009. Testing phylogenetic hypotheses for reconstructing the evolutionary history of *Dolichopoda* cave crickets in the eastern Mediterranean. J. Biogeography 36, 1785–1797.
Amos, W., Hoffman, J.I., Frodsham, A., Zhang, L., Best, S., Hill, A.V.S., 2007. Automated binning of microsatellite alleles: problems and solutions. Mol. Ecol. Notes 7, 10–14.
Antoniou, A., Kasapidis, P., Kotoulas, G., Mylonas, C.C., Magoulas, A., 2017. Genetic diversity of Atlantic Bluefin tuna in the Mediterranean Sea: insights from genome-wide SNPs and microsatellites. J. Biol. Res. (Thessalon) 24, 3.
Araújo, M.B., Guisan, A., 2006. Five (or so) challenges for species distribution modelling. J. Biogeography 33, 1677–1688.
Barbosa, S., Paupério, J., Herman, J.S., Ferreira, C.M., Pita, R., Vale-Gonçalves, H.M., Cabral, J.A., Garrido-García, J.A., Soriguer, R.C., Beja, P., Mira, A., Alves, P.C., Searle, J.B., 2017. Endemic species may have complex histories: within-refugium phylogeography of an endangered Iberian vole. Mol. Ecol. Notes 26, 951–967.
Belkhir, K., Borsa, P., Chikhi, L., Raufaste, N., Bonhomme, F., 2001. GENETIX, logiciel sous Windows TM pour la génétique des populations. Laboratoire Génome, Populations, Interactions CNRS UMR 5000: Université de Montpellier II, Montpellier, France.
Bilgin, R., 2007. Kgtests: a simple Excel Macro program to detect signatures of population expansion using microsatellites. Mol. Ecol. Notes 7, 416–417.
Bilton, D.T., Mirol, P.M., Mascheretti, S., Fredga, K., Zima, J., Searle, J.B., 1998. Mediterranean Europe as an area of endemism for small mammals rather than a source for northwards postglacial colonization. Proc. Biol. Sci. 265, 1219–1226.
Blois, J.L., 2012. update: Recent advances in using species distributional models to understand past distributions. Front. Biogeogr. 3, 123–124.
Blondel, J., Aronson, J., 1999. Biology and Wildlife of the Mediterranean Region. Oxford University Press.
Blondel, J., Aronson, J., Bodiou, J.Y., 2010. The Mediterranean Region: Biological Diversity through Time and Space. Oxford University Press.
Bouckaert, R.R., Heled, J., Kühnert, D., Vaughan, T.J., Wu, C., Xie, D., Suchard, M.A., Rambaut, A., Drummond, A.J., 2014. BEAST 2: A Software Platform for Bayesian Evolutionary Analysis. PLoS Comput. Biol. 10, e1003537.
Brown, R.P., Terrasa, B., Pırez-Mellado, V., Castro, J.A., Hoskisson, P.A., Picornell, A., Ramon, M.M., 2008. Bayesian estimation of post-Messinian divergence times in Balearic Island lizards. Mol. Phylogenet. Evol. 48, 350–358.
Bruford, M.W., Hanotte, O., Burke, T., 1998. Multi and single locus DNA fingerprinting. In: Hoelzel, A.R. (Ed.), Molecular Genetic Analysis of Populations: A Practical Approach. IRL Press, pp. 225–269.
Carstens, B.C., Lemmon, A.R., Lemmon, E.M., 2012. The promises and pitfalls of next-generation sequencing data in phylogeography. Syst. Biol. 61, 713–715.
Čerňanský, A., 2010. Earliest world record of green lizards (Lacertilia, Lacertidae) from the Lower Miocene of Central Europe. Biologia 65, 737–741.
Chifman, J., Kubatko, L.S., 2014. Quartet inference from SNP data under the coalescent model. Bioinformatics 30, 3317–3324.
Cornuet, J.M., Luikart, G., 1996. Description and power analysis of two tests for detecting recent population bottlenecks from allele frequency data. Genetics 144, 2001–2014.
Cox, S.C., Carranza, S., Brown, R.P., 2010. Divergence times and colonization of the Canary Islands by *Gallotia* lizards. Mol. Phylogenet. Evol. 56, 747–757.
Creutzburg, N., 1963. Paleogeographic evolution of Crete from Miocene till our days. Cretan Annals 15 (16), 336–342.
Crowley, T.J., North, G.R., 1991. Paleoclimatology. Oxford University Press, New York.
DaCosta, J.M., Sorenson, M.D., 2016. ddRAD-seq phylogenetics based on nucleotide, indel, and presence–absence polymorphisms: analyses of two avian genera with contrasting histories. Mol. Phylogenet. Evol. 94 (Part A), 122–135.
Darriba, D., Taboada, G.L., Doallo, R., Posada, D., 2012. jModelTest 2: more models, new heuristics and parallel computing. Nat. Meth. 9 772-772.

De Giuli, C., Masini, F., Valleri, G., 1987. Paleogeographic evolution of the Adriatic area since Oligocene to Pleistocene. Riv. It. Paleont. Strat. 93, 109–126.
Dermitzakis, D.M., 1989. The colonisation of Aegean islands in relation with the paleogeographic evolution (in greek). Biol. Gallo-Hellenica 14, 99–121.
Dermitzakis, D.M., 1990. Paleogeography, Geodynamic Processes and event Stratigraphy during the Late Cenozoic of the Aegean area. Atti Convegni Lincei 85, 263–288.
Dermitzakis, D.M., Papanikolaou, D.J., 1981. Paleogeography and geodynamics of the Aegean region during the Neogene. Annal. Geol. Pays Hellenic 30, 245–289.
Džukić, G., Kalezić, M.L., 2004. The Biodiversity of Amphibians and Reptiles in the Balkan Peninsula. In: Griffiths, H.I. (Ed.), Balkan Biodiversity: Pattern and Process in the European Hotspot. Kluwer Academic Publishers, Dordrecht, pp. 167–792.
Earl, D.A., vonHoldt, B.M., 2012. STRUCTURE HARVESTER: a website and program for visualizing STRUCTURE output and implementing the Evanno method. Conserv. Genet. Res. 4, 359–361.
Eaton, D.A.R., 2014. PyRAD: assembly of de novo RADseq loci for phylogenetic analyses. Bioinformatics 30, 1844–1848.
Estes, R., 1983. Handbuch der Paläoherpetologie, Part 10: Sauria terrestria. Gustav Fischer Verlag, Stuttgart, Amphisbaenia.
Evanno, G., Regnaut, S., Goudet, J., 2005. Detecting the number of clusters of individuals using the software STRUCTURE: a simulation study. Mol Ecol 14, 2611–2620.
Ferchaud, A., Ursenbacher, S., Cheylan, M., Luiselli, L., Jelić, D., Halpern, B., Major, Á., Kotenko, T., Keyan, N., Behrooz, R., Crnobrnja-Isailović, J., Tomović, L., Ghira, I., Ioannidis, Y., Arnal, V., Montgelard, C., 2012. Phylogeography of the *Vipera ursinii* complex (Viperidae): mitochondrial markers reveal an east–west disjunction in the Palaearctic region. J. Biogeogr. 39, 1836–1847.
Gariboldi, M.C., Túnez, J.I., Failla, M., Hevia, M., Panebianco, M.V., Paso Viola, M.N., Vitullo, A.D., Cappozzo, H.L., 2016. Patterns of population structure at microsatellite and mitochondrial DNA markers in the franciscana dolphin (*Pontoporia blainvillei*). Ecol. Evol. 6, 8764–8776.
Gkontas, I., Papadaki, S., Trichas, A., Poulakakis, N., 2016. First assessment on the molecular phylogeny and phylogeography of the species *Gnaptor boryi* distributed in Greece (Coleoptera: Tenebrionidae). Mitoch. DNA Part A 1–8.
Gomez, A., Lunt, D.H., 2007. Refugia within refugia: patterns of phylogeographic concordance in the Iberian Peninsula. In: Weiss, S., Ferrand, N. (Eds.), Phylogeography in Southern European Refugia: Evolutionary Perspectives On the Origins and Conservation of European Biodiversity. Springer, Berlin, pp. 155–188.
Goodwin, S., McPherson, J.D., McCombie, W.R., 2016. Coming of age: ten years of next-generation sequencing technologies. Nat. Rev. Gen. 17, 333.
Griffiths, H., Kryštufek, B., Reed, J., 2004. Balkan Biodiversity: Pattern and Process in the European Hotspot. Springer.
Guicking, D., Joger, U., Wink, M., 2009. Cryptic diversity in a Eurasian water snake (*Natrix tessellata*, Serpentes: Colubridae): evidence from mitochondrial sequence data and nuclear ISSR-PCR fingerprinting. Org. Divers. Evol. 9, 201–214.
Guillou, H., Carracedo, J.C., Torrado, F.P., Badiola, E.R., 1996. K-Ar ages and magnetic stratigraphy of a hotspot-induced, fast grown oceanic island: El Hierro, Canary Islands. J. Volcanol. Geoth. Res. 73, 141–155.
Gvoždík, V., Jandzik, D., Lymberakis, P., Jablonski, D., Moravec, J., 2010. Slow worm, *Anguis fragilis* (Reptilia: Anguidae) as a species complex: genetic structure reveals deep divergences. Mol. Phylogenet. Evol. 55, 460–472.
Harris, J.D., Arnold, N.E., 1999. Relationships of wall lizards, *Podarcis* (Reptilia: Lacertidae) based on mitochondrial DNA sequences. Copeia 749–754.
Hewitt, G., 2000. The genetic legacy of the Quaternary ice ages. Nature 405, 907–913.
Hewitt, G.M., 1999. Post-glacial re-colonization of European biota. Biol. J. Linnean Soc. 68, 87–112.
Hewitt, G.M., 2011. Mediterranean Peninsulas: The Evolution of Hotspots. Springer Publishers, Berlin Heidelberg, Biodiversity Hotspots.
Hijmans, R.J., Cameron, S.E., Parra, J.L., Jones, P.G., Jarvis, A., 2005. Very high resolution interpolated climate surfaces for global land areas. Int. J. Climatol. 25, 1965–1978.
Hsü, K.J., 1972. Origin of saline giants: a critical review after the discovery of the Mediterranean Evaporite. Earth-Science Rev. 8, 371–396.
Hurston, H., Voith, L., Bonanno, J., Foufopoulos, J., Pafilis, P., Valakos, E., Anthony, N., 2009. Effects of fragmentation on genetic diversity in island populations of the Aegean wall lizard *Podarcis erhardii* (Lacertidae, Reptilia). Mol. Phylogenet. Evol. 52, 395–405.
Jablonski, D., Jandzik, D., Mikulíček, P., Džukić, G., Ljubisavljević, K., Tzankov, N., Jelić, D., Thanou, E., Moravec, J., Gvoždík, V., 2016. Contrasting evolutionary histories of the legless lizards slow worms (*Anguis*) shaped by the topography of the Balkan Peninsula. BMC Evol. Biol. 16, 1–18.
Jakobsson, M., Rosenberg, N.A., 2007. CLUMPP: a cluster matching and permutation program for dealing with label switching and multimodality in analysis of population structure. Bioinformatics 23, 1801–1806.
Joger, U., Fritz, U., Guicking, D., Kalyabina-Hauf, S., Nagy, Z.T., Wink, M., 2007. Phylogeography of western Palaearctic reptiles – spatial and temporal speciation patterns. Zool. Anz. 246, 293–313.
Jolivet, L., Augier, R., Robin, C., Suc, J., Rouchy, J., 2006. Lithospheric-scale geodynamic context of the Messinian salinity crisis. Sediment. Geol. 188–189, 9–33.
Jombart, T., Ahmed, I., 2011. adegenet 1.3-1: new tools for the analysis of genome-wide SNP data. Bioinformatics.
Jombart, T., Devillard, S., Balloux, F., 2010. Discriminant analysis of principal components: a new method for the analysis of genetically structured populations. BMC Genetics 11, 1–15.
Kalinowski, S.T., Wagner, A.P., Taper, M.L., 2006. ml-relate: a computer program for maximum likelihood estimation of relatedness and relationship. Mol. Ecol. Notes 6, 576–579.
Kaliontzopoulou, A., Brito, J.C., Carretero, M.A., Larbes, S., Harris, D.J., 2008. Modelling the partially unknown distribution of wall lizards (*Podarcis*) in North Africa: ecological affinities, potential areas of occurrence, and methodological constraints. Canadian J. Zool. 86, 992–1001.
Katoh, K., Standley, D.M., 2013. MAFFT Multiple Sequence Alignment Software Version 7: Improvements in Performance and Usability. Mol. Biol. Evol. 30, 772–780.
Kenneth, J.H., Montadert, L., Bernoulli, D., Cita, M.B., Erickson, A., Garrison, R.E., Kidd, R.B., Melieres, F., Muller, C., Wright, R.A., 1977. History of the Mediterranean salinity crisis. Nature 267, 399–403.
Kindler, C., Böhme, W., Corti, C., Gvoždík, V., Jablonski, D., Jandzik, D., Metallinou, M., Široký, P., Fritz, U., 2013. Mitochondrial phylogeography, contact zones and taxonomy of grass snakes (*Natrix natrix*, *N. megalocephala*). Zool. Scripta 42, 458–472.
King, J.P., Kimmel, M., Chakraborty, R., 2000. A power analysis of microsatellite-based statistics for inferring past population growth. Mol. Biol. Evol. 17, 1859–1868.
Klossa-Kilia, E., Kilias, G., Tryfonopoulos, G., Koukou, K., Spyros, S., Parmakelis, A., 2006. Molecular phylogeny of the Greek populations of the genus *Ligidium* (Isopoda, Oniscidea) using three mtDNA gene segments. Zool. Scr. 35, 459–472.
Kornilios, P., Thanou, E., Kapli, P., Parmakelis, A., Chatzaki, M., 2016. Peeking through the trapdoor: historical biogeography of the Aegean endemic spider Cyrtocarenum Ausserer, 1871 with an estimation of mtDNA substitution rates for Mygalomorphae. Mol. Phylogenet. Evol.
Kotsakiozi, P., Parmakelis, A., Giokas, S., Papanikolaou, I., Valakos, E.D., 2012. Mitochondrial phylogeny and biogeographic history of the Greek endemic land-snail genus *Codringtonia* Kobelt 1898 (Gastropoda, Pulmonata, Helicidae). Mol. Phylogenet. Evol. 62, 681–692.
Kozlov, A.M., Aberer, A.J., Stamatakis, A., 2015. ExaML Version 3: A Tool for Phylogenomic Analyses on Supercomputers. Bioinformatics.
Krijgsman, W., Hilgen, F.J., Raffi, I., Sierro, F.J., Wilson, D.S., 1999. Chronology, causes and progression of the Messinian salinity crisis. Nature 400, 652–655.
Kryštufek, B., Buzan, E.V., Hutchinson, W.F., Hänfling, B., 2007. Phylogeography of the rare Balkan endemic Martino's vole, *Dinaromys bogdanovi*, reveals strong differentiation within the western Balkan Peninsula. Mol. Ecol. 16, 1221–1232.
Kuhlemann, J., 2007. Paleogeographic and paleotopographic evolution of the Swiss and Eastern Alps since the Oligocene. Glob. Planet. Change 58, 224–236.
Lambeck, K., 1996. Sea-level change and shore-line evolution in Aegean Greece since upper palaeolithic time. Antiquity 70, 588–611.
Leaché, A.D., Chavez, A.S., Jones, L.N., Grummer, J.A., Gottscho, A.D., Linkem, C.W., 2015. Phylogenomics of phrynosomatid lizards: conflicting signals from sequence capture versus restriction site associated DNA sequencing. Genome Biol. Evol. 7, 706–719.
Lemmon, E.M., Lemmon, A.R., 2013. High-throughput genomic data in systematics and phylogenetics. Annu. Rev. Ecol. Evol. Syst. 44, 99–121.
Lymberakis, P., Poulakakis, N., 2010. Three continents claiming an archipelago: the evolution of Aegean's herpetofaunal diversity. Diversity 2, 233–255.
Lymberakis, P., Poulakakis, N., Manthalou, G., Tsigenopoulos, C.S., Magoulas, A., Mylonas, M., 2007. Mitochondrial phylogeography of *Rana (Pelophylax)* populations in the Eastern Mediterranean region. Mol. Phylogenet. Evol. 44, 115–125.
Marzahn, E., Mayer, W., Joger, U., Ilgaz, Ç., Jablonski, D., Kindler, C., Kumlutaş, Y., Nistri, A., Schneeweiss, N., Vamberger, M., Žagar, A., Fritz, U., 2016. Phylogeography of the *Lacerta viridis* complex: mitochondrial and nuclear markers provide taxonomic insights. J. Zool. Syst. Evol. Res. 54, 85–105.
Mayer, W., Beyerlein, P., 2001. Genetic differentiation of the *Lacerta viridis/bilineata* complex and of *Lacerta trilineata* in Greece: mitochondrial DNA sequences. Mertensiella 13, 52–59.
Meulenkamp, J.E., 1985. Aspects of the Late Cenozoic Evolution of the Aegean Region. In: Stanley, D.J., Wezel, F.C. (Eds.), Geological Evolution of the Mediterranean Basin. Springer, New York, pp. 307–321.
Mizsei, E., Jablonski, D., Roussos, S.A., Dimaki, M., Ioannidis, Y., Nilson, G., Nagy, Z.T., 2017. Nuclear markers support the mitochondrial phylogeny of Vipera ursinii-renardi complex (Squamata: Viperidae) and species status for the Greek meadow viper. Zootaxa 4227, zootaxa.4227.4221.4224.
Musilová, R., Zavadil, V., Marková, S., Kotlík, P., 2010. Relics of the Europe's warm past: phylogeography of the Aesculapian snake. Mol. Phylogenet. Evol. 57, 1245–1252.
Myers, N., Mittermeier, R.A., Mittermeier, C.G., da Fonseca, G.A.B., Kent, J., 2000. Biodiversity hotspots for conservation priorities. Nature 403, 853–858.
Nei, M., 1987. Molecular Evolutionary Genetics. Columbia University Press, New York.
Nieto-Montes de Oca, A., Barley, A.J., Meza-Lázaro, R.N., García-Vázquez, U.O., Zamora-Abrego, J.G., Thomson, R.C., Leaché, A.D., 2017. Phylogenomics and species delimitation in the knob-scaled lizards of the genus *Xenosaurus* (Squamata: Xenosauridae) using ddRADseq data reveal a substantial underestimation of diversity. Mol. Phylogenet. Evol. 106, 241–253.
Ogilvie, H.A., Bouckaert, R.R., Drummond, A.J., 2017. StarBEAST2 brings faster species tree inference and accurate estimates of substitution rates. Mol. Biol. Evol.
Oliverio, M., Bologna, M.A., Mariottini, P., 2000. Molecular biogeography of the Mediterranean lizards *Podarcis* Wagler, 1830 and *Teira* Gray, 1838 (Reptilia, Lacertidae). J. Biogeography 27, 1403–1420.
Parmakelis, A., Klossa-Kilia, E., Kilias, G., Triantis, K.A., Sfenthourakis, S., 2008. Increased molecular divergence of two endemic *Trachelipus* (Isopoda, Oniscidea) species from Greece reveals patterns not congruent with current taxonomy. Biol. J. Linnean Soc. 95, 361–370.
Pattengale, N.D., Alipour, M., Bininda-Emonds, O.R., Moret, B.M., Stamatakis, A., 2010. How many bootstrap replicates are necessary? J. Comput. Biol.: J. Comput. Mol. Cell Biol. 17, 337–354.
Pavlicev, M., Mayer, W., 2009. Fast radiation of the subfamily Lacertinae (Reptilia: Lacertidae): History or methodical artefact? Mol. Phylogenet. Evol. 52, 727–734.
Perissoratis, C., Conispoliatis, N., 2003. The impacts of sea-level changes during latest Pleistocene and Holocene times on the morphology of the Ionian and Aegean seas (SE

Alpine Europe). Mar. Geol. 196, 145–156.
Peterson, B.K., Weber, J.N., Kay, E.H., Fisher, H.S., Hoekstra, H.E., 2012. Double digest RADseq: an inexpensive method for *De Novo* SNP discovery and genotyping in model and non-model species. PLoS ONE 7, e37135.
Phillips, J.S., Dudik, M., Schapire, E.R., 2004. A maximum entropy approach to species distribution modeling. In: Proc. 21st ICML. ACM, Banff, Alberta, Canada, p. 83.
Phillips, S.J., Anderson, R.P., Schapire, R.E., 2006. Maximum entropy modeling of species geographic distributions. Ecol. Model 190, 231–259.
Piry, S., Luikart, G., Cornuet, J.M., 1999. BOTTLENECK: a computer program for detecting recent reductions in the effective population size using allele frequency data. J. Heredity 90, 502–503.
Podnar, M., Madaric, B.B., Mayer, W., 2014. Non concordant phylogeographical patterns of three widely codistributed endemic Western Balkans lacertid lizards (Reptilia, Lacertidae) shaped by specific habitat requirements and different responses to Pleistocene climatic oscillations. J. Zool. Syst. Evol. Res. 52, 119–129.
Podnar, M., Mayer, W., Tvrtković, N., 2004. Mitochondrial phylogeography of the Dalmatian wall lizard, (Lacertidae). Org. Divers. Evol. 4, 307–317.
Popov, S.V., Rögl, F., Rozanov, A.Y., Steininger, F.F., Shcherba, I.G., Kovac, M., 2004. Lithological-Paleogeographic Maps of Paratethys. Schweizerbart'sche Verlagsbuchhandlung.
Potts, R., Behrensmeyer, A.K., 1992. Late Cenozoic terrestrial ecosystems. In: Behrensmeyer, A.K., Damuth, J., DiMichele, W., Potts, R., Sues, H.D., Wing, S. (Eds.), Terrestrial Ecosystems through Time. University of Chicago Press, Chicago, pp. 419–541.
Poulakakis, N., Kapli, P., Lymberakis, P., Trichas, A., Vardinoyannis, K., Sfenthourakis, S., Mylonas, M., 2014. A review of phylogeographic analyses of animal taxa from the Aegean and surrounding regions. J. Zool. Syst. Evol. Res. 53, 18–32.
Poulakakis, N., Lymberakis, P., Valakos, E., Pafilis, P., Zouros, E., Mylonas, M., 2005a. Phylogeography of Balkan wall lizard (*Podarcis taurica*) and its relatives inferred from mitochondrial DNA sequences. Mol Ecol 14, 2433–2443.
Poulakakis, N., Lymberakis, P., Valakos, E., Zouros, E., Mylonas, M., 2005b. Phylogenetic relationships and biogeography of *Podarcis* species from the Balkan Peninsula, by bayesian and maximum likelihood analyses of mitochondrial DNA sequences. Mol. Phylogenet. Evol. 37, 845–857.
Pritchard, J.K., Stephens, M., Donnelly, P., 2000. Inference of population structure using multilocus genotype data. Genetics 155, 945–959.
Psonis, N., Antoniou, A., Kukushkin, O., Jablonski, D., Petrov, B., Crnobrnja-Isailović, J., Sotiropoulos, K., Gherghel, I., Lymberakis, P., Poulakakis, N., 2017. Hidden diversity in the *Podarcis tauricus* (Sauria, Lacertidae) species subgroup in the light of multilocus phylogeny and species delimitation. Mol. Phylogenet. Evol. 106, 6–17.
Psonis, N., Lymberakis, P., Poursanidis, D., Poulakakis, N., 2016. Contribution to the study of *Acanthodactylus* (Sauria: Lacertidae) mtDNA diversity focusing on the *A. boskianus* species group. Mitochondrion 30, 78–94.
Psonis, N., Vardinoyannis, K., Mylonas, M., Poulakakis, N., 2015. Unraveling the evolutionary history of the *Chilostoma* Fitzinger, 1833 (Mollusca, Gastropoda, Pulmonata) lineages in Greece. Mol. Phylogenet. Evol. 91, 210–225.
Rato, C., Harris, D.J., Perera, A., Carvalho, S.B., Carretero, M.A., Rödder, D., 2015. A Combination of Divergence and Conservatism in the Niche Evolution of the Moorish Gecko, *Tarentola mauritanica* (Gekkota: Phyllodactylidae). PLoS ONE 10, e0127980.
Raymond, M., Rousset, F., 1995. Genepop (Version-1.2) - population-genetics software for exact tests and ecumenicism. J. Heredity 86, 248–249.
Ree, R.H., Smith, S.A., 2008. Maximum likelihood inference of geographic range evolution by dispersal, local extinction, and cladogenesis. Syst. Biol. 57, 4–14.
Reich, D.E., Feldman, M.W., Goldstein, D.B., 1999. Statistical properties of two tests that use multilocus data sets to detect population expansions. Mol. Biol. Evol. 16, 453–466.
Robinson, D.F., Foulds, L.R., 1981. Comparison of phylogenetic trees. Math. Biosci. 53, 131–147.
Rosenberg, N.A., 2004. distruct: a program for the graphical display of population structure. Mol. Ecol. Notes 4, 137–138.
Runemark, A., Hey, J., Hansson, B., Svensson, E.I., 2012. Vicariance divergence and gene flow among islet populations of an endemic lizard. Mol. Ecol. 21, 117–129.
Sagonas, K., Poulakakis, N., Lymberakis, P., Parmakelis, A., Pafilis, P., Valakos, E.D., 2014. Molecular systematics and historical biogeography of the green lizards (*Lacerta*) in Greece: insights from mitochondrial and nuclear DNA. Mol. Phylogenet. Evol. 76C, 144–154.
Salvi, D., Harris, D.J., Kaliontzopoulou, A., Carretero, M.A., Pinho, C., 2013. Persistence across Pleistocene ice ages in Mediterranean and extra-Mediterranean refugia: phylogeographic insights from the common wall lizard. BMC Evol. Biol. 13, 147.
Schoener, T.W., 1968. The *Anolis* Lizards of Bimini: resource partitioning in a complex Fauna. Ecology 49, 704–726.
Schule, W., 1993. Mammals, vegetation and the initial human settlement of the Mediterranean islands: a palaeoecological approach. J. Biogeography 20, 399–412.
Senczuk, G., Colangelo, P., De Simone, E., Aloise, G., Castiglia, R., 2017. A combination of long term fragmentation and glacial persistence drove the evolutionary history of the Italian wall lizard *Podarcis siculus*. BMC Evol. Biol. 17, 6.
Shriver, M.D., Jin, L., Chakraborty, R., Boerwinkle, E., 1993. VNTR allele frequency distributions under the stepwise mutation model: a computer simulation approach. Genetics 134, 983–993.
Sillero, N., Campos, J., Bonardi, A., Corti, C., Creemers, R., Crochet, P., Crnobrnja-Isailović, J., Denoël, M., Ficetola, G.F., Gonçalves, J., Kuzmin, S., Lymberakis, P., de Pous, P., Rodríguez, A., Sindaco, R., Speybroeck, J., Toxopeus, B., Vieites, D.R., Vences, M., 2014. Updated distribution and biogeography of amphibians and reptiles of Europe. Amphibia-Reptilia 35, 1–31.
Skourtanioti, E., Kapli, P., Ilgaz, Ç., Kumlutaş, Y., Avcı, A., Ahmadzadeh, F., Crnobrnja-Isailović, J., Gherghel, I., Lymberakis, P., Poulakakis, N., 2016. A reinvestigation of phylogeny and divergence times of the *Ablepharus kitaibelii* species complex (Sauria, Scincidae) based on mtDNA and nuDNA genes. Mol. Phylogenet. Evol. 103, 199–214.
Stamatakis, A., 2014. RAxML Version 8: a tool for phylogenetic analysis and post-analysis of large phylogenies. Bioinformatics 30, 1312–1313.
Steininger, F.F., Rögl, F., 1984. Paleogeography and palinspastic reconstruction of the Neogene of the Mediterranean and Paratethys. In: Dixon, J.E., Robertson, A.H.F. (Eds.), The Geological Evolution of the Eastern Meidterranean. Blackwell Scientific Publications, pp. 659–668.
Svenning, J., Fløjgaard, C., Marske, K.A., Nógues-Bravo, D., Normand, S., 2011. Applications of species distribution modeling to paleobiology. Quat. Sci. Rev. 30, 2930–2947.
Swofford, D.L., 2002. PAUP*. Phylogenetic analysis using parsimony (*and other methods). Version 4. Sinauer Associates, Sunderland, MA.
Taberlet, P., Fumagalli, L., Wust-Saucy, A.G., Cosson, J.F., 1998. Comparative phylogeography and postglacial colonization routes in Europe. Mol. Ecol. 7, 453–464.
Terrasa, B., Picornell, A., Castro, J.A., Ramon, M.M., 2004. Genetic variation within endemic *Podarcis* lizards from the Balearic Islands inferred from partial Cytochrome b sequences. Amphibia-Reptilia 25, 407–414.
Toonen, R.J., Hughes, S., 2001. Increased throughput for fragment analysis on an ABI PRISM 377 automated sequencer using a membrane comb and STRand software. Biotechniques 31, 1320–1324.
Tryfonopoulos, G., Thanou, E., Fraguedakis-Tsolis, S., Chondropoulos, B., 2010. New data on the distribution and genetic structure of Greek moles of the genus *Talpa* (Mammalia, Talpidae). J. Zool. Syst. Evol. Res. 48, 188–193.
Ursenbacher, S., Schweiger, S., Tomovic, L., Crnobrnja-Isailovic, J., Fumagalli, L., Mayer, W., 2008. Molecular phylogeography of the nose-horned viper (*Vipera ammodytes*, Linnaeus (1758)): evidence for high genetic diversity and multiple refugia in the Balkan peninsula. Mol. Phylogenet. Evol. 46, 1116–1128.
Vähä, J., Erkinaro, J., NiemelÄ, E., Primmer, C.R., 2007. Life-history and habitat features influence the within-river genetic structure of Atlantic salmon. Mol. Ecol. 16, 2638–2654.
Valakos, E., Pafilis, P., Sotiropoulos, K., Lymberakis, P., Maragou, P., Foufopoulos, J., 2008. The Amphibians and Reptiles of Greece. Chimaira, Frankfurt am Main.
van Andel, T.H., Shackleton, J.C., 1982. Late Paleolithic and Mesolithic Coastlines of Greece and the Aegean. J. Field Archaeology 9, 445–454.
van der Vaart, A.W., 1998. Asymptotic statistics. Cambridge University Press, Cambridge.
van Oosterhout, C., Hutchinson, W.F., Wills, D.P.M., Shipley, P., 2004. MICRO-CHECKER: software for identifying and correcting genotyping errors in microsatellite data. Mol. Ecol. Notes 4, 535–538.
Venczel, M., 2006. Lizards from the late Miocene of Polgárdi (W-Hungary). Nymphaea 33.
Warren, D.L., Glor, R.E., Turelli, M., 2008. Environmental niche equivalency versus conservatism: quantitative approaches to niche ecolution. Evolution 62, 2868–2883.
Warren, D.L., Glor, R.E., Turelli, M., 2010. ENMTools: a toolbox for comparative studies of environmental niche models. Ecography 33, 607–611.
Weir, B.S., Cockerham, C.C., 1984. Estimating F-statistics for the analysis of population-structure. Evolution 38, 1358–1370.
Welter-Schultes, F., 2012. European Non-Marine Molluscs, A Guide for Species Identification. Planet Poster Editions, Göttingen.
Wielstra, B., Crnobrnja-Isailovic, J., Litvinchuk, S., Reijnen, B., Skidmore, A., Sotiropoulos, K., Toxopeus, A., Tzankov, N., Vukov, T., Arntzen, J.W., 2013. Tracing glacial refugia of *Triturus* newts based on mitochondrial DNA phylogeography and species distribution modeling. Front. Zool. 10, 13.
Wilson, G.A., Rannala, B., 2003. Bayesian inference of recent migration rates using multilocus genotypes. Genetics 163, 1177–1191.
Yu, Y., Harris, A.J., He, X., 2013. RASP (Reconstruct Ancestral State in Phylogenies) 2.1 beta. Available at http://mnh.scu.edu.cn/soft/blog/RASP.
Zachos, J., Pagani, M., Sloan, L., Thomas, E., Billups, K., 2001. Trends, rhythms, and aberrations in global climate 65 Ma to present. Science 292, 686–693.
Zelilidis, A., Kontopoulos, N., Avramidis, P., Piper, D.J.W., 1998. Tectonic and sedimentological evolution of the Pliocene-Quaternary basins of Zakynthos island, Greece: case study of the transition from compressional to extensional tectonics. Basin Res. 10, 393–408.
Zinenko, O., Stümpel, N., Mazanaeva, L., Bakiev, A., Shiryaev, K., Pavlov, A., Kotenko, T., Kukushkin, O., Chikin, Y., Duisebayeva, T., Nilson, G., Orlov, N.L., Tuniyev, S., Ananjeva, N.B., Murphy, R.W., Joger, U., 2015. Mitochondrial phylogeny shows multiple independent ecological transitions and northern dispersion despite of Pleistocene glaciations in meadow and steppe vipers (*Vipera ursinii* and *Vipera renardi*). Mol. Phylogenet. Evol. 84, 85–100.

Figure S1. Taxa (individuals/samples) representation of the three clustering threshold datasets (A. 0.85, B. 0.90, and C. 0.95) of the ddRADseq data, before applying the min_taxa filter. It informs about the percentage of loci (y axis) that are present in a specific percentage of samples (x axis).

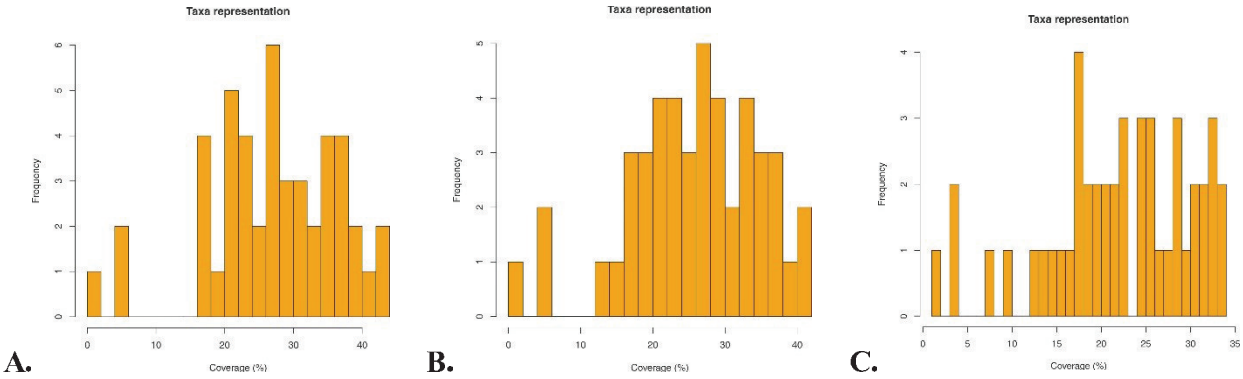

Figure S2. Percentage of taxa (individuals/samples) per locus, gappyness and percentage of variable sites regarding the ddRADseq data before and after applying the following values of orthology clustering threshold and min_taxa=4 filter, respectivelly: **A.** 0.85, **B.** 0.90, and **C** 0.95.

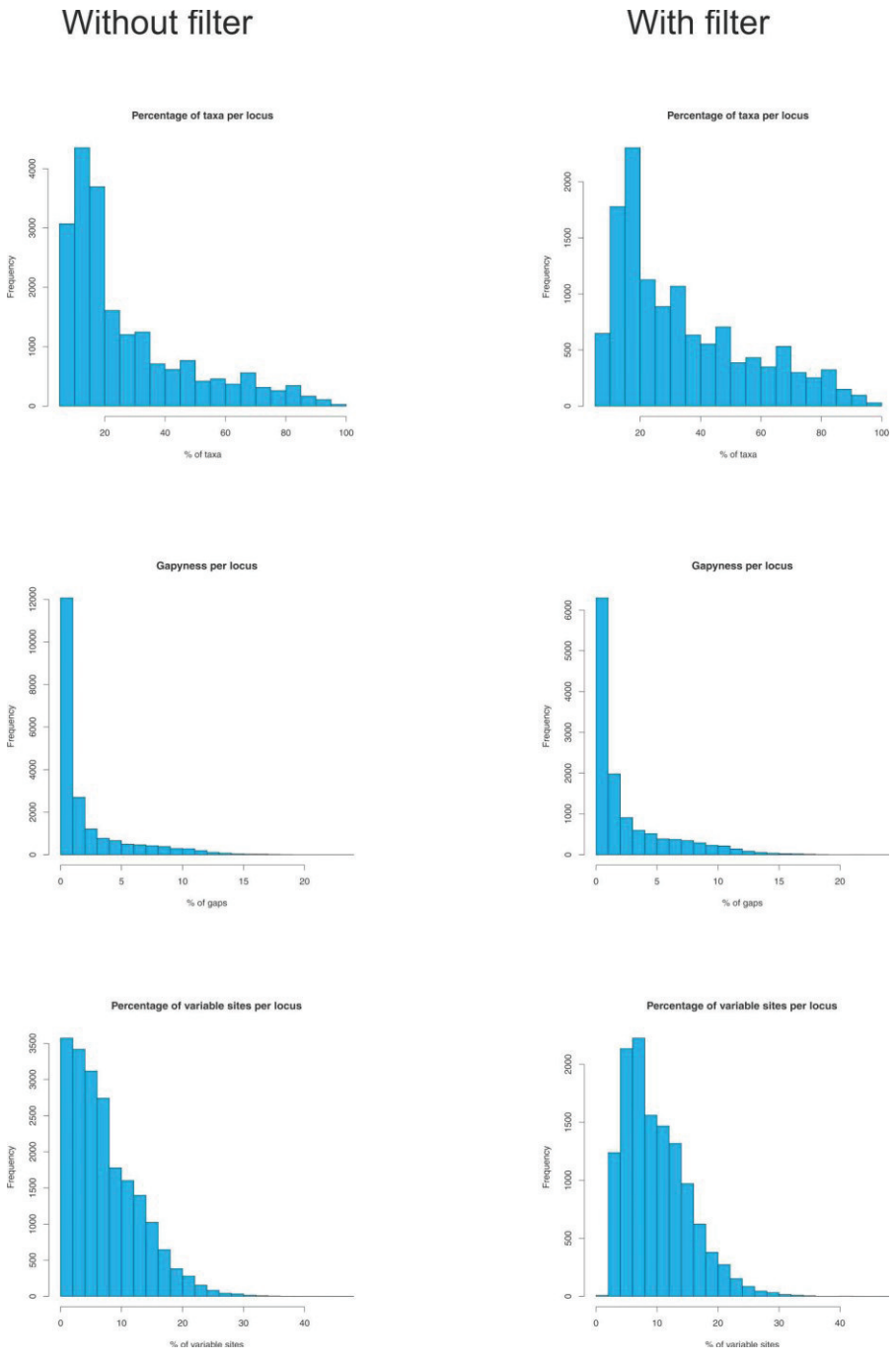

A

Without filter

With filter

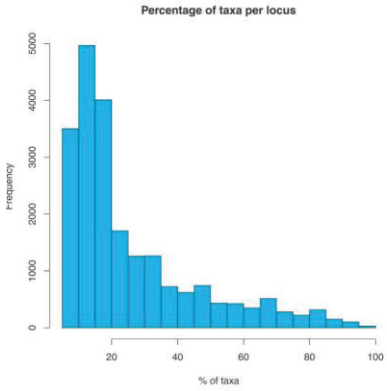

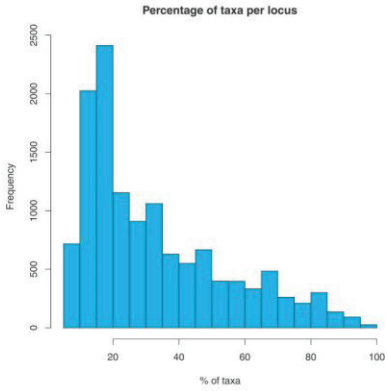

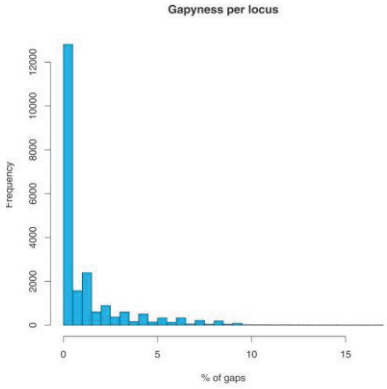

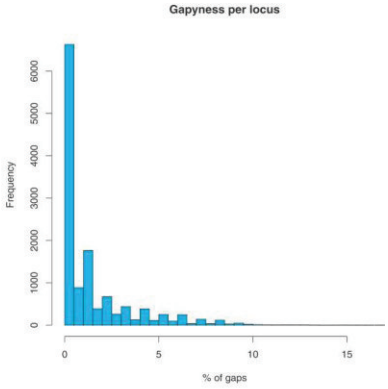

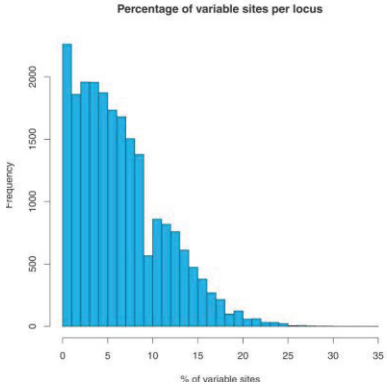

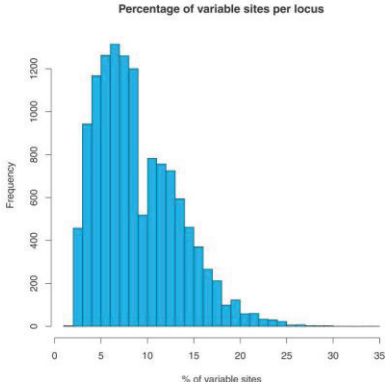

B

Without filter

With filter

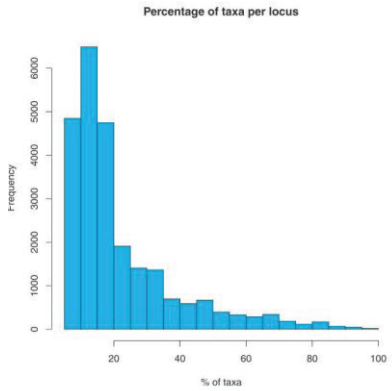

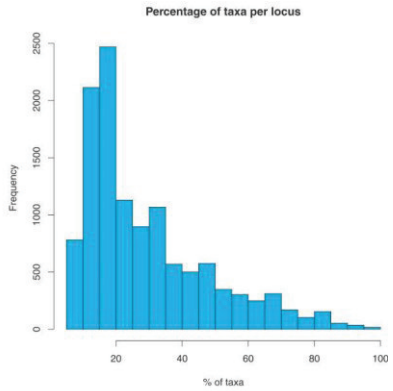

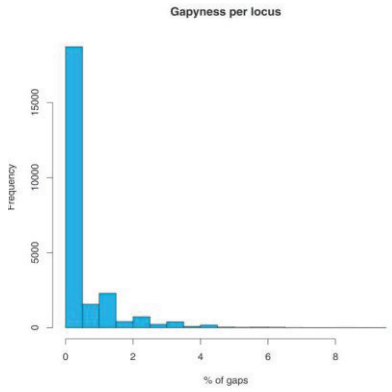

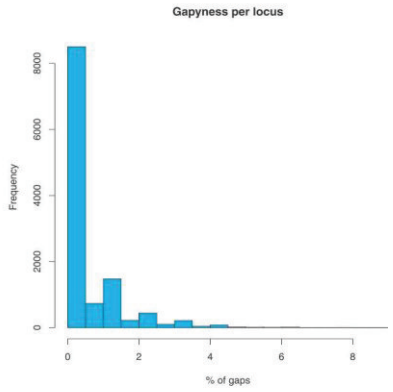

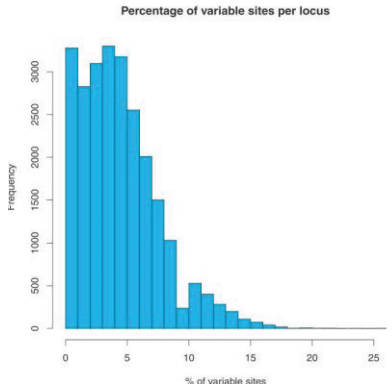

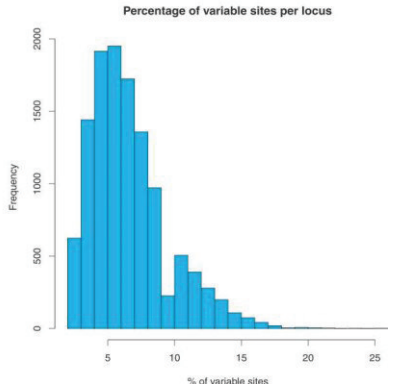

C

Figure S3. Three of the four resulted best ML scoring tree topologies that is the least consistent across datasets (1/12 datasets in each case) regarding the main phylogenetic clades and subclades. The parameters used for clustering threshold and min_taxa filter was A. 0.95 – 4 B. 0.95 – 7 and 0.95 – 9, and C. 0.95 – 11.

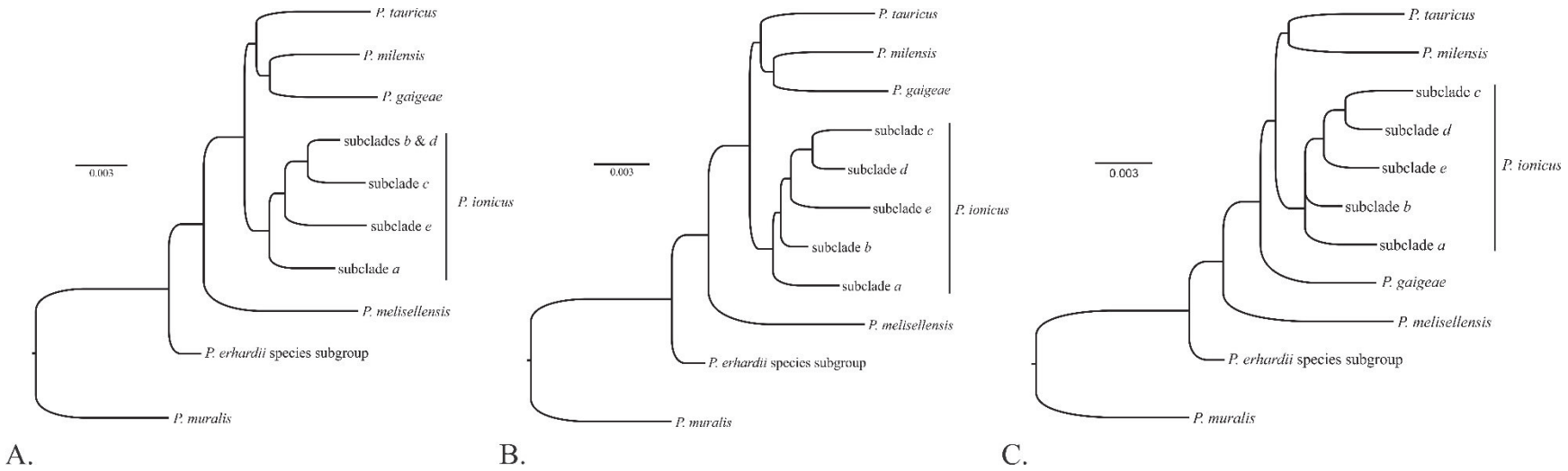

Figure S4. The estimated population structure of the *P. tauricus* species subgroup after four steps of the hierarchical STRUCTURE analysis using microsatellites. Every individual is represented by a thin horizontal line that consist of *K* number of colors. The Q value corresponds to the percentage of estimated assignment of the individual to each one of the *K* clusters. The arrows show the process of this hierarchical approach, in which subgroups of data are analyzed subsequently. The symbols of finger pointer emphasize the clustering position of specific individuals of interest, which are discussed in the text.

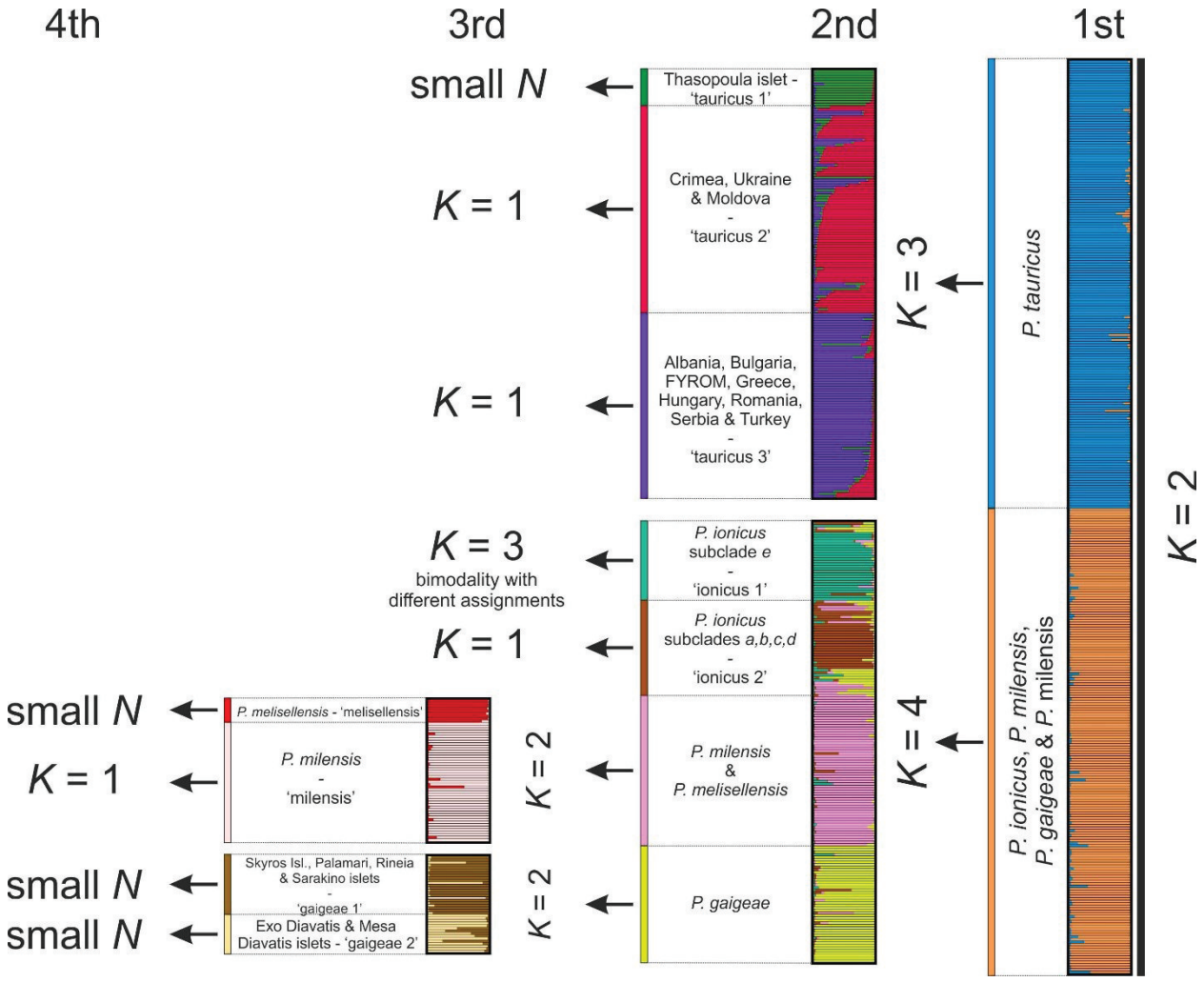

Comment S1. Details regarding the population structure results shown on Figure S1.

S1A: The first step of the hierarchical analysis led to *K*=2; the first cluster ('tauricus') corresponds to *P. tauricus* and the second ('non-tauricus') to the rest of the specimens (*P. ionicus, P. gaigeae, P. milensis,* and *P. melisellensis*). The second step led to *K*=3 for the first cluster and *K*=4 for the second one. Within the tauricus cluster, the three clusters that were revealed (Q>90) correspond to geographically well-defined groups. The first cluster ('tauricus 1') included individuals from Thasopoula islet (North Aegean between Thasos Isl. and Kavala prefecture) and a single specimen from northeastern Greece (Feres, sample code 078), the second cluster ('tauricus 2') consisted of individuals from the Balkans (Albania, Bulgaria, FYROM, Greece, Romania, and Serbia), Hungary, and NW Turkey, and the third cluster ('tauricus 3') comprised individuals from eastern Europe (Crimean Peninsula, Ukraine, and Moldavia). Within the second main cluster (*P. tauricus* species subgroup excluding *P. tauricus*) the four different clusters correspond to: (a) *P. ionicus* ('ionicus 1'), which corresponds to the subclade *e* of Psonis et al. (2017) and present study, (b) *P. ionicus* ('ionicus 2'), which corresponds to the subclade *c* and *d* of Psonis et al. (2017) and the present stud), (c) *P. milensis* and *P. melisellensis* ('milensis and melisellensis') and (d) *P. gaigeae* ('gaigeae'). Subclades *a* and *b* of Psonis et al. (2017) and present study were not identified as separate clusters, with most of their samples grouping into the four aforementioned clusters with Q<90. The third hierarchical STRUCTURE analysis step was applied only to clusters having sufficient number of samples (N>20). All, except three, led to *K*=1. The clusters of 'ionicus 1', 'milensis and melisellensis', and 'gaigeae' showed population substructure with *K*=3, *K*=2, and *K*=2, respectively. The first cluster exhibited multimodality for *K*=3 having different individual assignments with equal probability. The second is subdivided into two clusters corresponding to the two species i.e. *P. melisellensis* ('melisellensis') and *P. milensis* ('milensis'). The third that includes only *P. gaigeae* samples is divided into two clusters containing samples from Skyros Isl. and the islets of Palamari, Rineia, and Sarakino ('gaigeae 1') and from the islets of Exo Diavatis and Mesa Diavatis ('gaigeae 2'), respectively. Finally, the forth STRUCTURE step was conducted only for 'milensis' cluster and resulted in *K*=1.

Figure S5. Microsatellite based DAPC plot using **A.** the first (x axis) and the second (y axis) and **B.** the first (x axis) and the third (y axis) most important discriminant function (DF). The influence of each DF to the observed diversity is shown in the DA eigenvalues diagram. 1: *P. gaigeae*, 2: *P. melisellensis*, 3: *P. milensis*, 4: *P. ionicus* subclade *a*, 5: *P. ionicus* subclade *b*, 6: *P. ionicus* subclade *c*, 7: *P. ionicus* subclade *d*, 8: *P. ionicus* subclade *e*, 9: *P. tauricus*.

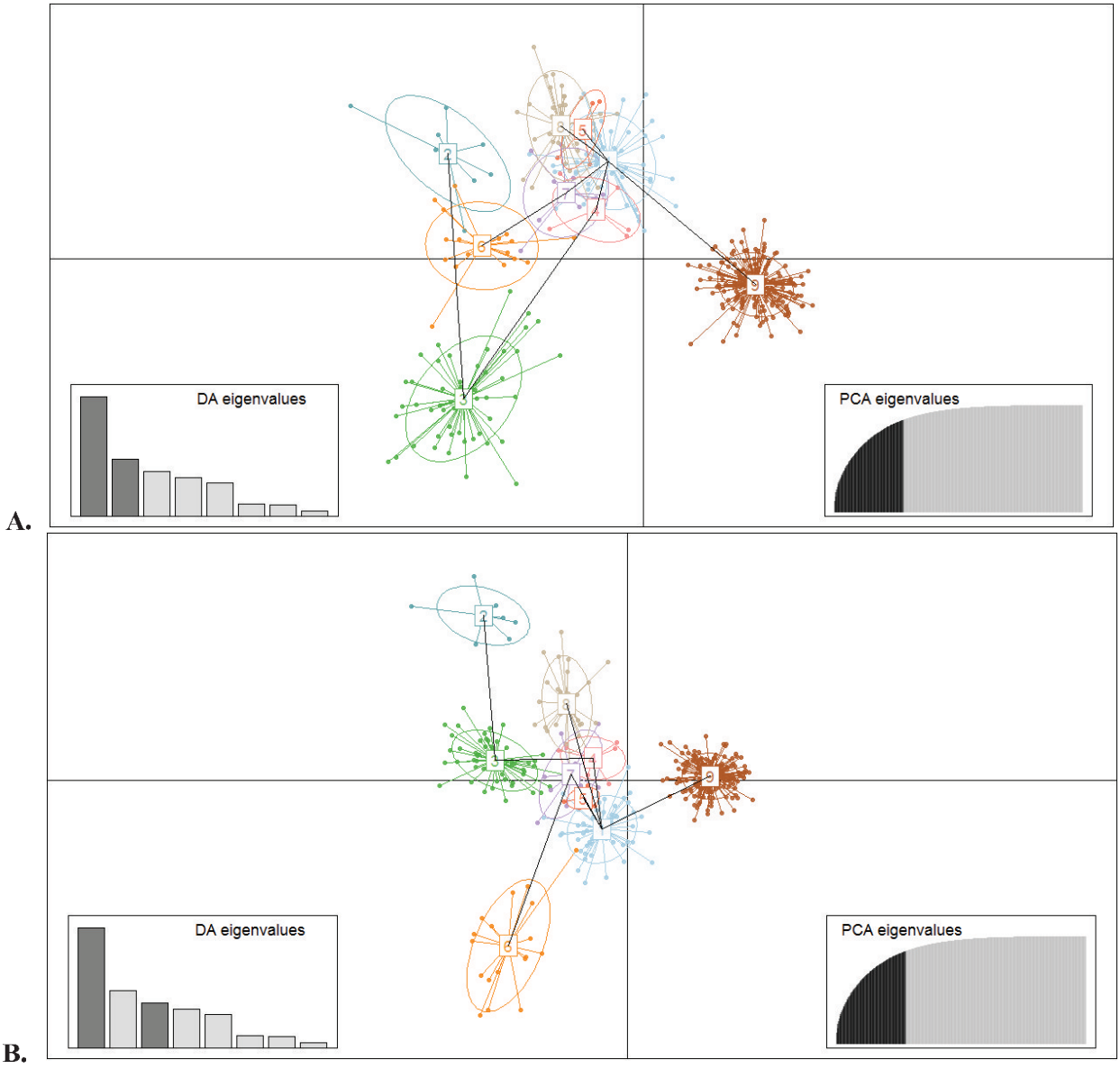

Figure S6. SNP based DAPC plot using **A.** the first (x axis) and the second (y axis) and **B.** the first (x axis) and the third (y axis) most important discriminant function (DF). The influence of each DF to the observed diversity is shown in the DA eigenvalues diagram. 1: *P. gaigeae*, 2: *P. ionicus* subclade *a*, 3: *P. ionicus* subclade *b*, 4: *P. ionicus* subclade *c*, 5: *P. ionicus* subclade *d*, 6: *P. ionicus* subclade *e*, 7: *P. melisellensis*, 8: *P. milensis*, 9: *P. tauricus*.

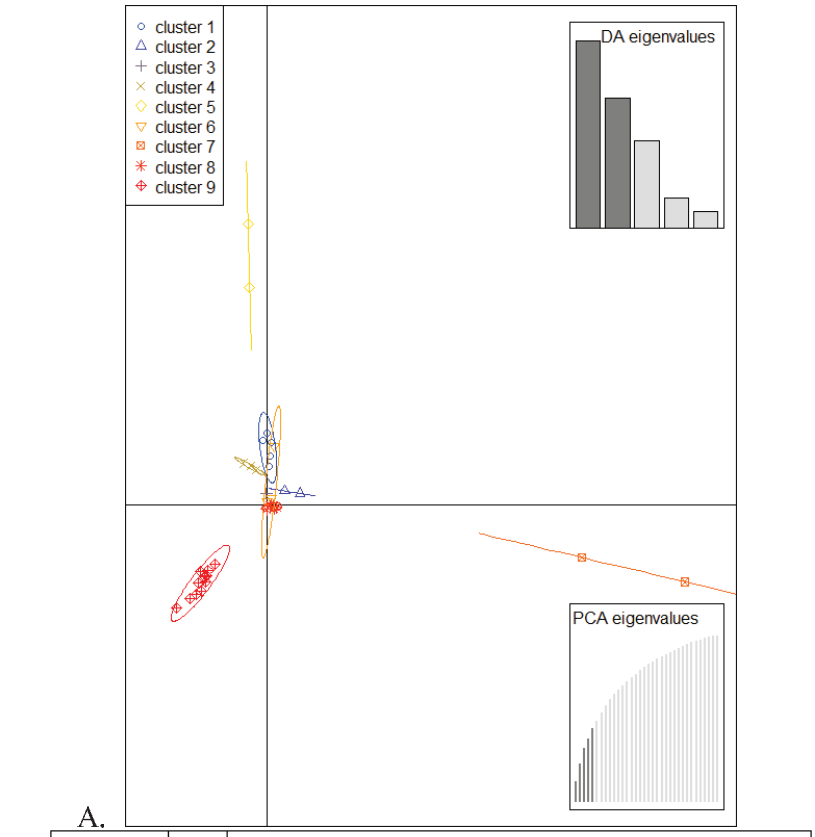

A.

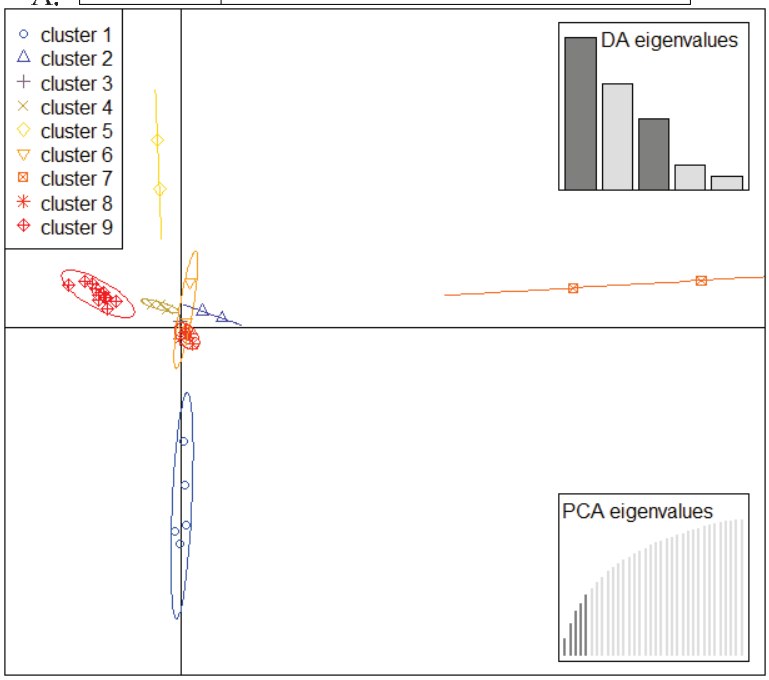

B.

Figure S7. Haplotype network of mtDNA sequences belonging to *P. gaigeae* and their correspondence to the geographic map and the phylogenetic tree inferred by Psonis et al. (2017). In the network, the size of the circle is linked to the haplotype frequency and dark dots indicate nucleotide substitutions. Dots in the phylogenetic tree show high statistical support.

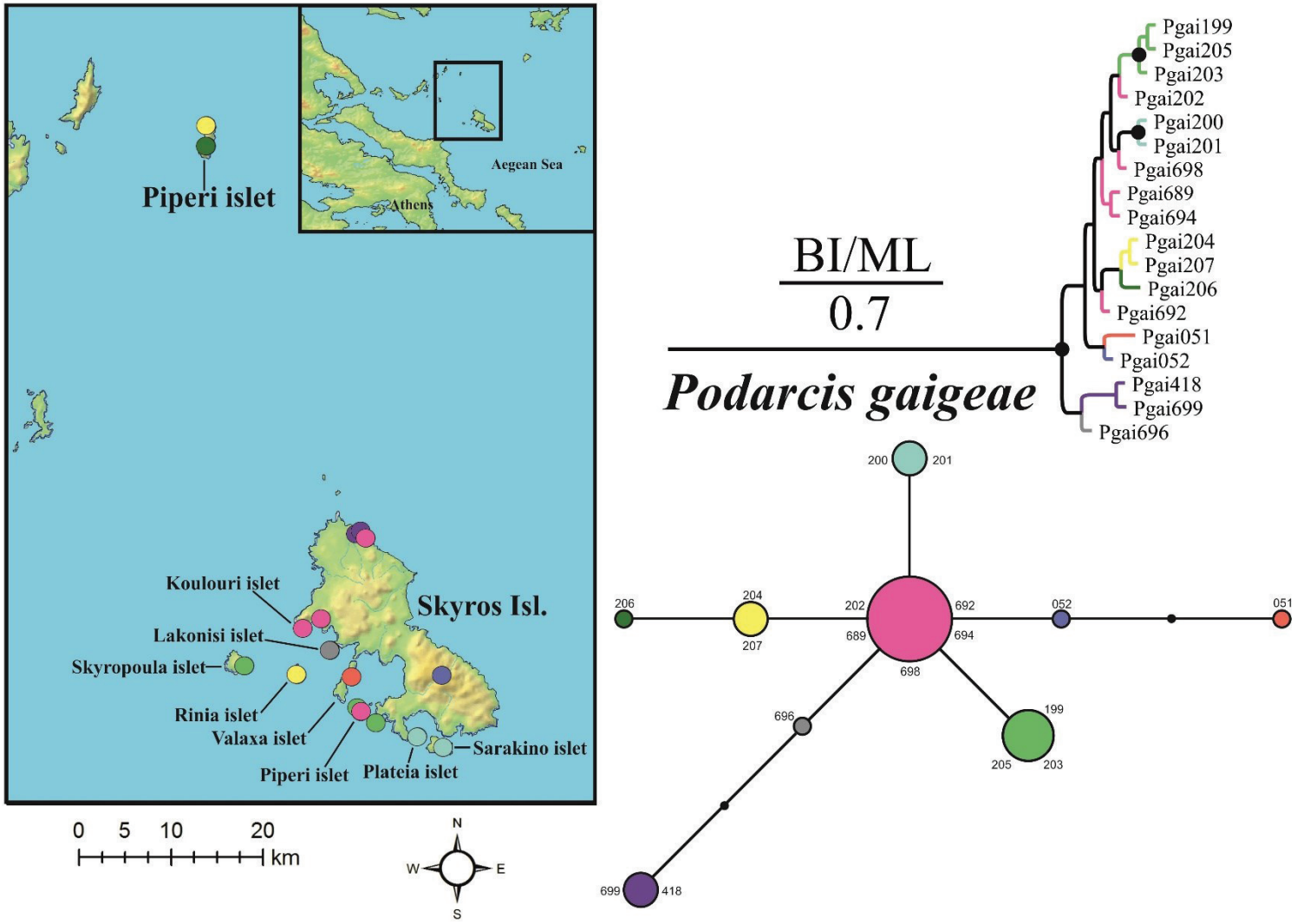

Figure S8. Haplotype network of mtDNA sequences belonging to *P. milensis* and their correspondence to the geographic map and the phylogenetic tree inferred by Psonis et al. (2017). In the network the size of the circle is linked to the haplotype frequency and dark dots indicate nucleotide substitutions. Dots in the phylogenetic tree show high statistical support.

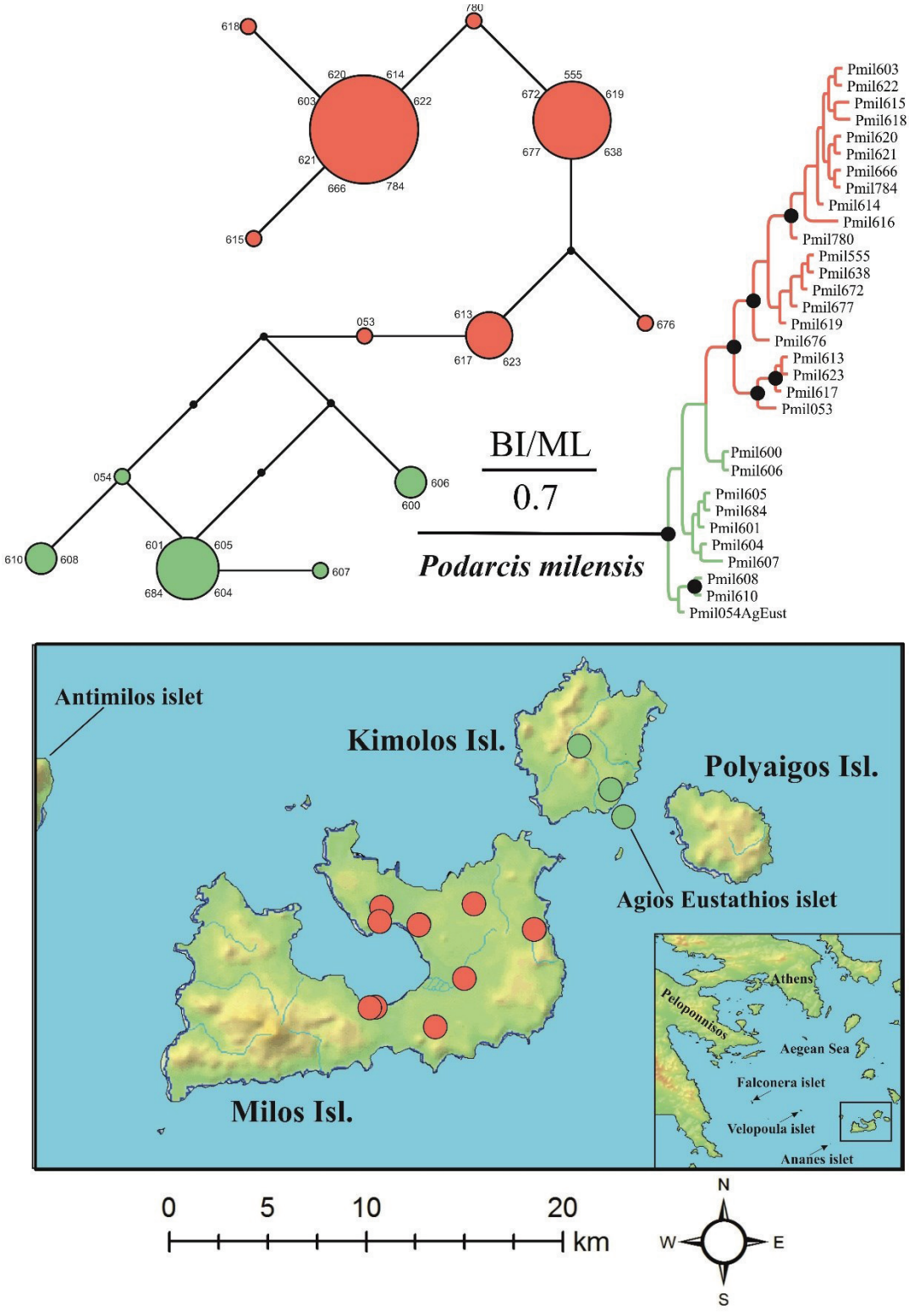

Figure S9. Haplotype network of mtDNA sequences belonging to *P. tauricus* and their correspondence to the geographic map and the phylogenetic tree inferred by Psonis et al. (2017). In the network the size of the circle is linked to the haplotype frequency, except for the two largest (red and dark blue) the size of which has been reduced into half for better display. Dark dots indicate nucleotide substitutions. Dots in the phylogenetic tree show high statistical support.

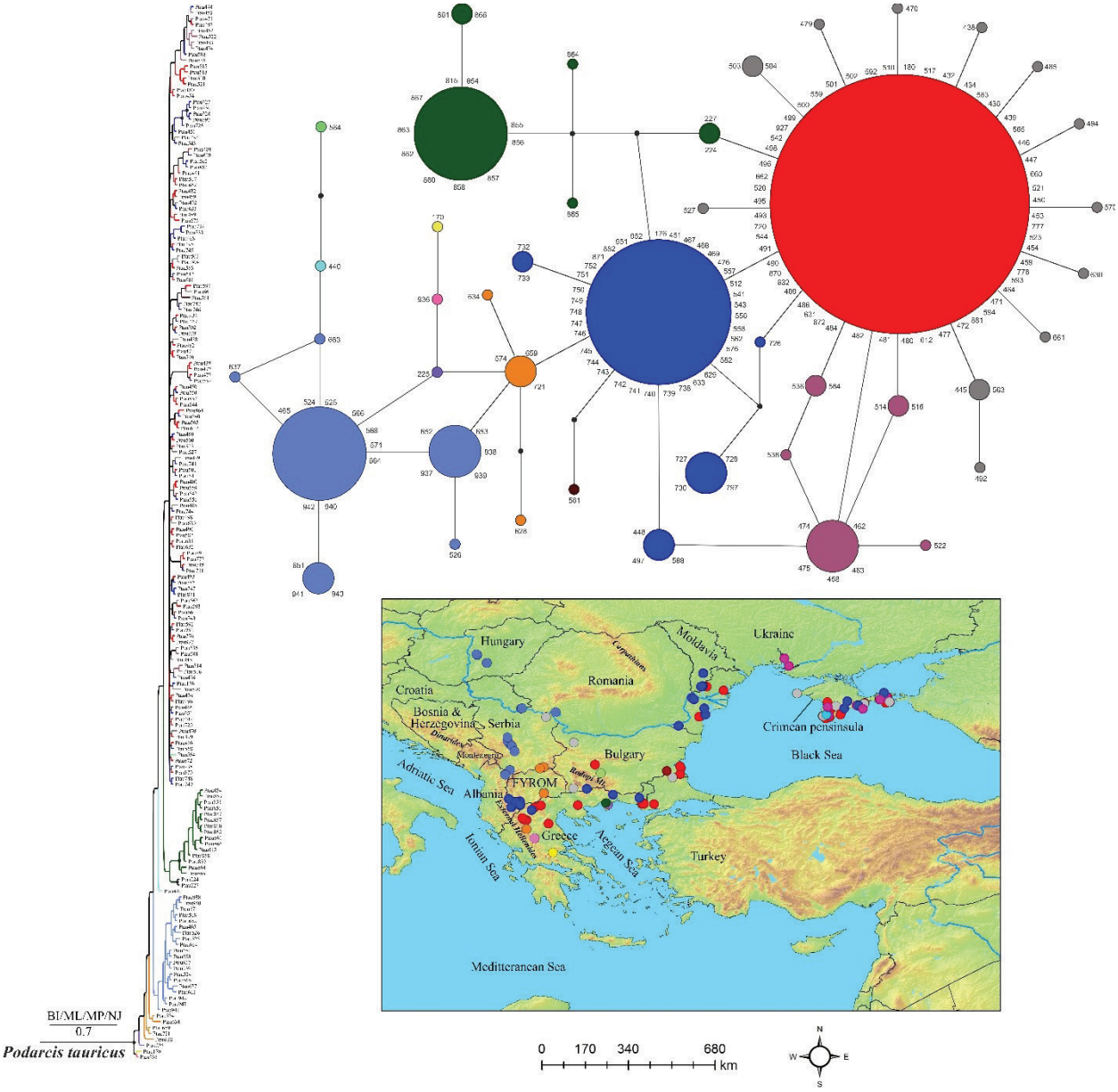

Figure S10. Haplotype network of mtDNA sequences belonging to *P. ionicus* subclades *a* and *b* and their correspondence to the geographic map and the phylogenetic tree inferred by Psonis et al. (2017). In the network the size of the circle is linked to the haplotype frequency and dark dots indicate nucleotide substitutions. Dots in the phylogenetic tree show high statistical support.

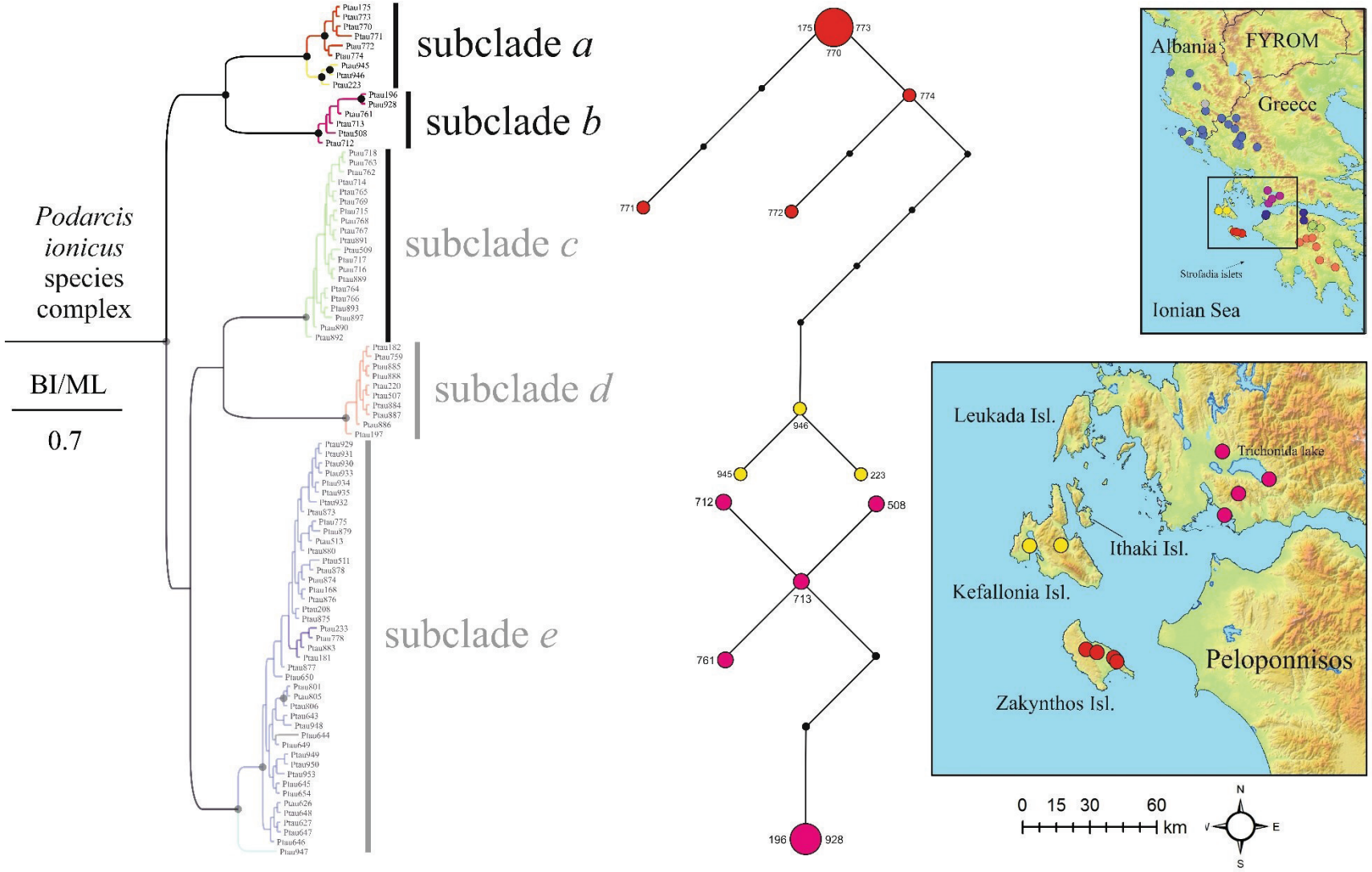

Figure S11. Haplotype network of mtDNA sequences belonging to *P. ionicus* subclades *c* and *d* and their correspondence to the geographic map and the phylogenetic tree inferred by Psonis et al. (2017). In the network the size of the circle is linked to the haplotype frequency and dark dots indicate nucleotide substitutions. Dots in the phylogenetic tree show high statistical support.

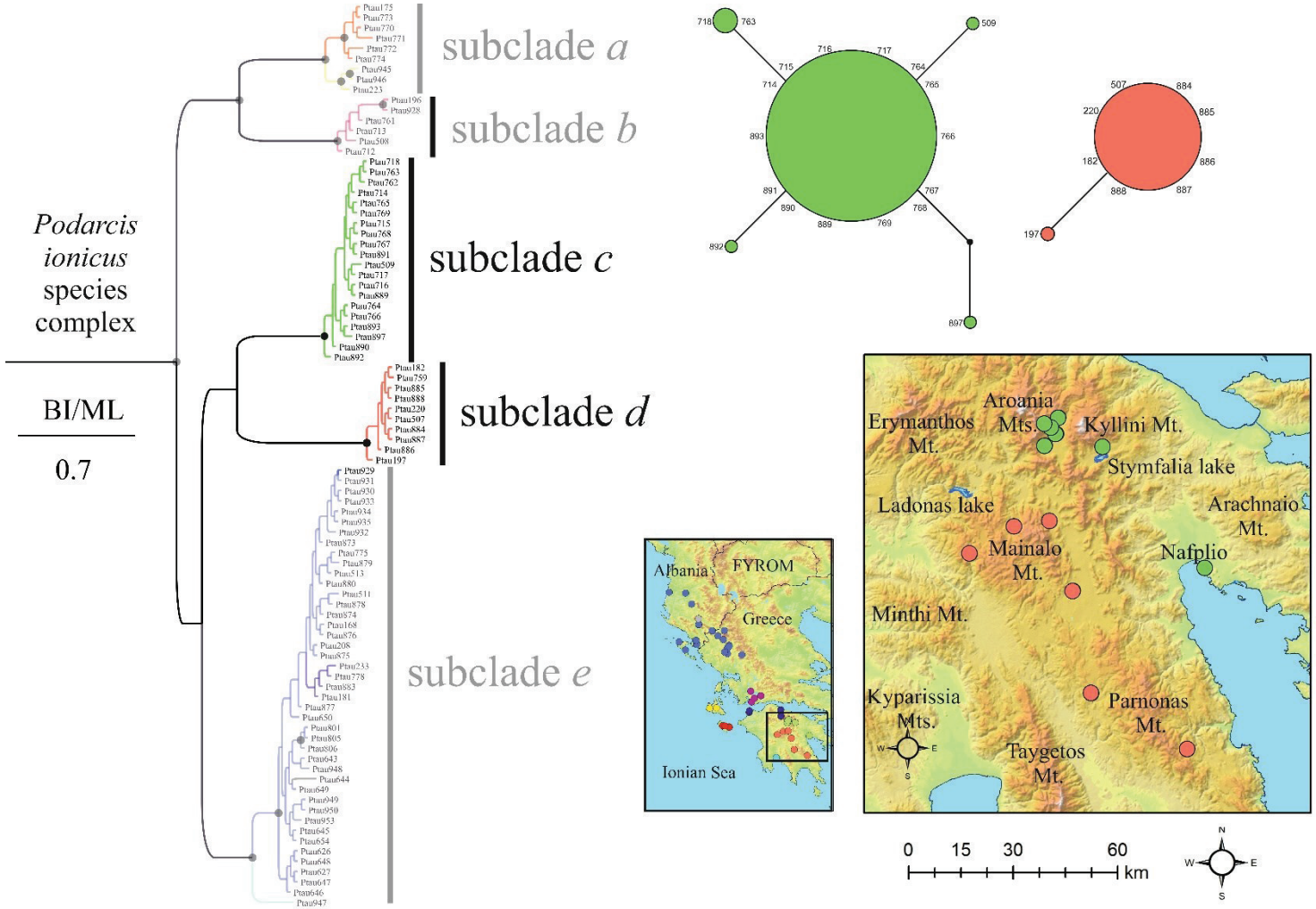

Figure S12. Haplotype network of mtDNA sequences belonging to *P. ionicus* subclade *e* and their correspondence to the geographic map and the phylogenetic tree inferred by Psonis et al. (2017). In the network the size of the circle is linked to the haplotype frequency and dark dots and number indicate nucleotide substitutions. Dots in the phylogenetic tree show high statistical support.

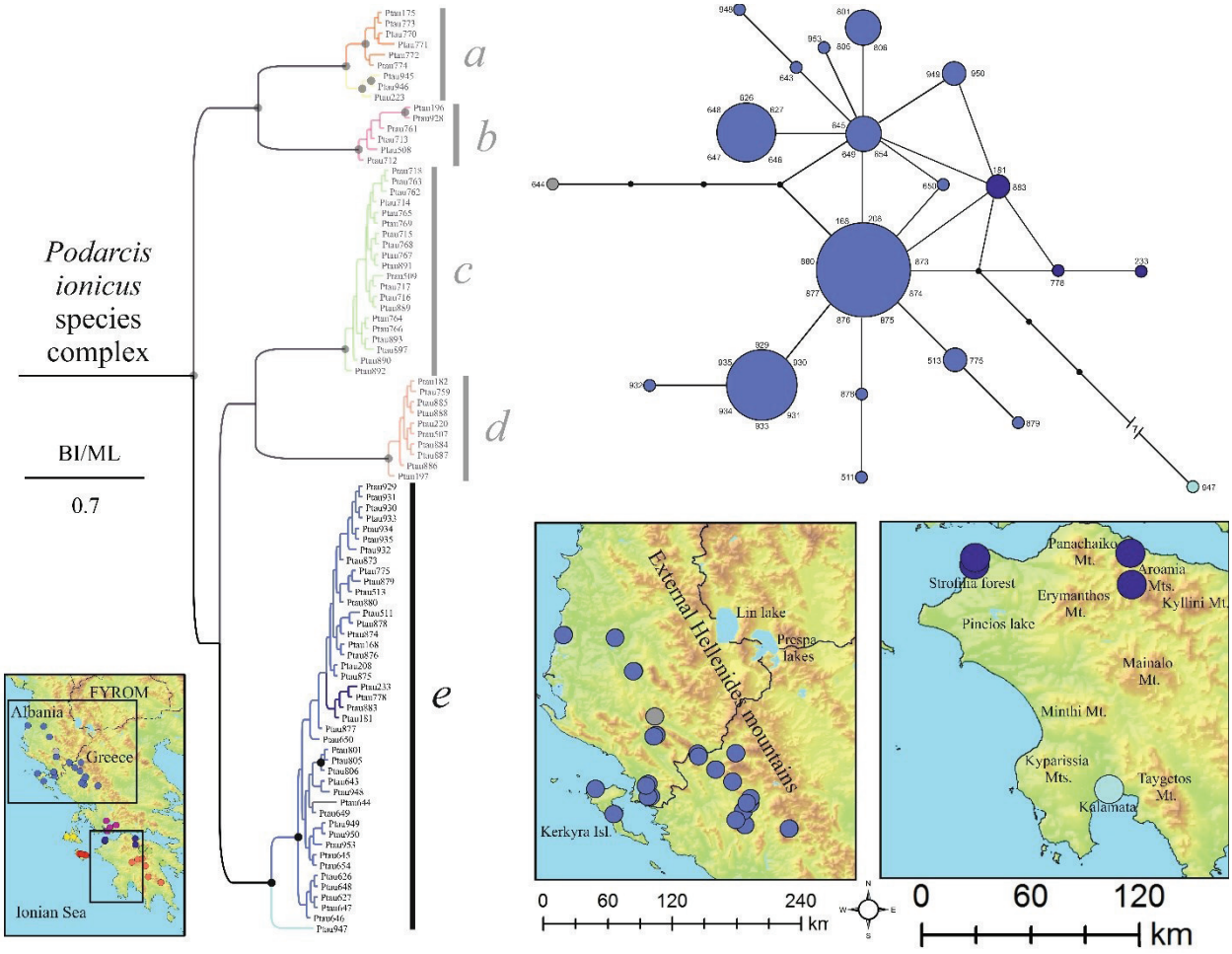

Figure S13. Mismatch distribution analysis for each species of *P. tauricus* subgroup, as well as for each subclade (*a* to *e*) of *P. ionicus* based on mtDNA sequencing data. The continuous line corresponds to the expected values of demographic equilibrium, whereas the dashed line to the observed values.

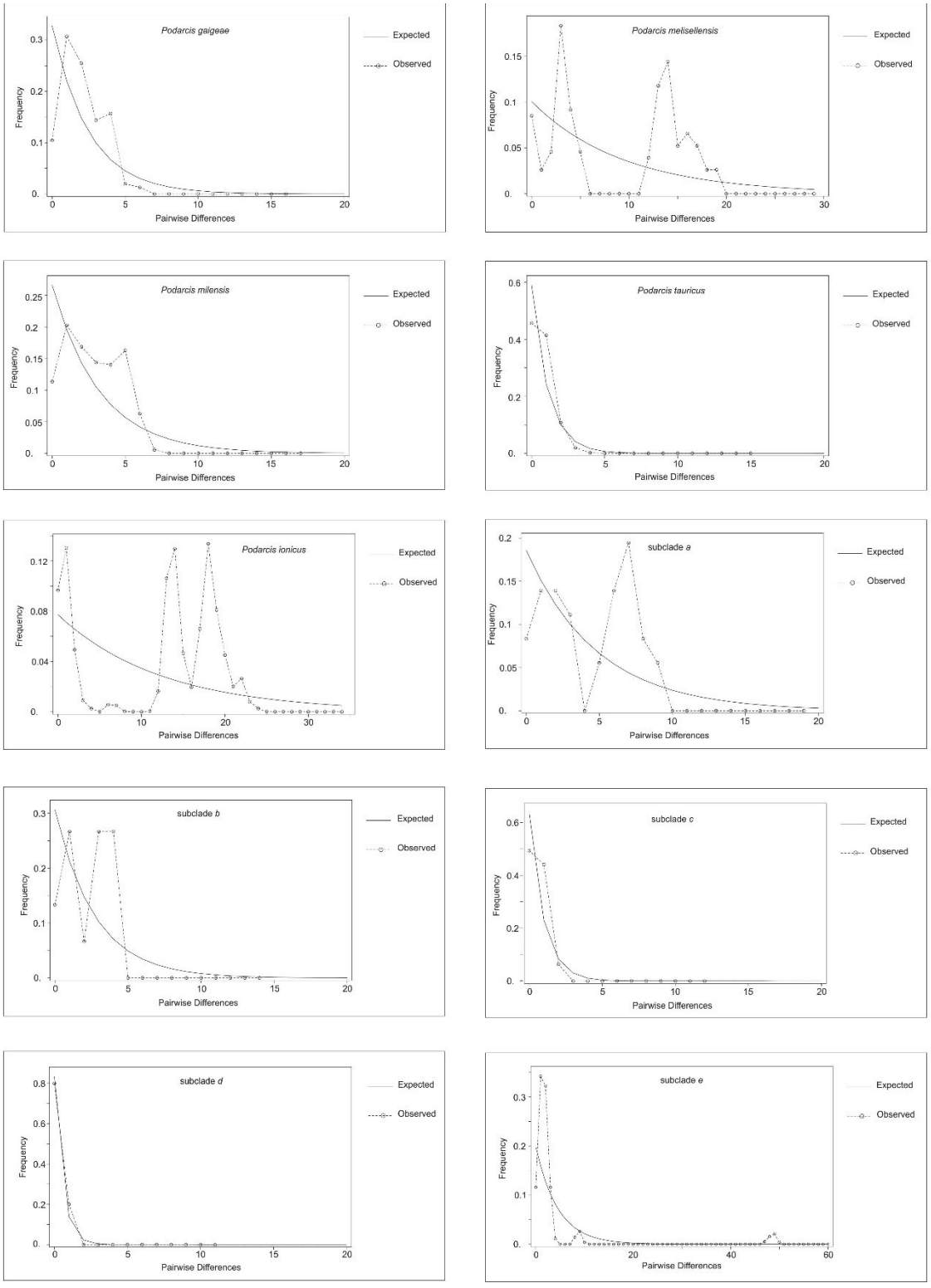

Figure S14. Bayesian Skyline Plots for the focal species of *P. tauricus* subgroup, as well as for the subclades *a*, *c*, and *e* of *P. ionicus* using mtDNA sequencing data. The black line corresponds to the median, whereas the purple to the standard deviation. The analysis for subclades *b* and *d* was not able to be performed due to small sample size and/or low genetic variability.

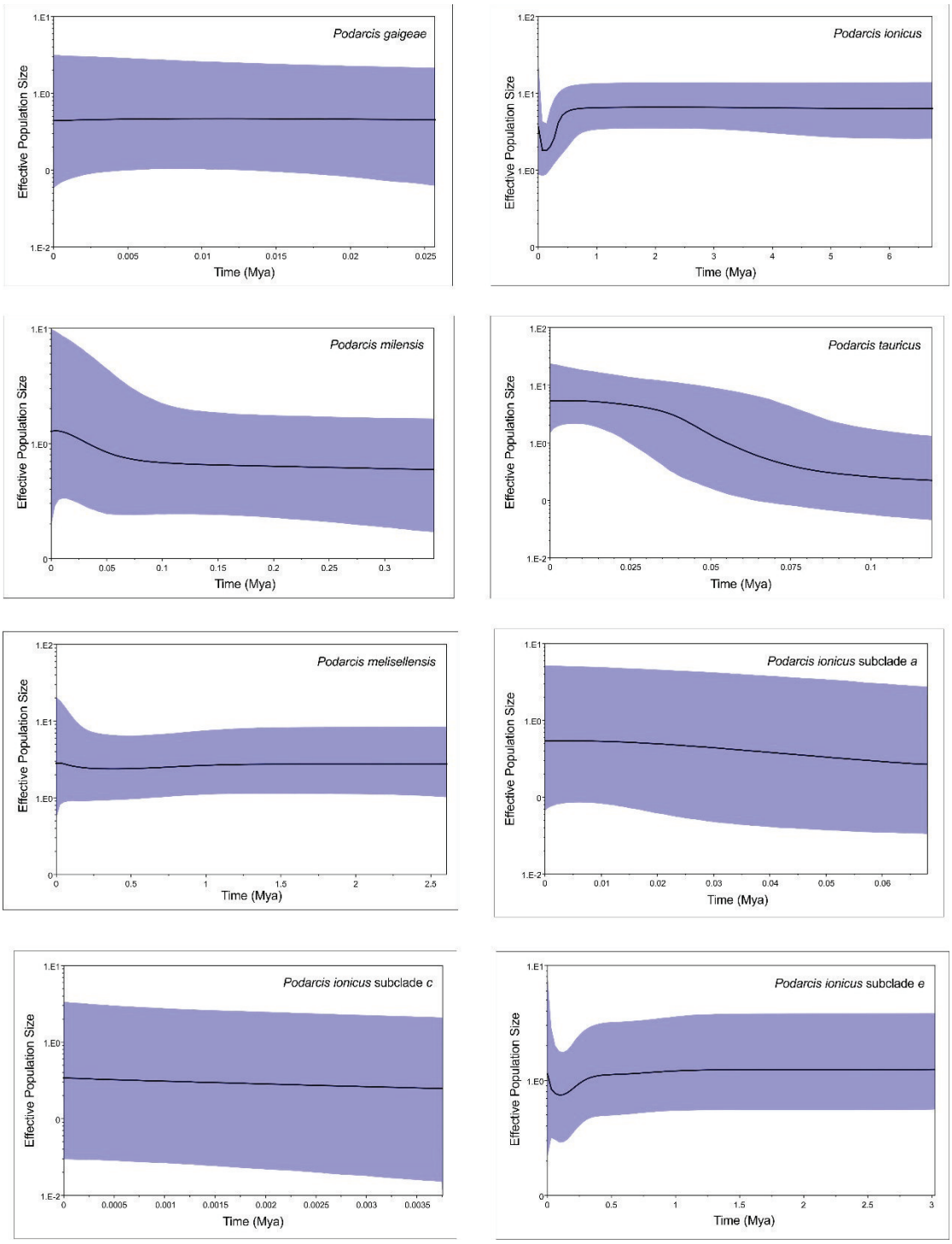

Figure S15. ROC curve and mean AUC calculated value, as well as the result of the Jackknife test of the MaxEnt analysis for A) *P. gaigeae* (AUC=0.999), B) *P. milensis* (AUC=0.999), C) *P. melisellensis* (AUC=0.991), D) *P. tauricus* (AUC=0.991), E) *P. ionicus* (AUC=0.987), F) the entire *P. tauricus* species subgroup (AUC=0.929),

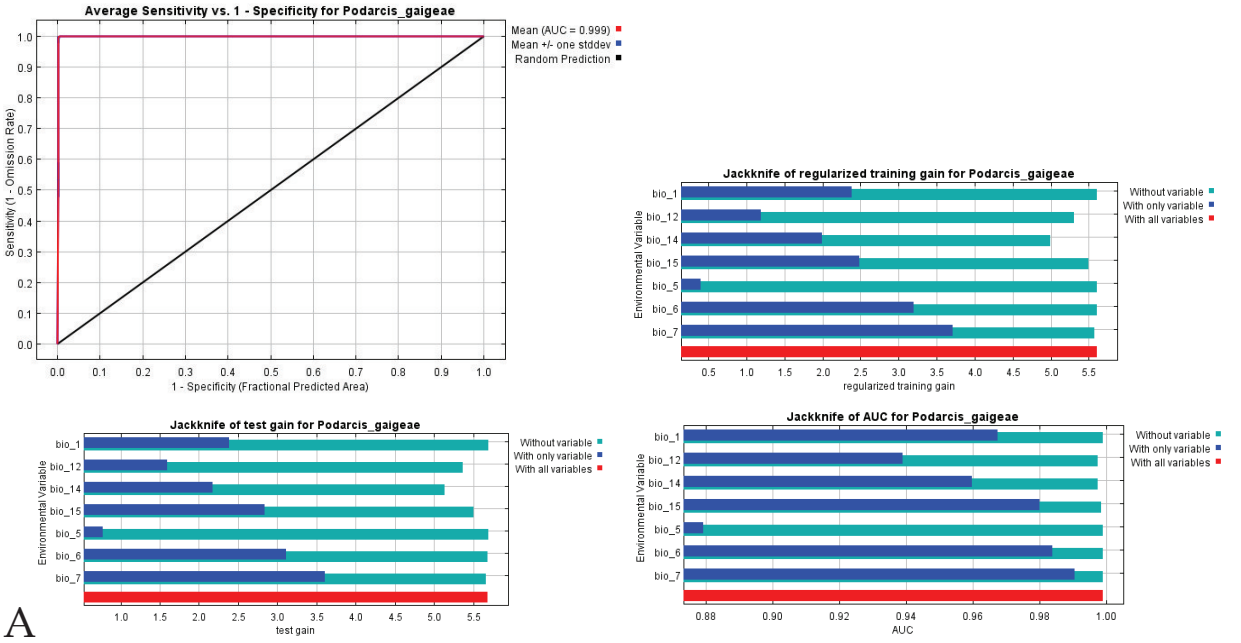

A

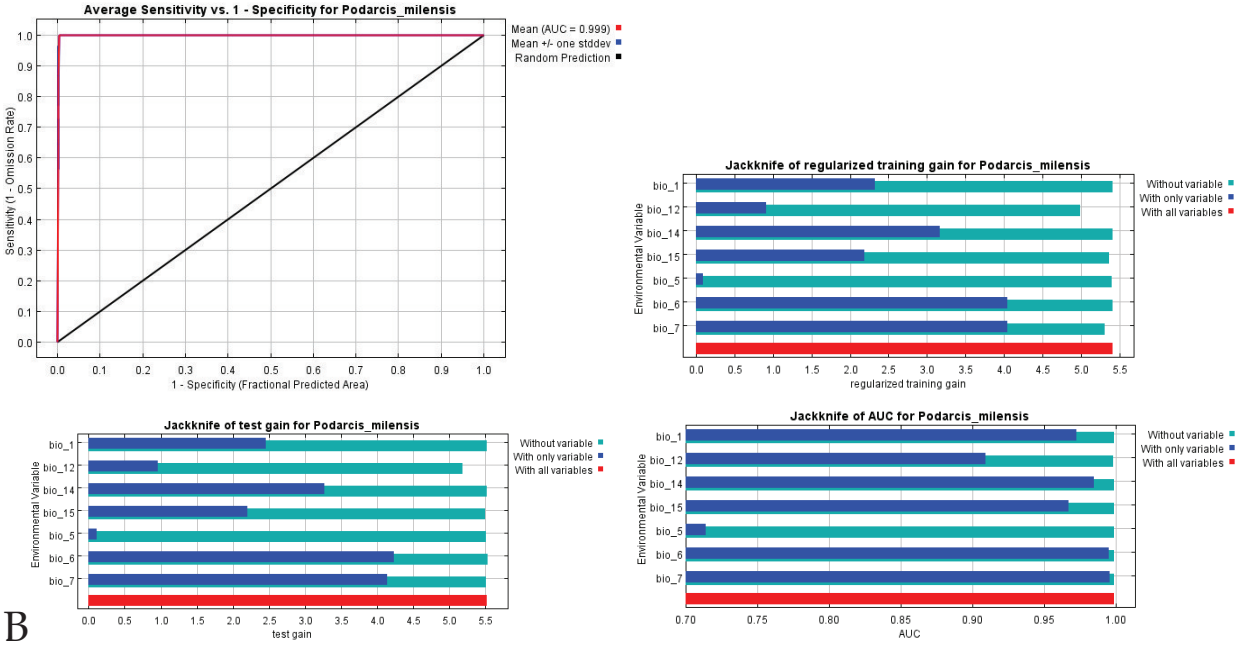

B

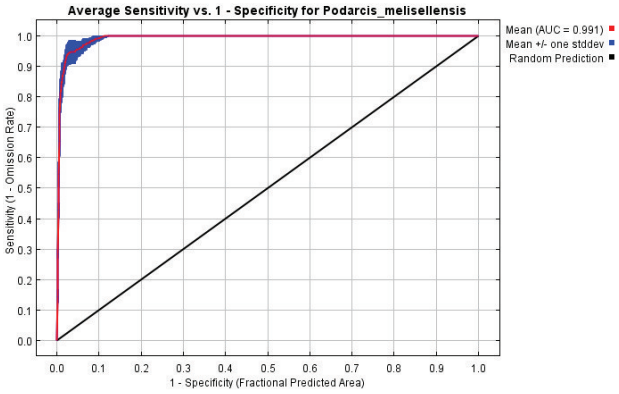
Average Sensitivity vs. 1 - Specificity for Podarcis_melisellensis
Mean (AUC = 0.991)
Mean +/- one stddev
Random Prediction
Sensitivity (1 - Omission Rate)
1 - Specificity (Fractional Predicted Area)

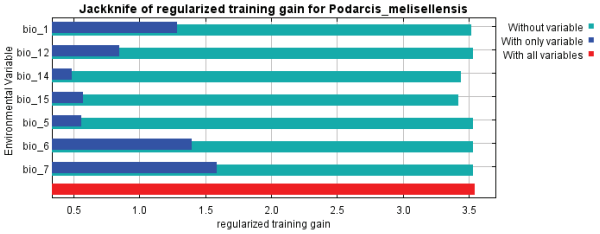
Jackknife of regularized training gain for Podarcis_melisellensis
Without variable
With only variable
With all variables
Environmental Variable
bio_1
bio_12
bio_14
bio_15
bio_5
bio_6
bio_7
regularized training gain

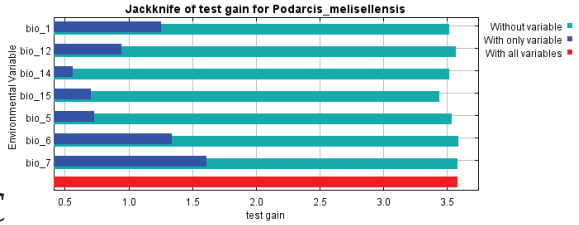
Jackknife of test gain for Podarcis_melisellensis
Without variable
With only variable
With all variables
Environmental Variable
test gain

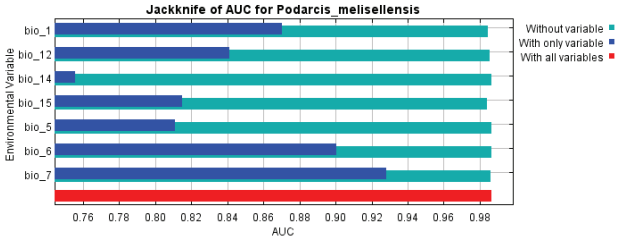
Jackknife of AUC for Podarcis_melisellensis
Without variable
With only variable
With all variables
Environmental Variable
AUC

C

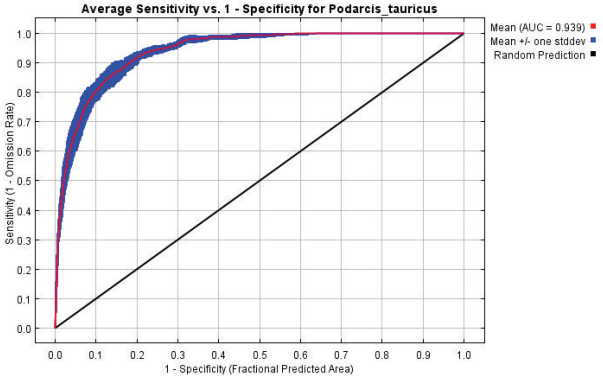
Average Sensitivity vs. 1 - Specificity for Podarcis_tauricus
Mean (AUC = 0.939)
Mean +/- one stddev
Random Prediction
Sensitivity (1 - Omission Rate)
1 - Specificity (Fractional Predicted Area)

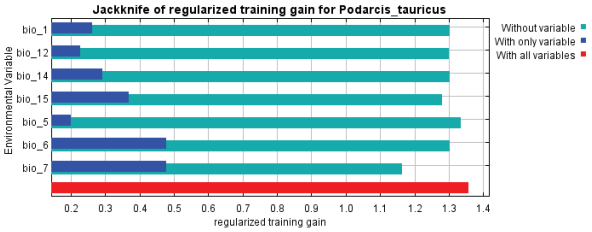
Jackknife of regularized training gain for Podarcis_tauricus
Without variable
With only variable
With all variables
Environmental Variable
regularized training gain

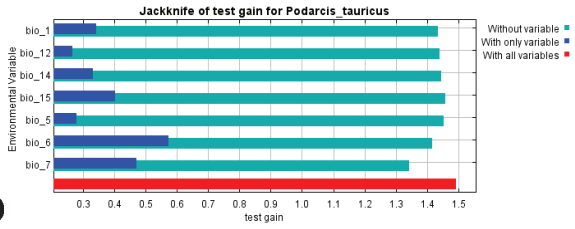
Jackknife of test gain for Podarcis_tauricus
Without variable
With only variable
With all variables
Environmental Variable
test gain

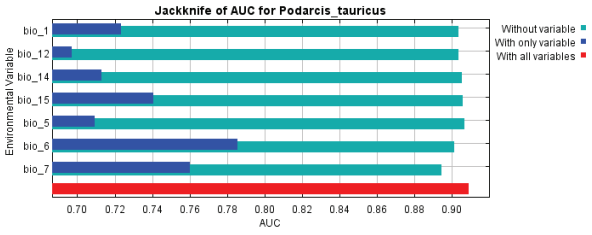
Jackknife of AUC for Podarcis_tauricus
Without variable
With only variable
With all variables
Environmental Variable
AUC

D

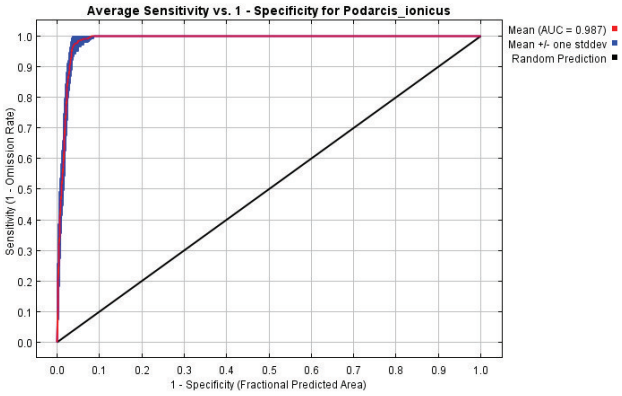
Average Sensitivity vs. 1 - Specificity for Podarcis_ionicus
Mean (AUC = 0.987)
Mean +/- one stddev
Random Prediction
Sensitivity (1 - Omission Rate)
1 - Specificity (Fractional Predicted Area)

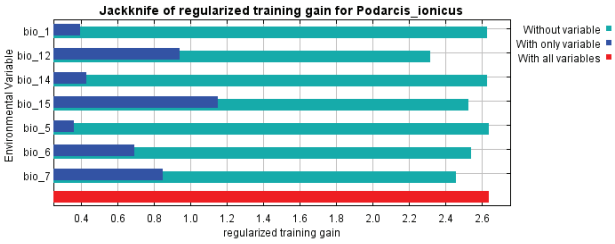
Jackknife of regularized training gain for Podarcis_ionicus
Without variable
With only variable
With all variables
Environmental Variable
bio_1
bio_12
bio_14
bio_15
bio_5
bio_6
bio_7
regularized training gain

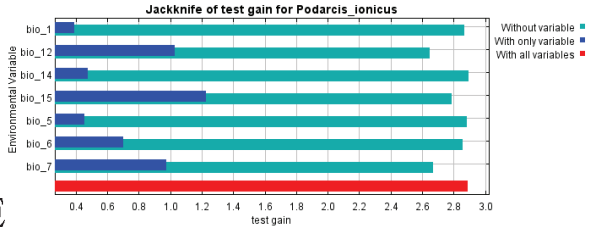
Jackknife of test gain for Podarcis_ionicus
Without variable
With only variable
With all variables
Environmental Variable
test gain

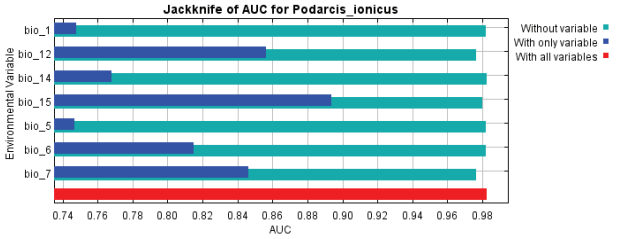
Jackknife of AUC for Podarcis_ionicus
Without variable
With only variable
With all variables
Environmental Variable
AUC

E

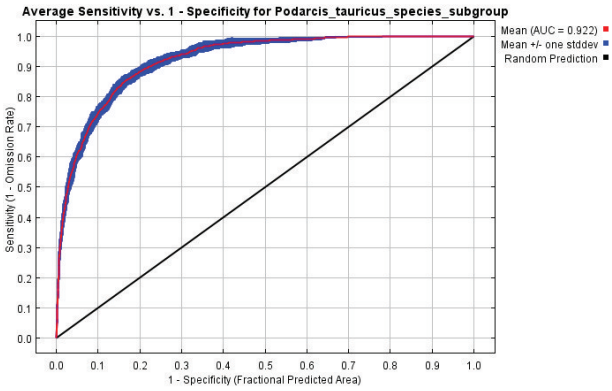
Average Sensitivity vs. 1 - Specificity for Podarcis_tauricus_species_subgroup
Mean (AUC = 0.922)
Mean +/- one stddev
Random Prediction
Sensitivity (1 - Omission Rate)
1 - Specificity (Fractional Predicted Area)

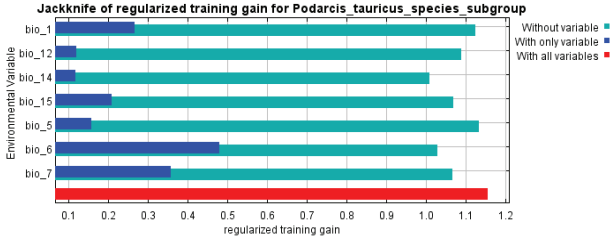
Jackknife of regularized training gain for Podarcis_tauricus_species_subgroup
Without variable
With only variable
With all variables
Environmental Variable
regularized training gain

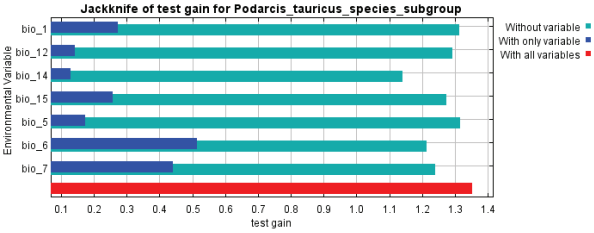
Jackknife of test gain for Podarcis_tauricus_species_subgroup
Without variable
With only variable
With all variables
Environmental Variable
test gain

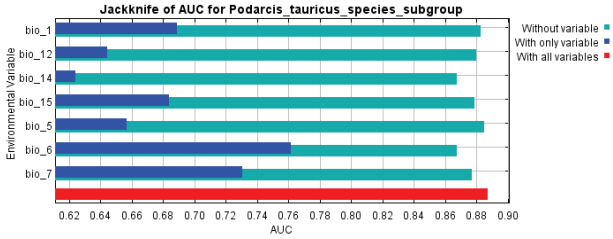
Jackknife of AUC for Podarcis_tauricus_species_subgroup
Without variable
With only variable
With all variables
Environmental Variable
AUC

F

Figure S16. Species distribution modelling using the MaxEnt model for each focal species and for the entire *P. tauricus* species subgroup. The projections correspond to three time periods: Current, Last Glacial Maximum (LGM), and Last Interglacial period (LIG).

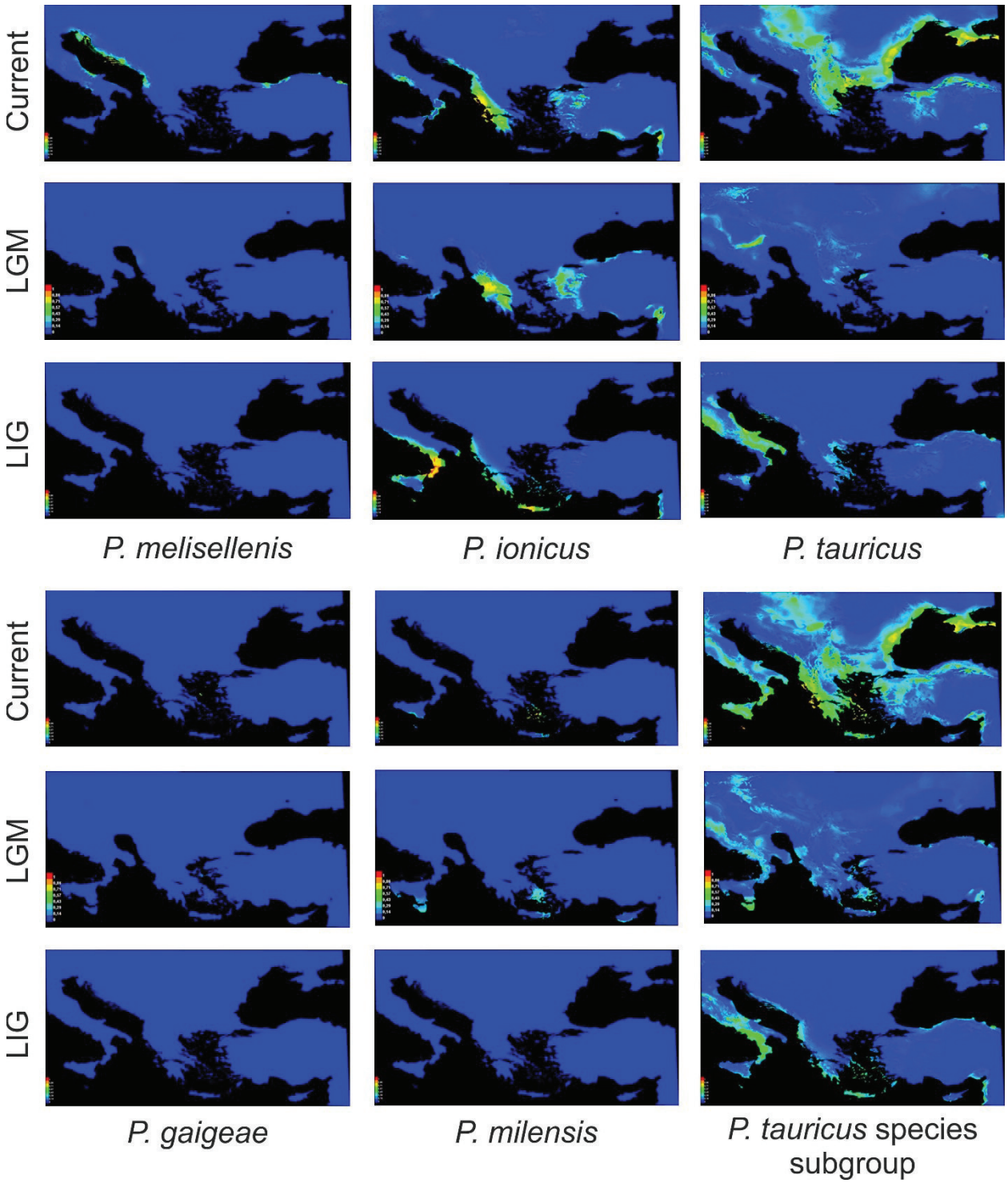

Bibliography

Psonis, N., Antoniou, A., Kukushkin, O., Jablonski, D., Petrov, B., Crnobrnja-Isailović, J., Sotiropoulos, K., Gherghel, I., Lymberakis, P., Poulakakis, N., 2017. Hidden diversity in the *Podarcis tauricus* (Sauria, Lacertidae) species subgroup in the light of multilocus phylogeny and species delimitation. Mol. Phylogenet. Evol. 106, 6-17.

Table S1. Alphabetically ordered by taxon name list of specimens examined in the present study with their corresponding sample codes, taxon names, Natural History Museum of Crete (NHMC) voucher numbers (or isolate codes of NCBI Sanger sequences), country/region/locality names (detailed only where available), reference of the study in which they were used, and accession numbers in GenBank, as well as sample assignment to datasets (I to V) declared by "X". For the samples that do not belong to NHMC there is no sample number, and instead their use (CALIB: calibration in Molecular Dating; DEMO: Demography and/or Haplotype Networks; INDATE: ingroup in Molecular Dating; OUT: outgroup in ddRADseq Phylogeny) in the analyses of the present work is mentioned.

Sample Code	Taxon Name	NHMC Voucher Numbers (or isolate codes of NCBI sequences)	Country – Region – Locality	Study	Sanger / ddRADseq Sequences Accession Numbers (16S rRNA/cyt *b*/MC1R/Pod15b/Pod55)	I. Phylogeny (Sanger data) by Psonis et al. 2017	II. Demography and mtDNA haplotype networks (Sanger data)	III. Molecular Dating (Sanger data)	IV. Microsatellites data	V. ddRADseq data
CALIB	*Gallotia caesaris caesaris*	GagaH1	Spain – Canary Islands – El Hierro Isl.	(Carranza *et al.* 2006) (16S rRNA) / (Carranza *et al.* 2004) (cyt b)	DQ298684 / AY151843 / -			X		
CALIB	*Gallotia caesaris gomerae*	GagaG1	Spain – Canary Islands – La Gomera Isl.	(Carranza *et al.* 2006) (16S rRNA) / (Carranza *et al.* 2004) (cyt b)	DQ298683 / AY151842 / -			X		
CALIB	*Lacerta agilis*	NHMC 80.3.64.3	Greece – Makedonia – Drama	(Sagonas *et al.* 2014)	KJ940218 / KJ940307 / - / - / -	X		X		
CALIB	*Lacerta agilis*	Lagi1	Spain	(Nunes *et al.* 2011)	- / - / JF732966 / - / -	X		X		
CALIB	*Lacerta bilineata*	YCN-1	Italy – Puglia, Noce	(Mayer & Beyerlein 2001)	AF149973 / - / -			X		
CALIB	*Lacerta bilineata*	-	Italy – Melfi, Basilicata	(Brueckner & Duering 2001)	- / AF233419 / -			X		
CALIB	*Lacerta bilineata*	NHMC 80.3.61.26 clone 1	Greece - Ioannina	(Sagonas *et al.* 2014)	KJ940220 / KJ940309 / -			X		
CALIB	*Lacerta strigata*	isolate_3	Georgia	(Godinho *et al.* 2005)	DQ097098 / DQ097091 / -			X		
CALIB	*Lacerta viridis guentherpetersi*	NHMC 80.3.61.1	Greece - Pieria	(Sagonas *et al.* 2014)	KJ940234 / KJ940323 / -			X		
INDATE	*Podarcis bocagei*	Gpb6	Spain – Lugo	(Pinho *et al.* 2006) (16S rRNA) / (Harris & Sá-Sousa 2002) (cyt *b*)	DQ081075 / AF469426 / - / - / -	X		X		
INDATE	*Podarcis bocagei*	Sar1	Spain – Lugo	(Pinho *et al.* 2010) (MC1R) / (Pereira *et al.* 2013) (Pod55 & Pod15b)	- / - / GU180961 / KC681232 / KC681696	X		X		

Sample Code	Taxon Name	NHMC Voucher Numbers (or isolate codes of NCBI sequences)	Country – Region – Locality	Study	Sanger / ddRADseq Sequences Accession Numbers (16S rRNA/cyt *b*/MC1R/Pod15b/Pod55)	I. Phylogeny (Sanger data) by Psonis et al. 2017	II. Demography and mtDNA haplotype networks (Sanger data)	III. Molecular Dating (Sanger data)	IV. Microsatellites data	V. ddRADseq data
INDATE	*Podarcis bocagei*	MP3	Portugal – Porto – Madalena	(Pinho *et al.* 2006) (16S rRNA) / (Harris & Sá-Sousa 2002) (cyt *b*)	DQ081076 / AF469424 / - / - / -	X		X		
INDATE	*Podarcis bocagei*	Vair5	Portugal – Porto – Vairao	(Pinho *et al.* 2010)	- / - / GU180965 / - / -	X		X		
INDATE	*Podarcis bocagei*	3.120	Portugal – Porto – Madalena	(Pereira *et al.* 2013)	- / - / - / KC681228 / KC681693	X		X		
070	*Podarcis cretensis*	NHMC 80.3.51.176	Greece – Crete Isl.– Samaria gorge	(Poulakakis *et al.* 2003) (isolate PE-12; cyt *b*) / (Psonis et al., 2017) (16S rRNA & nDNA markers)	KX658177 / AF486202 / KX658476 / KX658529 / KX658582	X		X		
093	*Podarcis cretensis*	NHMC 80.3.51.327	Greece – Crete Isl. – Koufonisi islet	(Poulakakis *et al.* 2005c) (Pe93 isolate; 16S rRNA) / (Poulakakis *et al.* 2003) (isolate PE-23; cyt *b*) / (Psonis et al., 2017) (nDNA markers)	AY896147 / AF486213 / KX658477 / KX658530 / KX658583	X		X		
824	*Podarcis cretensis*	NHMC 80.3.51.2593	Greece – Crete Isl. – Chania prefecture – Gramvousa	Present Study	ddRADseq: TBP					X
956	*Podarcis cretensis*	NHMC 80.3.51.2491	Greece – Crete Isl. – Lasithi prefecture – Chrysi islet	Present Study	ddRADseq: TBP					X
015	*Podarcis erhardii*	NHMC 80.3.51.583	Greece – Sarantaporos	(Poulakakis *et al.* 2005c) (Pe15 isolate; mtDNA markers) / (Psonis et al., 2017) (nDNA markers)	AY896198 / AY896062 / KX658478 / KX658531 / KX658584	X		X		
636	*Podarcis erhardii*	NHMC 80.3.51.2407	FYROM – Mikri Prespa lake	(Psonis et al., 2017)	KX658178 / KX657876 / KX658479 / KX658532 / KX658585	X		X		
658	*Podarcis erhardii*	NHMC 80.3.51.2462	Serbia – Crnovska River	(Psonis et al., 2017)	KX658179 / KX657877 / KX658480 / KX658533 / KX658586	X		X		

Sample Code	Taxon Name	NHMC Voucher Numbers (or isolate codes of NCBI sequences)	Country – Region – Locality	Study	Sanger / ddRADseq Sequences Accession Numbers (16S rRNA/cyt *b*/MC1R/Pod15b/Pod55)	I. Phylogeny (Sanger data) by Psonis et al. 2017	II. Demography and mtDNA haplotype networks (Sanger data)	III. Molecular Dating (Sanger data)	IV. Microsatellites data	V. ddRADseq data
972	*Podarcis erhardii*	NHMC 80.3.51.2616	Greece – Kyklades island complex – Thira Isl. (Santorini Isl.)	Present Study	ddRADseq: TBP					X
982	*Podarcis erhardii*	NHMC 80.3.51.2637	Greece – Florina prefecture – Prespa lakes	Present Study	ddRADseq: TBP					X
INDATE	*Podarcis filfolensis*	Fil01	Malta – Comino	(Buades *et al.* 2013)	- / JX852112 / - / - / -	X		X		
INDATE	*Podarcis filfolensis*	12_1	Malta – Comino	(Salvi *et al.* 2014)	- / - / KJ027748 / KJ027908 / KJ027961	X		X		
INDATE	*Podarcis filfolensis*	Fil02	Malta – Maltese archipelago	(Rodríguez *et al.* 2013)	- / KF022052 / - / - / -	X		X		
INDATE	*Podarcis filfolensis*	17_2	Malta – Malta Isl. – Balzan	(Salvi *et al.* 2014)	- / - / KJ027769 / KJ027930 / KJ027975	X		X		
051	*Podarcis gaigeae*	NHMC 80.3.56.1	Greece – Sporades, Skyros Isl. – Valaxa islet	(Poulakakis *et al.* 2005c) (16S rRNA) / (Poulakakis *et al.* 2005b) (cyt *b*) / (Psonis et al., 2017) (nDNA markers)	AY768739 / AY768775/ KX658481 / KX658534 / KX658587	X	X	X	X	
052	*Podarcis gaigeae*	NHMC 80.3.56.34	Greece – Sporades, Skyros Isl. – Kochylas Mt.	(Poulakakis *et al.* 2005c) (16S rRNA) / (Poulakakis *et al.* 2005b) (cyt *b*)	AY768731 / AY768767 / - / - / -	X	X		X	
1008	*Podarcis gaigeae*	NHMC 80.3.56.118	Greece – Sporades island complex – Skyros Isl. – Palamari	Present Study	ddRADseq: TBP					X
1009	*Podarcis gaigeae*	NHMC 80.3.56.119	Greece – Sporades island complex – Skyros Isl. – Palamari	Present Study	ddRADseq: TBP					X
199	*Podarcis gaigeae*	NHMC 80.3.56.11	Greece – Sporades, Skyros Isl. –	(Poulakakis *et al.* 2005c) (16S rRNA) /	AY76879 / AY768765 / - / - / -	X	X		X	

Sample Code	Taxon Name	NHMC Voucher Numbers (or isolate codes of NCBI sequences)	Country – Region – Locality	Study	Sanger / ddRADseq Sequences Accession Numbers (16S rRNA/cyt *b*/MC1R/Pod15b/Pod55)	I. Phylogeny (Sanger data) by Psonis et al. 2017	II. Demography and mtDNA haplotype networks (Sanger data)	III. Molecular Dating (Sanger data)	IV. Microsatellites data	V. ddRADseq data
200	*Podarcis gaigeae*	NHMC 80.3.56.14	Greece – Sporades, Skyros Isl. – Mesa Diavatis islet – Sarakino islet	(Poulakakis *et al.* 2005b) (cyt *b*) / (Poulakakis *et al.* 2005c) (16S rRNA) / (Poulakakis *et al.* 2005b) (cyt *b*)	AY768737 / AY768773 / - / - / -	X	X		X	
201	*Podarcis gaigeae*	NHMC 80.3.56.15	Greece – Sporades, Skyros Isl. – Plateia islet	(Poulakakis *et al.* 2005c) (16S rRNA) / (Poulakakis *et al.* 2005b) (cyt *b*) / (Psonis et al., 2017) (nDNA markers)	AY768735 / AY768771 / KX658482 / KX658535 / KX658588	X	X	X	X	
202	*Podarcis gaigeae*	NHMC 80.3.56.29	Greece – Sporades, Skyros Isl. – Koulouri islet	(Poulakakis *et al.* 2005c) (16S rRNA) / (Poulakakis *et al.* 2005b) (cyt *b*)	AY768730 / AY768766 / - / - / -	X	X		X	
203	*Podarcis gaigeae*	NHMC 80.3.56.25	Greece – Sporades, Skyros Isl. – Lakonisi islet	(Poulakakis *et al.* 2005c) (16S rRNA) / (Poulakakis *et al.* 2005b) (cyt *b*)	AY768732 / AY768768 / - / - / -	X	X		X	
204	*Podarcis gaigeae*	NHMC 80.3.56.16	Greece – Sporades, Skyros Isl. – Rineia islet	(Poulakakis *et al.* 2005c) (16S rRNA) / (Poulakakis *et al.* 2005b) (cyt *b*)	AY768717 / AY768772 / - / - / -	X	X		X	
205	*Podarcis gaigeae*	NHMC 80.3.56.22	Greece – Sporades, Skyros Isl. – Skyropoula islet	(Poulakakis *et al.* 2005c) (16S rRNA) / (Poulakakis *et al.* 2005b) (cyt *b*)	AY768738 / AY768774 / - / - / -	X	X		X	
411	*Podarcis gaigeae*	NHMC 80.3.56.63	Greece – Sporades island complex – Skyros archipelago – Palamari islet	Present Study					X	
412	*Podarcis gaigeae*	NHMC 80.3.56.64	Greece – Sporades island complex – Skyros archipelago – Palamari islet	Present Study					X	

Sample Code	Taxon Name	NHMC Voucher Numbers (or isolate codes of NCBI sequences)	Country – Region – Locality	Study	Sanger / ddRADseq Sequences Accession Numbers (16S rRNA/cyt *b*/MC1R/Pod15b/Pod55)	I. Phylogeny (Sanger data) by Psonis et al. 2017	II. Demography and mtDNA haplotype networks (Sanger data)	III. Molecular Dating (Sanger data)	IV. Microsatellites data	V. ddRADseq data
413	*Podarcis gaigeae*	NHMC 80.3.56.65	Greece – Sporades island complex – Skyros archipelago – Palamari islet	Present Study					X	
414	*Podarcis gaigeae*	NHMC 80.3.56.66	Greece – Sporades island complex – Skyros archipelago – Palamari islet	Present Study					X	
415	*Podarcis gaigeae*	NHMC 80.3.56.67	Greece – Sporades island complex – Skyros archipelago – Palamari islet	Present Study					X	
416	*Podarcis gaigeae*	NHMC 80.3.56.68	Greece – Sporades island complex – Skyros archipelago – Palamari islet	Present Study					X	
417	*Podarcis gaigeae*	NHMC 80.3.56.69	Greece – Sporades island complex – Skyros archipelago – Palamari islet	Present Study					X	
418	*Podarcis gaigeae*	NHMC 80.3.56.70	Greece – Sporades, Skyros Isl. – Palamari islet	(Psonis et al., 2017)	KX658180 / KX657878 / - / - / -	X	X		X	
419	*Podarcis gaigeae*	NHMC 80.3.56.71	Greece – Sporades, Skyros Isl. – Palamari islet	Present Study					X	

Sample Code	Taxon Name	NHMC Voucher Numbers (or isolate codes of NCBI sequences)	Country – Region – Locality	Study	Sanger / ddRADseq Sequences Accession Numbers (16S rRNA/cyt *b*/MC1R/Pod15b/Pod55)	I. Phylogeny (Sanger data) by Psonis et al. 2017	II. Demography and mtDNA haplotype networks (Sanger data)	III. Molecular Dating (Sanger data)	IV. Microsatellites data	V. ddRADseq data
420	*Podarcis gaigeae*	NHMC 80.3.56.72	Greece – Sporades, Skyros Isl. – Exo Diavatis islet	Present Study					X	
421	*Podarcis gaigeae*	NHMC 80.3.56.73	Greece – Sporades, Skyros Isl. – Exo Diavatis islet	Present Study					X	
422	*Podarcis gaigeae*	NHMC 80.3.56.74	Greece – Sporades, Skyros Isl. – Exo Diavatis islet	Present Study					X	
423	*Podarcis gaigeae*	NHMC 80.3.56.75	Greece – Sporades, Skyros Isl. – Exo Diavatis islet	Present Study					X	
424	*Podarcis gaigeae*	NHMC 80.3.56.76	Greece – Sporades, Skyros Isl. – Exo Diavatis islet	Present Study					Discarded	
425	*Podarcis gaigeae*	NHMC 80.3.56.77	Greece – Sporades, Skyros Isl. – Exo Diavatis islet	Present Study					X	
426	*Podarcis gaigeae*	NHMC 80.3.56.78	Greece – Sporades, Skyros Isl. – Exo Diavatis islet	Present Study					X	
427	*Podarcis gaigeae*	NHMC 80.3.56.79	Greece – Sporades, Skyros Isl. – Exo Diavatis islet	Present Study					X	

Sample Code	Taxon Name	NHMC Voucher Numbers (or isolate codes of NCBI sequences)	Country – Region – Locality	Study	Sanger / ddRADseq Sequences Accession Numbers (16S rRNA/cyt *b*/MC1R/Pod15b/Pod55)	I. Phylogeny (Sanger data) by Psonis et al. 2017	II. Demography and mtDNA haplotype networks (Sanger data)	III. Molecular Dating (Sanger data)	IV. Microsatellites data	V. ddRADseq data
685	*Podarcis gaigeae*	NHMC 80.3.56.80	Greece – Sporades, Skyros Isl. – Exo Diavatis islet	Present Study					X	
686	*Podarcis gaigeae*	NHMC 80.3.56.81	Greece – Sporades, Skyros Isl. – Exo Diavatis islet	Present Study					X	
687	*Podarcis gaigeae*	NHMC 80.3.56.82	Greece – Sporades, Skyros Isl. – Exo Diavatis islet	Present Study					X	
688	*Podarcis gaigeae*	NHMC 80.3.56.83	Greece – Sporades, Skyros Isl. – Exo Diavatis islet	Present Study					X	
689	*Podarcis gaigeae*	NHMC 80.3.56.84	Greece – Sporades, Skyros Isl. – Exo Diavatis islet	(Psonis et al., 2017)	KX658181 / KX657879 / - / - / -	X	X		X	
690	*Podarcis gaigeae*	NHMC 80.3.56.85	Greece – Sporades island complex – Skyros archipelago – Exo Diavatis islet	Present Study					X	
691	*Podarcis gaigeae*	NHMC 80.3.56.86	Greece – Sporades island complex – Skyros archipelago – Exo Diavatis islet	Present Study					Discarded	
692	*Podarcis gaigeae*	NHMC 80.3.56.87	Greece – Sporades –	(Psonis et al., 2017)	KX658182 / KX657880 / - / - / -	X	X		X	

Sample Code	Taxon Name	NHMC Voucher Numbers (or isolate codes of NCBI sequences)	Country – Region – Locality	Study	Sanger / ddRADseq Sequences Accession Numbers (16S rRNA/cyt *b*/MC1R/Pod15b/Pod55)	I. Phylogeny (Sanger data) by Psonis et al. 2017	II. Demography and mtDNA haplotype networks (Sanger data)	III. Molecular Dating (Sanger data)	IV. Microsatellites data	V. ddRADseq data
693	*Podarcis gaigeae*	NHMC 80.3.56.88	Greece – Sporades island complex – Skyros Isl., Agios Fokas, quarry	Present Study					X	
694	*Podarcis gaigeae*	NHMC 80.3.56.89	Greece – Sporades, Skyros Isl. – Exo Diavatis islet	(Psonis et al., 2017)	KX658183 / KX657881 / - / - / -	X	X		X	
695	*Podarcis gaigeae*	NHMC 80.3.56.90	Greece – Sporades, Skyros Isl. – Lakkonisi islet	Present Study					Discarded	
696	*Podarcis gaigeae*	NHMC 80.3.56.91	Greece – Sporades, Skyros Isl. – Lakkonisi islet	(Psonis et al., 2017)	KX658184 / KX657882 / - / - / -	X	X		X	
697	*Podarcis gaigeae*	NHMC 80.3.56.92	Greece – Sporades island complex - Skyros Isl. – Palamari	Present Study					X	
698	*Podarcis gaigeae*	NHMC 80.3.56.93	Greece – Sporades, Skyros Isl. – Palamari	(Psonis et al., 2017)	KX658185 / KX657883 / - / - / -	X	X			
699	*Podarcis gaigeae*	NHMC 80.3.56.94	Greece – Sporades, Skyros Isl. – Palamari	(Psonis et al., 2017)	KX658186 / KX657884 / - / - / -	X	X		X	
700	*Podarcis gaigeae*	NHMC 80.3.56.95	Greece – Sporades, Skyros Isl. – Palamari	Present Study					Discarded	
701	*Podarcis gaigeae*	NHMC 80.3.56.96	Greece – Sporades	Present Study					X	

Sample Code	Taxon Name	NHMC Voucher Numbers (or isolate codes of NCBI sequences)	Country – Region – Locality	Study	Sanger / ddRADseq Sequences Accession Numbers (16S rRNA/cyt *b*/MC1R/Pod15b/Pod55)	I. Phylogeny (Sanger data) by Psonis et al. 2017	II. Demography and mtDNA haplotype networks (Sanger data)	III. Molecular Dating (Sanger data)	IV. Microsatellites data	V. ddRADseq data
702	*Podarcis gaigeae*	NHMC 80.3.56.97	Greece – Sporades island complex - Skyros Isl. – Palamari	Present Study					X	
703	*Podarcis gaigeae*	NHMC 80.3.56.98	Greece – Sporades island complex - Skyros Isl. – Palamari	Present Study					X	
704	*Podarcis gaigeae*	NHMC 80.3.56.99	Greece – Sporades island complex - Skyros Isl. – Palamari	Present Study					Discarded	
705	*Podarcis gaigeae*	NHMC 80.3.56.100	Greece – Sporades island complex - Skyros Isl. – Palamari	Present Study					Discarded	
706	*Podarcis gaigeae*	NHMC 80.3.56.101	Greece – Sporades island complex - Skyros Isl. – Palamari	Present Study					Discarded	
707	*Podarcis gaigeae*	NHMC 80.3.56.102	Greece – Sporades island complex - Skyros archipelago – Skyropoula islet	Present Study					X	
708	*Podarcis gaigeae*	NHMC 80.3.56.103	Greece – Sporades island complex	Present Study					X	

Sample Code	Taxon Name	NHMC Voucher Numbers (or isolate codes of NCBI sequences)	Country – Region – Locality	Study	Sanger / ddRADseq Sequences Accession Numbers (16S rRNA/cyt *b*/MC1R/Pod15b/Pod55)	I. Phylogeny (Sanger data) by Psonis et al. 2017	II. Demography and mtDNA haplotype networks (Sanger data)	III. Molecular Dating (Sanger data)	IV. Microsatellites data	V. ddRADseq data
709	*Podarcis gaigeae*	NHMC 80.3.56.104	Greece – Sporades island complex - Skyros Isl. – Kareflou – Skyros archipelago – Mesa Diavatis islet	Present Study					Discarded	
710	*Podarcis gaigeae*	NHMC 80.3.56.106	Greece – Sporades island complex – Skyros archipelago – Mesa Diavatis islet	Present Study	ddRADseq: TBP					X
711	*Podarcis gaigeae*	NHMC 80.3.56.107	Greece – Sporades island complex – Skyros archipelago – Mesa Diavatis islet	Present Study	ddRADseq: TBP					X
789	*Podarcis gaigeae*	NHMC 80.3.56.108	Greece – Sporades island complex - Skyros Isl. – Palamari	Present Study					X	
790	*Podarcis gaigeae*	NHMC 80.3.56.109	Greece – Sporades island complex - Skyros Isl. – Palamari	Present Study					X	
791	*Podarcis gaigeae*	NHMC 80.3.56.110	Greece – Sporades island complex - Skyros Isl. – Palamari	Present Study					X	

Sample Code	Taxon Name	NHMC Voucher Numbers (or isolate codes of NCBI sequences)	Country – Region – Locality	Study	Sanger / ddRADseq Sequences Accession Numbers (16S rRNA/cyt *b*/MC1R/Pod15b/Pod55)	I. Phylogeny (Sanger data) by Psonis et al. 2017	II. Demography and mtDNA haplotype networks (Sanger data)	III. Molecular Dating (Sanger data)	IV. Microsatellites data	V. ddRADseq data
792	*Podarcis gaigeae*	NHMC 80.3.56.111	Greece – Sporades island complex - Skyros Isl. – Palamari	Present Study					X	
793	*Podarcis gaigeae*	NHMC 80.3.56.112	Greece – Sporades island complex - Skyros Isl. – Palamari	Present Study					X	
794	*Podarcis gaigeae*	NHMC 80.3.56.113	Greece – Sporades island complex - Skyros Isl. – Palamari	Present Study					X	
795	*Podarcis gaigeae*	NHMC 80.3.56.114	Greece – Sporades island complex - Skyros Isl. – Palamari	Present Study					X	
796	*Podarcis gaigeae*	NHMC 80.3.56.115	Greece – Sporades island complex - Skyros Isl. – Palamari	Present Study					X	
810	*Podarcis gaigeae*	NHMC 80.3.56.120	Greece – Sporades island complex – Skyros archipelago – Mesa Diavatis islet	Present Study	ddRADseq: TBP					X
206	*Podarcis gaigeae*	NHMC 80.3.56.37	Greece – Sporades – Piperi islet	(Poulakakis *et al.* 2005c) (16S rRNA) / (Poulakakis *et al.* 2005b) (cyt *b*) / (Psonis et al., 2017) (nDNA markers)	AY768733 / AY768769 / KX658483 / KX658536 / KX658589	X	X	X	X	

Sample Code	Taxon Name	NHMC Voucher Numbers (or isolate codes of NCBI sequences)	Country – Region – Locality	Study	Sanger / ddRADseq Sequences Accession Numbers (16S rRNA/cyt *b*/MC1R/Pod15b/Pod55)	I. Phylogeny (Sanger data) by Psonis et al. 2017	II. Demography and mtDNA haplotype networks (Sanger data)	III. Molecular Dating (Sanger data)	IV. Microsatellites data	V. ddRADseq data
207	*Podarcis gaigeae*	NHMC 80.3.56.38	Greece – Sporades – Piperi islet	(Poulakakis *et al.* 2005c) (16S rRNA) / (Poulakakis *et al.* 2005b) (cyt *b*)	AY768734 / AY768770 / - / - / -	X	X		X	
168	*Podarcis ionicus*	NHMC 80.3.50.22	Greece – Eptanisa Islands – Kerkyra Isl.	(Poulakakis *et al.* 2005c) (16S rRNA) / (Poulakakis *et al.* 2005b) (cyt *b*)	AY768714 / AY768750 / - / - / -	X	X		X	
175	*Podarcis ionicus*	NHMC 80.3.50.20	Greece – Eptanisa Islands – Zakynthos Isl.	(Poulakakis *et al.* 2005c) (16S rRNA) / (Poulakakis *et al.* 2005b) (cyt *b*)	AY768728 / AY768764 / - / - / -	X	X		X	
181	*Podarcis ionicus*	NHMC 80.3.50.18	Greece – Achaia, Kalavryta	(Poulakakis *et al.* 2005c) (16S rRNA) / (Poulakakis *et al.* 2005b) (cyt *b*)	AY768712 / AY768748 / - / - / -	X	X		X	
182	*Podarcis ionicus*	NHMC 80.3.50.17	Greece – Arkadia, Dimitsana	(Poulakakis *et al.* 2005c) (16S rRNA) / (Poulakakis *et al.* 2005b) (cyt *b*)	AY768708 / AY768744 / - / - / -	X	X		X	
192	*Podarcis ionicus*	NHMC 80.3.50.3	Greece – Eptanisa Islands – Strofades Isls.	Present Study					Discarded	
196	*Podarcis ionicus*	NHMC 80.3.50.15	Greece – Aitoloakarnania, Agrinio	(Poulakakis *et al.* 2005c) (16S rRNA) / (Poulakakis *et al.* 2005b) (cyt b)	AY768706 / AY768742 / - / - / -	X	X		X	
197	*Podarcis ionicus*	NHMC 80.3.50.21	Greece – Arkadia, Vytina	(Poulakakis *et al.* 2005c) (16S rRNA) / (Poulakakis *et al.* 2005b) (cyt *b*)	AY768727 / AY768721 / - / - / -	X	X		X	
208	*Podarcis ionicus*	NHMC 80.3.50.2	Greece – Ioannina, Theriakisi	(Poulakakis *et al.* 2005c) (16S rRNA) / (Poulakakis *et al.* 2005b) (cyt *b*)	AY768726 / AY768762 / - / - / -	X	X		X	
220	*Podarcis ionicus*	NHMC 80.3.50.23	Greece – Arkadia, Levidi	(Poulakakis *et al.* 2005c) (16S rRNA) / (Poulakakis *et al.* 2005b) (cyt *b*)	AY768717 / AY768753 / - / - / -	X	X		X	

Sample Code	Taxon Name	NHMC Voucher Numbers (or isolate codes of NCBI sequences)	Country – Region – Locality	Study	Sanger / ddRADseq Sequences Accession Numbers (16S rRNA/cyt *b*/MC1R/Pod15b/Pod55)	I. Phylogeny (Sanger data) by Psonis et al. 2017	II. Demography and mtDNA haplotype networks (Sanger data)	III. Molecular Dating (Sanger data)	IV. Microsatellites data	V. ddRADseq data
221	*Podarcis ionicus*	NHMC 80.3.50.24	Greece – Korinthia, Stymfalia lake	Present Study					Discarded	
223	*Podarcis ionicus*	NHMC 80.3.50.26	Greece – Ionian Islands – Kefallonia Isl.	(Poulakakis *et al.* 2005c) (16S rRNA) / (Poulakakis *et al.* 2005b) (cyt *b*) / (Psonis et al., 2017) (nDNA markers) / Present Study (ddRADseq data)	AY768713 / AY768749 / KX658504 / KX658557 / KX658610 ddRADseq: TBP	X	X	X	X	X
233	*Podarcis ionicus*	NHMC 80.3.50.1	Greece – Ileia – Strofilia near to Kalogria	(Poulakakis *et al.* 2005b)	AY768721 / AY768757 / - / - / -	X	X		X	
506	*Podarcis ionicus*	NHMC 80.3.50.14	Greece – Korinthia, Chelmos Mt.	Present Study					Discarded	
507	*Podarcis ionicus*	NHMC 80.3.50.40	Greece – Arkadia – Tripoli	(Psonis et al., 2017)	KX658283 / KX657979 / - / - / -	X	X		X	
508	*Podarcis ionicus*	NHMC 80.3.50.42	Greece – Aitoloakarnania – Messologi, 2/39 Syntagma Evzonon	(Psonis et al., 2017)	KX658284 / KX657980 / - / - / -	X	X		X	
509	*Podarcis ionicus*	NHMC 80.3.50.44	Greece – Korinthia – Feneos	(Psonis et al., 2017)	KX658285 / KX657981 / - / - / -	X	X			
511	*Podarcis ionicus*	NHMC 80.3.50.55	Greece – Ioannina– Tzoumerka Mt.	(Psonis et al., 2017)	KX658287 / KX657983 / - / - / -	X	X		X	
513	*Podarcis ionicus*	NHMC 80.3.50.65	Greece – Ioannina – Nemertsika Mt., Vitsikopoulo	(Psonis et al., 2017)	KX658289 / KX657985 / - / - / -	X	X		X	
626	*Podarcis ionicus*	NHMC 80.3.50.223	Albania – Kodër	(Psonis et al., 2017)	KX658330 / KX658028 / - / - / -	X	X		X	
627	*Podarcis ionicus*	NHMC 80.3.50.224	Albania – Kodër	(Psonis et al., 2017)	KX658331 / KX658029 / - / - / -	X	X		X	

Sample Code	Taxon Name	NHMC Voucher Numbers (or isolate codes of NCBI sequences)	Country – Region – Locality	Study	Sanger / ddRADseq Sequences Accession Numbers (16S rRNA/cyt *b*/MC1R/Pod15b/Pod55)	I. Phylogeny (Sanger data) by Psonis et al. 2017	II. Demography and mtDNA haplotype networks (Sanger data)	III. Molecular Dating (Sanger data)	IV. Microsatellites data	V. ddRADseq data
643	*Podarcis ionicus*	NHMC 80.3.50.235	Albania – Golemaj	(Psonis et al., 2017)	KX658340 / KX658038 / KX658509 / KX658562 / KX658615	X	X	X	X	
644	*Podarcis ionicus*	NHMC 80.3.50.236	Albania – Golemaj	(Psonis et al., 2017)	KX658341 / KX658039 / - / - / -	X	X		X	
645	*Podarcis ionicus*	NHMC 80.3.50.237	Albania – Vagalat	(Psonis et al., 2017)	KX658342 / KX658040 / - / - / -	X	X		X	
646	*Podarcis ionicus*	NHMC 80.3.50.238	Albania – Vagalat	(Psonis et al., 2017)	KX658343 / KX658041 / - / - / -	X	X		X	
647	*Podarcis ionicus*	NHMC 80.3.50.239	Albania – Vagalat	(Psonis et al., 2017)	KX658344 / KX658042 / - / - / -	X	X		X	
648	*Podarcis ionicus*	NHMC 80.3.50.240	Albania – Kodër	(Psonis et al., 2017)	KX658345 / KX658043 / - / - / -	X	X		X	
649	*Podarcis ionicus*	NHMC 80.3.50.241	Albania – Vagalat	(Psonis et al., 2017)	KX658346 / KX658044 / - / - / -	X	X		X	
650	*Podarcis ionicus*	NHMC 80.3.50.242	Albania – Halo	(Psonis et al., 2017)	KX658347 / KX658045 / - / - / -	X	X		X	
654	*Podarcis ionicus*	NHMC 80.3.50.246	Albania – Kodër	(Psonis et al., 2017)	KX658351 / KX658049 / - / - / -	X	X		X	
712	*Podarcis ionicus*	NHMC 80.3.50.252	Greece – Aitoloakarnania – Trichonida lake	(Psonis et al., 2017)	KX658358 / KX658056 / KX658510 / KX658563 / KX658616	X	X	X	X	
713	*Podarcis ionicus*	NHMC 80.3.50.253	Greece – Aitoloakarnania – Trichonida lake	(Psonis et al., 2017)	KX658359 / KX658057 / KX658511 / KX658564 / KX658617	X	X	X	X	
714	*Podarcis ionicus*	NHMC 80.3.50.254	Greece – Korinthia – Ancient Feneos	(Psonis et al., 2017)	KX658360 / KX658058 / - / - / -	X	X		X	
715	*Podarcis ionicus*	NHMC 80.3.50.255	Greece – Korinthia – Ancient Feneos	(Psonis et al., 2017)	KX658361 / KX658059 / - / - / -	X	X		X	
716	*Podarcis ionicus*	NHMC 80.3.50.256	Greece – Korinthia – Ancient Feneos	(Psonis et al., 2017) (Sanger data) / Present Study (ddRADseq)	KX658362 / KX658060 / - / - / - ddRADseq: TBP	X	X		X	X
717	*Podarcis ionicus*	NHMC 80.3.50.257	Greece – Korinthia – Ancient Feneos	(Psonis et al., 2017) / Present Study (ddRADseq)	KX658363 / KX658061 / - / - / - ddRADseq: TBP	X	X		X	X

Sample Code	Taxon Name	NHMC Voucher Numbers (or isolate codes of NCBI sequences)	Country – Region – Locality	Study	Sanger / ddRADseq Sequences Accession Numbers (16S rRNA/cyt *b*/MC1R/Pod15b/Pod55)	I. Phylogeny (Sanger data) by Psonis et al. 2017	II. Demography and mtDNA haplotype networks (Sanger data)	III. Molecular Dating (Sanger data)	IV. Microsatellites data	V. ddRADseq data
718	*Podarcis ionicus*	NHMC 80.3.50.258	Greece – Korinthia – Ancient Feneos	(Psonis et al., 2017) / Present Study (ddRADseq)	KX658364 / KX658062 / KX658512 / KX658565 / KX658618 ddRADseq: TBP	X	X	X	X	X
753	*Podarcis ionicus*	NHMC 80.3.50.5	Greece – Eptanisa Islands – Strofades Isls.	Present Study					Discarded	
754	*Podarcis ionicus*	NHMC 80.3.50.6	Greece – Eptanisa Islands – Strofades Isls.	Present Study					Discarded	
755	*Podarcis ionicus*	NHMC 80.3.50.7	Greece – Eptanisa Islands – Strofades Isls.	Present Study					Discarded	
756	*Podarcis ionicus*	NHMC 80.3.50.10	Greece – Achaia, Kalavryta	Present Study					Discarded	
757	*Podarcis ionicus*	NHMC 80.3.50.11	Greece – Achaia, Kalavryta	Present Study					Discarded	
758	*Podarcis ionicus*	NHMC 80.3.50.12	Greece – Achaia, Kalavryta	Present Study					Discarded	
759	*Podarcis ionicus*	NHMC 80.3.50.38	Greece – Arkadia – Tripoli	(Psonis et al., 2017)	- / KX658087 / - / - / -	X			X	
760	*Podarcis ionicus*	NHMC 80.3.50.39	Greece – Arkadia – Tripoli	Present Study					Discarded	
761	*Podarcis ionicus*	NHMC 80.3.50.41	Greece – Aitolokarnania – Messologi, 2/39 Syntagma Evzonon	(Psonis et al., 2017)	KX658389 / KX658088 / KX658514 / KX658567 / KX658620	X	X	X	X	
763	*Podarcis ionicus*	NHMC 80.3.50.45	Greece – Korinthia – Stymfalia lake	(Psonis et al., 2017)	KX658390 / KX658090 / KX658515 / KX658568 / KX658621	X	X	X	X	
764	*Podarcis ionicus*	NHMC 80.3.50.46	Greece – Korinthia – Stymfalia lake	(Psonis et al., 2017)	KX658391 / KX658091 / - / - / -	X	X		X	
765	*Podarcis ionicus*	NHMC 80.3.50.49	Greece – Korinthia –	(Psonis et al., 2017)	KX658392 / KX658092 / - / - / -	X	X		X	

Sample Code	Taxon Name	NHMC Voucher Numbers (or isolate codes of NCBI sequences)	Country – Region – Locality	Study	Sanger / ddRADseq Sequences Accession Numbers (16S rRNA/cyt *b*/MC1R/Pod15b/Pod55)	I. Phylogeny (Sanger data) by Psonis et al. 2017	II. Demography and mtDNA haplotype networks (Sanger data)	III. Molecular Dating (Sanger data)	IV. Microsatellites data	V. ddRADseq data
766	*Podarcis ionicus*	NHMC 80.3.50.50	Greece – Korinthia – Feneos, Doxis lake	(Psonis et al., 2017)	KX658393 / KX658093 / - / - / -	X	X		X	
767	*Podarcis ionicus*	NHMC 80.3.50.51	Greece – Korinthia – Feneos, Doxis lake	(Psonis et al., 2017)	KX658394 / KX658094 / - / - / -	X	X		X	
768	*Podarcis ionicus*	NHMC 80.3.50.52	Greece – Korinthia – Feneos, Doxis lake	(Psonis et al., 2017)	KX658395 / KX658095 / - / - / -	X	X		X	
769	*Podarcis ionicus*	NHMC 80.3.50.53	Greece – Korinthia – Feneos, Doxis lake	(Psonis et al., 2017)	KX658396 / KX658096 / - / - / -	X	X		X	
770	*Podarcis ionicus*	NHMC 80.3.50.56	Greece – Eptanisa Islands– Zakynthos, near Keri lake	(Psonis et al., 2017)	KX658397 / KX658097 / KX658516 / KX658569 / KX658622	X	X	X	X	
771	*Podarcis ionicus*	NHMC 80.3.50.57	Greece – Eptanisa Islands– Zakynthos, in the center of the town	(Psonis et al., 2017)	KX658398 / KX658098 / - / - / -	X	X		X	
772	*Podarcis ionicus*	NHMC 80.3.50.58	Greece – Eptanisa Islands– Zakynthos, Chora to Argasi	(Psonis et al., 2017) (Sanger data) / Present Study (ddRADseq)	KX658399 / KX658099 / KX658517 / KX658570 / KX658623 ddRADseq: TBP	X	X	X	X	X
773	*Podarcis ionicus*	NHMC 80.3.50.59	Greece – Eptanisa Islands – Zakynthos, Chora to Argasi	(Psonis et al., 2017)	KX658400 / KX658100 / - / - / -	X	X		X	
774	*Podarcis ionicus*	NHMC 80.3.50.60	Greece – Eptanisa Islands – Zakynthos,	(Psonis et al., 2017)	KX658401 / KX658101 / - / - / -	X	X		X	

Sample Code	Taxon Name	NHMC Voucher Numbers (or isolate codes of NCBI sequences)	Country – Region – Locality	Study	Sanger / ddRADseq Sequences Accession Numbers (16S rRNA/cyt *b*/MC1R/Pod15b/Pod55)	I. Phylogeny (Sanger data) by Psonis et al. 2017	II. Demography and mtDNA haplotype networks (Sanger data)	III. Molecular Dating (Sanger data)	IV. Microsatellites data	V. ddRADseq data
775	*Podarcis ionicus*	NHMC 80.3.50.62	Greece – Ioannina – Nemertsika Mt. – Paliochori Kalipades region	(Psonis et al., 2017)	KX658402 / KX658102 / - / - / -	X	X		X	
778	*Podarcis ionicus*	NHMC 80.3.50.221	Greece – Achaia – Strofilia forest	(Psonis et al., 2017)	KX658405 / KX658105 / - / - / -	X	X		X	
801	*Podarcis ionicus*	NHMC 80.3.50.296	Albania – Cajupit pass	(Psonis et al., 2017) (Sanger data) / Present Study (ddRADseq)	KX658407 / KX658107 / - / - / - ddRADseq: TBP	X	X		X	X
802	*Podarcis ionicus*	NHMC 80.3.50.297	Albania – Cajupit pass	Present Study					Discarded	
803	*Podarcis ionicus*	NHMC 80.3.50.298	Albania – Cajupit pass	Present Study					Discarded	
804	*Podarcis ionicus*	NHMC 80.3.50.299	Albania – Cajupit pass	Present Study					Discarded	
805	*Podarcis ionicus*	NHMC 80.3.50.300	Albania – Cajupit pass	(Psonis et al., 2017)	KX658408 / KX658108 / - / - / -	X	X		X	
806	*Podarcis ionicus*	NHMC 80.3.50.301	Albania – Cajupit pass	(Psonis et al., 2017)	KX658409 / KX658109 / - / - / -	X	X		X	
873	*Podarcis ionicus*	NHMC 80.3.50.337	Greece – Ioannina – island of Ioannina lake	(Psonis et al., 2017)	KX658427 / KX658128 / - / - / -	X	X		X	
874	*Podarcis ionicus*	NHMC 80.3.50.338	Greece – Ioannina – Ioannina University, building E1	(Psonis et al., 2017) (Sanger data) / Present Study (ddRADseq)	KX658428 / KX658129 / - / - / - ddRADseq: TBP	X	X		X	X
875	*Podarcis ionicus*	NHMC 80.3.50.339	Greece – Ioannina – Mitsikeli Mt., Liggiades	(Psonis et al., 2017)	KX658429 / KX658130 / - / - / -	X	X		X	
876	*Podarcis ionicus*	NHMC 80.3.50.340	Greece – Ioannina – Zagori, Mesovouni	(Psonis et al., 2017)	KX658430 / KX658131 / - / - / -	X	X		X	
877	*Podarcis ionicus*	NHMC 80.3.50.341	Greece – Ioannina – Dodoni	(Psonis et al., 2017)	KX658431 / KX658132 / - / - / -	X	X		X	

Sample Code	Taxon Name	NHMC Voucher Numbers (or isolate codes of NCBI sequences)	Country – Region – Locality	Study	Sanger / ddRADseq Sequences Accession Numbers (16S rRNA/cyt *b*/MC1R/Pod15b/Pod55)	I. Phylogeny (Sanger data) by Psonis et al. 2017	II. Demography and mtDNA haplotype networks (Sanger data)	III. Molecular Dating (Sanger data)	IV. Microsatellites data	V. ddRADseq data
878	*Podarcis ionicus*	NHMC 80.3.50.342	Greece – Ioannina – Zagori, Dilofo, Agios Minas	(Psonis et al., 2017)	KX658432 / KX658133 / KX658522 / KX658575 / KX658628	X	X	X	X	
879	*Podarcis ionicus*	NHMC 80.3.50.343	Greece – Ioannina – Konitsa	(Psonis et al., 2017)	KX658433 / KX658134 / KX658523 / KX658576 / KX658629	X	X	X	X	
880	*Podarcis ionicus*	NHMC 80.3.50.344	Greece – Ioannina – opposite of the island of Ioannina lake	(Psonis et al., 2017)	KX658434 / KX658135 / - / - / -	X	X		X	
883	*Podarcis ionicus*	NHMC 80.3.50.347	Greece – Achaia – Klokos Mt.	(Psonis et al., 2017)	KX658437 / KX658138 / KX658524 / KX658577 / KX658630	X	X	X	X	
884	*Podarcis ionicus*	NHMC 80.3.50.320	Greece – Arkadia – Kosmas	(Psonis et al., 2017)	KX658438 / KX658139 / - / - / -	X	X		X	
885	*Podarcis ionicus*	NHMC 80.3.50.321	Greece – Arkadia – Kosmas	(Psonis et al., 2017)	KX658439 / KX658140 / KX658525 / KX658578 / KX658631	X	X	X	X	
886	*Podarcis ionicus*	NHMC 80.3.50.322	Greece – Arkadia – Kosmas	(Psonis et al., 2017) (Sanger data) / Present Study (ddRADseq)	KX658440 / KX658141 / - / - / - ddRADseq: TBP	X	X		X	X
887	*Podarcis ionicus*	NHMC 80.3.50.323	Greece – Lakonia – Karyes	(Psonis et al., 2017) (Sanger data) / Present Study (ddRADseq)	KX658441 / KX658142 / KX658526 / KX658579 / KX658632 ddRADseq: TBP	X	X	X	X	X
888	*Podarcis ionicus*	NHMC 80.3.50.324	Greece – Lakonia – Karyes	(Psonis et al., 2017)	KX658442 / KX658143 / KX658527 / KX658580 / KX658633	X	X	X	X	
889	*Podarcis ionicus*	NHMC 80.3.50.325	Greece – Korinthia – Doxis lake	(Psonis et al., 2017)	KX658443 / KX658144 / - / - / -	X	X		X	
890	*Podarcis ionicus*	NHMC 80.3.50.326	Greece – Korinthia – Doxis lake	(Psonis et al., 2017)	KX658444 / KX658145 / - / - / -	X	X		X	
891	*Podarcis ionicus*	NHMC 80.3.50.327	Greece – Korinthia – Doxis lake	(Psonis et al., 2017)	KX658445 / KX658146 / - / - / -	X	X		X	

Sample Code	Taxon Name	NHMC Voucher Numbers (or isolate codes of NCBI sequences)	Country – Region – Locality	Study	Sanger / ddRADseq Sequences Accession Numbers (16S rRNA/cyt *b*/MC1R/Pod15b/Pod55)	I. Phylogeny (Sanger data) by Psonis et al. 2017	II. Demography and mtDNA haplotype networks (Sanger data)	III. Molecular Dating (Sanger data)	IV. Microsatellites data	V. ddRADseq data
892	*Podarcis ionicus*	NHMC 80.3.50.328	Greece – Korinthia – Louzi	(Psonis et al., 2017)	KX658446 / KX658147 / - / - / -	X	X		X	
893	*Podarcis ionicus*	NHMC 80.3.50.329	Greece – Korinthia – Sikionas	(Psonis et al., 2017)	KX658447 / KX658148 / - / - / -	X	X		X	
897	*Podarcis ionicus*	NHMC 80.3.50.332	Greece – Argolida – Nafplio	(Psonis et al., 2017)	KX658448 / KX658149 / - / - / -	X	X		X	
928	*Podarcis ionicus*	NHMC 80.3.50.61	Greece – Aitoloakarnania – Arakinthos Mt., Karitsa	(Psonis et al., 2017) (Sanger data) / Present Study (ddRADseq)	KX658450 / KX658151 / - / - / - ddRADseq: TBP	X	X			X
929	*Podarcis ionicus*	NHMC 80.3.50.348	Greece – Eptanisa Islands – Kerkyra Isl., Sidari	(Psonis et al., 2017)	KX658451 / KX658152 / - / - / -	X	X			
930	*Podarcis ionicus*	NHMC 80.3.50.349	Greece – Eptanisa Islands – Kerkyra Isl., Sidari	(Psonis et al., 2017)	KX658452 / KX658153 / - / - / -	X	X			
931	*Podarcis ionicus*	NHMC 80.3.50.350	Greece – Eptanisa Islands – Kerkyra Isl., Sidari	(Psonis et al., 2017)	KX658453 / KX658154 / - / - / -	X	X			
932	*Podarcis ionicus*	NHMC 80.3.50.351	Greece – Eptanisa Islands – Kerkyra Isl., Sidari	(Psonis et al., 2017)	KX658454 / KX658155 / - / - / -	X	X			
933	*Podarcis ionicus*	NHMC 80.3.50.352	Greece – Eptanisa Islands – Kerkyra Isl., Sidari	(Psonis et al., 2017) (Sanger data) / Present Study (ddRADseq)	KX658455 / KX658156 / - / - / - ddRADseq: TBP	X	X			X
934	*Podarcis ionicus*	NHMC 80.3.50.353	Greece – Eptanisa Islands – Kerkyra Isl., Sidari	(Psonis et al., 2017)	KX658456 / KX658157 / - / - / -	X	X			
935	*Podarcis ionicus*	NHMC 80.3.50.354	Greece – Eptanisa Islands – Kerkyra Isl., Sidari	(Psonis et al., 2017)	KX658457 / KX658158 / - / - / -	X	X			

Sample Code	Taxon Name	NHMC Voucher Numbers (or isolate codes of NCBI sequences)	Country – Region – Locality	Study	Sanger / ddRADseq Sequences Accession Numbers (16S rRNA/cyt *b*/MC1R/Pod15b/Pod55)	I. Phylogeny (Sanger data) by Psonis et al. 2017	II. Demography and mtDNA haplotype networks (Sanger data)	III. Molecular Dating (Sanger data)	IV. Microsatellites data	V. ddRADseq data
945	*Podarcis ionicus*	NHMC 80.3.50.367	Greece – Eptanisa Islands – Kefallonia Isl., Lixouri	(Psonis et al., 2017)	KX658466 / KX658167 / - / - / -	X	X			
946	*Podarcis ionicus*	NHMC 80.3.50.368	Greece – Eptanisa Islands – Kefallonia Isl. , Lixouri	(Psonis et al., 2017)	KX658467 / KX658168 / - / - / -	X	X			
947	*Podarcis ionicus*	NHMC 80.3.50.63	Greece – Messinia – Pamisos river, near Kalamata airport	(Psonis et al., 2017)	KX658468 / KX658169 / - / - / -	X	X			
948	*Podarcis ionicus*	NHMC 80.3.50.170	Albania – Uznovë	(Psonis et al., 2017)	KX658469 / KX658170 / - / - / -	X	X			
949	*Podarcis ionicus*	NHMC 80.3.50.171	Albania – Divjakë-Karavastë NP	(Psonis et al., 2017)	KX658470 / KX658171 / - / - / -	X	X			
950	*Podarcis ionicus*	NHMC 80.3.50.172	Albania – Divjakë-Karavastë NP	(Psonis et al., 2017)	KX658471 / KX658172 / - / - / -	X	X			
953	*Podarcis ionicus*	NHMC 80.3.50.175	Albania – Fierzë	(Psonis et al., 2017)	KX658474 / KX658175 / - / - / -	X	X			
094	*Podarcis levendis*	NHMC 80.3.51.279	Greece – Antikythira Isl. – Pori islet	(Poulakakis *et al.* 2005c) (isolate Pe94; 16S rRNA) / (Poulakakis *et al.* 2003) (isolate PE-31; cyt *b*) / (Psonis et al., 2017) (nDNA markers)	AY896170 / AF486221 / KX658484 / KX658537 / KX658590	X		X		
096	*Podarcis levendis*	NHMC 80.3.51.288	Greece – Antikythira Isl. – Pori islet	(Poulakakis *et al.* 2005c) (isolate Pe96; 16S rRNA) / (Poulakakis *et al.* 2003) (isolate PE-32; cyt *b*) / (Psonis et al., 2017) (nDNA markers)	AY896171 / AF486222 / KX658485 / KX658538 / KX658591	X		X		
830	*Podarcis levendis*	NHMC 80.3.51.2529	Greece – Antikythira	Present Study	ddRADseq: TBP					X

Sample Code	Taxon Name	NHMC Voucher Numbers (or isolate codes of NCBI sequences)	Country – Region – Locality	Study	Sanger / ddRADseq Sequences Accession Numbers (16S rRNA/cyt *b*/MC1R/Pod15b/Pod55)	I. Phylogeny (Sanger data) by Psonis et al. 2017	II. Demography and mtDNA haplotype networks (Sanger data)	III. Molecular Dating (Sanger data)	IV. Microsatellites data	V. ddRADseq data
852	*Podarcis levendis*	NHMC 80.3.51.2535	archipelago – Pori islet Greece – Antikythira archipelago – Lagouvardos islet (Poreti islet)	Present Study	ddRADseq: TBP					X
639	*Podarcis lilfordi*	NHMC 80.3.59.2	Spain – Mallorca Isl.	(Kapli *et al.* 2013) (isolate Plil1; cyt *b*) / (Psonis et al., 2017) (16S rRNA & nDNA markers)	KX658187 / KF003361 / KX658486 / KX658539 / KX658592	X		X		
640	*Podarcis lilfordi*	NHMC 80.3.59.3	Spain – Mallorca Isl.	(Kapli *et al.* 2013) (isolate Plil2; cyt *b*) / (Psonis et al., 2017) (16S rRNA & nDNA markers)	KX658188 / KF003362 / KX658487 / KX658540 / KX658593	X		X		
545	*Podarcis melisellensis*	NHMC 80.3.57.4	Montenegro – Ada Bojana	(Psonis et al., 2017)	KX658189 / KX657885 / KX658488 / KX658541 / KX658594	X	X (only demography)	X	X	
547	*Podarcis melisellensis*	NHMC 80.3.57.6	Montenegro – Ada Bojana	Present Study					X	
548	*Podarcis melisellensis*	NHMC 80.3.57.7	Montenegro – Ada Bojana	Present Study					X	
549	*Podarcis melisellensis*	NHMC 80.3.57.8	Montenegro – Ada Bojana	Present Study					X	
55	*Podarcis melisellensis*	NHMC 80.3.57.1	Yugoslavia	Present Study					Discarded	
550	*Podarcis melisellensis*	NHMC 80.3.57.9	Montenegro – Niksic	Present Study					X	
624	*Podarcis melisellensis*	NHMC 80.3.57.2	Croatia – Cres Isl.	Present Study					Discarded	
655	*Podarcis melisellensis*	NHMC 80.3.57.10	Montenegro – Ada Bojana	(Psonis et al., 2017)	KX658190 / KX657886 / - / - / -	X	X (only demography)		X	
656	*Podarcis melisellensis*	NHMC 80.3.57.11	Bosnia and Herzegovina – Nevesinje	(Psonis et al., 2017) (Sanger data) / Present Study (ddRADseq data)	KX658191 / KX657887 / KX658489 / KX658542 / KX658595 ddRADseq: TBP	X	X (only demography)	X	X	X

Sample Code	Taxon Name	NHMC Voucher Numbers (or isolate codes of NCBI sequences)	Country – Region – Locality	Study	Sanger / ddRADseq Sequences Accession Numbers (16S rRNA/cyt *b*/MC1R/Pod15b/Pod55)	I. Phylogeny (Sanger data) by Psonis et al. 2017	II. Demography and mtDNA haplotype networks (Sanger data)	III. Molecular Dating (Sanger data)	IV. Microsatellites data	V. ddRADseq data
657	*Podarcis melisellensis*	NHMC 80.3.57.12 (NMP6V 74157)*	Bosnia and Herzegovina – Prozor	(Psonis et al., 2017)	KX658192 / KX657888 / - / - / -	X	X (only demography)		X	X
DEMO	*Podarcis melisellensis*	BIS3	Croatia – Vis archipelago - Biševo Island	(Podnar *et al.* 2004)	AY185019 / AY185062 / - / - / -	X	X (only demography)			
DEMO	*Podarcis melisellensis*	BRU1	Croatia – Vis archipelago - Brusnik islet	(Podnar *et al.* 2004)	AY185017 / AY185057 / - / - / -	X	X (only demography)			
DEMO	*Podarcis melisellensis*	CAV	Croatia – Cavtat	(Podnar *et al.* 2004)	AY185012 / AY185023 / - / - / -	X	X (only demography)			
DEMO	*Podarcis melisellensis*	GLA	Croatia – Lastovo archipelago - Glavat islet	(Podnar *et al.* 2004)	AY185014 / AY185042 / - / - / -	X	X (only demography)			
DEMO	*Podarcis melisellensis*	HVA	Croatia – Hvar Island	(Podnar *et al.* 2004)	AY185011 / AY185020 / - / - / -	X	X (only demography)			
DEMO	*Podarcis melisellensis*	JAB1	Croatia – Vis archipelago - Jabuka islet	(Podnar *et al.* 2004)	AY185018 / AY185097 / - / - / -	X	X (only demography)			
DEMO	*Podarcis melisellensis*	KCA	Croatia – Korčula Island	(Podnar *et al.* 2004)	AY185013 / AY185028 / - / - / -	X	X (only demography)			
DEMO	*Podarcis melisellensis*	KOR	Croatia – Istria – Koromačno	(Podnar *et al.* 2004)	AY185010 / AY185029 / - / - / -	X	X (only demography)			
DEMO	*Podarcis melisellensis*	LAS1	Croatia – Lastovo Island	(Podnar *et al.* 2004)	AY185015 / AY185036 / - / - / -	X	X (only demography)			
DEMO	*Podarcis melisellensis*	PUR	Croatia – Kornati archipelago - Purara islet	(Podnar *et al.* 2004)	AY185009 / AY185052 / - / - / -	X	X (only demography)			
DEMO	*Podarcis melisellensis*	VZP	Croatia – Vis Island - Zlopolje	(Podnar *et al.* 2004)	AY185016 / AY185097 / - / - / -	X	X (only demography)			
053	*Podarcis milensis*	NHMC 80.3.52.2	Greece – Kyklades – Milos Isl., Achivadolimni lake	(Poulakakis *et al.* 2005c) (16S rRNA) / (Poulakakis *et al.* 2005b) (cyt *b*) / (Psonis et al., 2017) (nDNA markers)	AY768741 / AY768777 / KX658490 / KX658543 / KX658596	X	X	X	X	
054	*Podarcis milensis*	NHMC 80.3.52.3	Greece – Kyklades –	(Poulakakis *et al.* 2005c) (16S rRNA) /	AY768740 / AY768776 / - / - / -	X	X		X	

Sample Code	Taxon Name	NHMC Voucher Numbers (or isolate codes of NCBI sequences)	Country – Region – Locality	Study	Sanger / ddRADseq Sequences Accession Numbers (16S rRNA/cyt *b*/MC1R/Pod15b/Pod55)	I. Phylogeny (Sanger data) by Psonis et al. 2017	II. Demography and mtDNA haplotype networks (Sanger data)	III. Molecular Dating (Sanger data)	IV. Microsatellites data	V. ddRADseq data
			Milos Isl. – Agios Efstathios islet	(Poulakakis *et al.* 2005b) (cyt *b*)						
555	*Podarcis milensis*	NHMC 80.3.52.66	Greece – Kyklades, Milos Isl. – Milos excavations	(Psonis et al., 2017)	KX658193 / KX657890 / KX658491 / KX658544 / KX658597	X	X	X	X	
600	*Podarcis milensis*	NHMC 80.3.52.5	Greece – Kyklades – Kimolos Isl.	(Psonis et al., 2017)	KX658194 / KX657891 / - / - / -	X	X		X	
601	*Podarcis milensis*	NHMC 80.3.52.10	Greece – Kyklades – Kimolos Isl.	(Psonis et al., 2017)	KX658195 / KX657892 / KX658492 / KX658545 / KX658598	X	X	X	X	
603	*Podarcis milensis*	NHMC 80.3.52.78	Greece – Kyklades – Milos Isl.	(Psonis et al., 2017)	KX658196 / KX657893 / - / - / -	X	X		X	
604	*Podarcis milensis*	NHMC 80.3.52.4	Greece – Kyklades – Kimolos Isl.	(Psonis et al., 2017)	KX658197 / KX657894 / - / - / -	X	X		X	
605	*Podarcis milensis*	NHMC 80.3.52.6	Greece – Kyklades – Kimolos Isl.	(Psonis et al., 2017)	KX658198 / KX657895 / - / - / -	X	X		X	
606	*Podarcis milensis*	NHMC 80.3.52.7	Greece – Kyklades – Kimolos Isl.	(Psonis et al., 2017)	KX658199 / KX657896 / - / - / -	X	X		X	
607	*Podarcis milensis*	NHMC 80.3.52.8	Greece – Kyklades – Kimolos Isl.	(Psonis et al., 2017)	KX658200 / KX657897 / - / - / -	X	X		X	
608	*Podarcis milensis*	NHMC 80.3.52.9	Greece – Kyklades – Kimolos Isl.	(Psonis et al., 2017)	KX658201 / KX657898 / - / - / -	X	X			
609	*Podarcis milensis*	NHMC 80.3.52.11	Greece – Kyklades island complex – Kimolos Isl.	Present Study					X	
610	*Podarcis milensis*	NHMC 80.3.52.12	Greece – Kyklades – Kimolos Isl.	(Psonis et al., 2017)	KX658202 / KX657899 / - / - / -	X	X		X	
613	*Podarcis milensis*	NHMC 80.3.52.67	Greece – Kyklades – Milos Isl.	(Psonis et al., 2017)	KX658203 / KX657900 / - / - / -	X	X		X	

Sample Code	Taxon Name	NHMC Voucher Numbers (or isolate codes of NCBI sequences)	Country – Region – Locality	Study	Sanger / ddRADseq Sequences Accession Numbers (16S rRNA/cyt *b*/MC1R/Pod15b/Pod55)	I. Phylogeny (Sanger data) by Psonis et al. 2017	II. Demography and mtDNA haplotype networks (Sanger data)	III. Molecular Dating (Sanger data)	IV. Microsatellites data	V. ddRADseq data
614	*Podarcis milensis*	NHMC 80.3.52.68	Greece – Kyklades – Milos Isl.	(Psonis et al., 2017)	KX658204 / KX657901 / - / - / -	X	X		X	
615	*Podarcis milensis*	NHMC 80.3.52.69	Greece – Kyklades – Milos Isl.	(Psonis et al., 2017)	KX658205 / KX657902 / - / - / -	X	X		X	
617	*Podarcis milensis*	NHMC 80.3.52.71	Greece – Kyklades – Milos Isl.	(Psonis et al., 2017)	KX658206 / KX657904 / - / - / -	X	X		X	
618	*Podarcis milensis*	NHMC 80.3.52.72	Greece – Kyklades – Milos Isl.	(Psonis et al., 2017)	KX658207 / KX657905 / - / - / -	X	X		X	
619	*Podarcis milensis*	NHMC 80.3.52.73	Greece – Kyklades – Milos Isl.	(Psonis et al., 2017)	KX658208 / KX657906 / - / - / -	X	X		X	
620	*Podarcis milensis*	NHMC 80.3.52.74	Greece – Kyklades – Milos Isl.	(Psonis et al., 2017)	KX658209 / KX657907 / - / - / -	X	X		X	
621	*Podarcis milensis*	NHMC 80.3.52.75	Greece – Kyklades – Milos Isl.	(Psonis et al., 2017)	KX658210 / KX657908 / - / - / -	X	X		X	
622	*Podarcis milensis*	NHMC 80.3.52.76	Greece – Kyklades – Milos Isl.	(Psonis et al., 2017)	KX658211 / KX657909 / - / - / -	X	X		X	
623	*Podarcis milensis*	NHMC 80.3.52.77	Greece – Kyklades – Milos Isl.	(Psonis et al., 2017)	KX658212 / KX657910 / - / - / -	X	X		X	
638	*Podarcis milensis*	NHMC 80.3.52.79	Greece – Kyklades – Milos Isl., Adamas	(Psonis et al., 2017)	KX658213 / KX657911 / KX658493 / KX658546 / KX658599	X	X	X	X	
665	*Podarcis milensis*	NHMC 80.3.52.80	Greece – Kyklades – Milos Isl., Achivadolimni lake, at Agios Konstantinos church	Present Study					X	
666	*Podarcis milensis*	NHMC 80.3.52.81	Greece – Kyklades – Milos Isl.,	(Psonis et al., 2017)	KX658214 / KX657912 / - / - / -	X	X		X	

Sample Code	Taxon Name	NHMC Voucher Numbers (or isolate codes of NCBI sequences)	Country – Region – Locality	Study	Sanger / ddRADseq Sequences Accession Numbers (16S rRNA/cyt *b*/MC1R/Pod15b/Pod55)	I. Phylogeny (Sanger data) by Psonis et al. 2017	II. Demography and mtDNA haplotype networks (Sanger data)	III. Molecular Dating (Sanger data)	IV. Microsatellites data	V. ddRADseq data
667	*Podarcis milensis*	NHMC 80.3.52.82	Greece – Kyklades – Milos Isl., Achivadolimni lake, at Agios Konstantinos church	Present Study					X	
669	*Podarcis milensis*	NHMC 80.3.52.84	Greece – Kyklades – Milos Isl., Achivadolimni lake, at Agios Konstantinos church	Present Study					X	
670	*Podarcis milensis*	NHMC 80.3.52.85	Greece – Kyklades – Milos Isl., Achivadolimni lake, at Agios Konstantinos church	Present Study					X	
671	*Podarcis milensis*	NHMC 80.3.52.86	Greece – Kyklades island complex – Milos Isl. – Papikinou beach	Present Study	ddRADseq: TBP					X
672	*Podarcis milensis*	NHMC 80.3.52.87	Greece – Kyklades – Milos Isl., Parasporos	(Psonis et al., 2017)	KX658215 / KX657913 / - / - / -	X	X		X	
673	*Podarcis milensis*	NHMC 80.3.52.88	Greece – Kyklades island complex – Milos Isl. – Parasporos	Present Study	ddRADseq: TBP				X	X

Sample Code	Taxon Name	NHMC Voucher Numbers (or isolate codes of NCBI sequences)	Country – Region – Locality	Study	Sanger / ddRADseq Sequences Accession Numbers (16S rRNA/cyt *b*/MC1R/Pod15b/Pod55)	I. Phylogeny (Sanger data) by Psonis et al. 2017	II. Demography and mtDNA haplotype networks (Sanger data)	III. Molecular Dating (Sanger data)	IV. Microsatellites data	V. ddRADseq data
674	*Podarcis milensis*	NHMC 80.3.52.89	Greece – Kyklades island complex – Milos Isl. – Parasporos	Present Study	ddRADseq: TBP				X	X
675	*Podarcis milensis*	NHMC 80.3.52.90	Greece – Kyklades – Milos Isl., Komia	Present Study					X	
676	*Podarcis milensis*	NHMC 80.3.52.91	Greece – Kyklades – Milos Isl., Komia	(Psonis et al., 2017)	KX658216 / KX657914 / - / - / -	X	X		X	
677	*Podarcis milensis*	NHMC 80.3.52.92	Greece – Kyklades – Milos Isl., Adamas NW, on the way to Vato	(Psonis et al., 2017)	KX658217 / KX657915 / - / - / -	X	X		X	
678	*Podarcis milensis*	NHMC 80.3.52.93	Greece – Kyklades – Milos Isl., Adamas NW, on the way to Vato	Present Study					X	
679	*Podarcis milensis*	NHMC 80.3.52.94	Greece – Kyklades island complex – Milos Isl. – NW of Adamas at the way to Vato	Present Study	ddRADseq: TBP				X	X
680	*Podarcis milensis*	NHMC 80.3.52.95	Greece – Kyklades island complex – Kimolos Isl. – Psathi to Chorio	Present Study					X	
681	*Podarcis milensis*	NHMC 80.3.52.96	Greece – Kyklades island complex – Kimolos Isl.	Present Study	ddRADseq: TBP				X	X

Sample Code	Taxon Name	NHMC Voucher Numbers (or isolate codes of NCBI sequences)	Country – Region – Locality	Study	Sanger / ddRADseq Sequences Accession Numbers (16S rRNA/cyt *b*/MC1R/Pod15b/Pod55)	I. Phylogeny (Sanger data) by Psonis et al. 2017	II. Demography and mtDNA haplotype networks (Sanger data)	III. Molecular Dating (Sanger data)	IV. Microsatellites data	V. ddRADseq data
682	*Podarcis milensis*	NHMC 80.3.52.97	– Psathi to Chorio Greece – Kyklades island complex – Kimolos Isl.	Present Study					X	
683	*Podarcis milensis*	NHMC 80.3.52.98	– Psathi to Chorio Greece – Kyklades island complex – Kimolos Isl.	Present Study					X	
684	*Podarcis milensis*	NHMC 80.3.52.99	– Psathi to Chorio Greece – Kyklades – Kimolos Isl.	(Psonis et al., 2017)	KX658218 / KX657916 / - / - / -	X	X		X	
779	*Podarcis milensis*	NHMC 80.3.52.100							X	
780	*Podarcis milensis*	NHMC 80.3.52.101	Greece – Kyklades – Milos Isl., Achivadolimni lake	(Psonis et al., 2017)	KX658219 / KX657917 / - / - / -	X	X		X	
781	*Podarcis milensis*	NHMC 80.3.52.102	Greece – Kyklades – Milos Isl., Achivadolimni lake	Present Study					X	
782	*Podarcis milensis*	NHMC 80.3.52.103	Greece – Kyklades – Milos Isl., Achivadolimni lake	Present Study					X	
783	*Podarcis milensis*	NHMC 80.3.52.104	Greece – Kyklades – Milos Isl., Achivadolimni lake	Present Study					X	

Sample Code	Taxon Name	NHMC Voucher Numbers (or isolate codes of NCBI sequences)	Country – Region – Locality	Study	Sanger / ddRADseq Sequences Accession Numbers (16S rRNA/cyt *b*/MC1R/Pod15b/Pod55)	I. Phylogeny (Sanger data) by Psonis et al. 2017	II. Demography and mtDNA haplotype networks (Sanger data)	III. Molecular Dating (Sanger data)	IV. Microsatellites data	V. ddRADseq data
784	*Podarcis milensis*	NHMC 80.3.52.106	Greece – Kyklades– Milos Isl., Zefyria	(Psonis et al., 2017)	KX658220 / KX657918 / - / - / -	X	X		X	
785	*Podarcis milensis*	NHMC 80.3.52.107	Greece – Kyklades– Milos Isl., Zefyria	Present Study					X	
786	*Podarcis milensis*	NHMC 80.3.52.108	Greece – Kyklades– Milos Isl., Zefyria	Present Study					X	
787	*Podarcis milensis*	NHMC 80.3.52.109	Greece – Kyklades– Milos Isl., Zefyria	Present Study					X	
788	*Podarcis milensis*	NHMC 80.3.52.110	Greece – Kyklades– Milos Isl., Zefyria	Present Study					X	
809	*Podarcis milensis*	NHMC 80.3.52.65	Greece – Kyklades island complex – Antimilos Isl.	Present Study					Discarded	
988	*Podarcis milensis*	NHMC 80.3.52.105	Greece – Kyklades island complex – Milos Isl. – Achivadolimni lake	Present Study	ddRADseq: TBP					X
552	*Podarcis milensis*	NHMC 80.3.52.54	Greece – Kyklades island complex – Milos Isl. – Falconera islet	Present Study					Discarded	
553	*Podarcis milensis*	NHMC 80.3.52.57	Greece – Kyklades island complex – Milos Isl. – Ananes islet	Present Study					Discarded	

Sample Code	Taxon Name	NHMC Voucher Numbers (or isolate codes of NCBI sequences)	Country – Region – Locality	Study	Sanger / ddRADseq Sequences Accession Numbers (16S rRNA/cyt *b*/MC1R/Pod15b/Pod55)	I. Phylogeny (Sanger data) by Psonis et al. 2017	II. Demography and mtDNA haplotype networks (Sanger data)	III. Molecular Dating (Sanger data)	IV. Microsatellites data	V. ddRADseq data
807	*Podarcis milensis*	NHMC 80.3.52.52	Greece – Kyklades island complex – Milos Isl. – Falconera islet	Present Study					Discarded	
808	*Podarcis milensis*	NHMC 80.3.52.53	Greece – Kyklades island complex – Milos Isl. – Falconera islet	Present Study					Discarded	
014	*Podarcis muralis*	NHMC 80.3.53.79	Greece – Karditsa – Kazarma	(Poulakakis *et al.* 2005c) (mtDNA markers)/ (Psonis et al., 2017) (nDNA markers)	AY896187 / AY896134 / KX658494 / KX658547 / KX658600	X		X		
595	*Podarcis muralis*	NHMC 80.3.53.541	Ukraine – Lower Danube area, near Ukrainian–Romanian state border, trading river port of the town of Reni, Odessa Province, Reni Distr.	(Psonis et al., 2017)	KX658221 / KX657919 / KX658495 / KX658548 / KX658601	X		X		
596	*Podarcis muralis*	NHMC 80.3.53.544	Ukraine – NW coast of the Lake Kagul, Odessa Province, Reni Distr..	(Psonis et al., 2017)	KX658222 / KX657920 / KX658496 / KX658549 / KX658602	X		X		
635	*Podarcis muralis*	NHMC 80.3.53.545	Greece – Kastoria – Eptachori	(Psonis et al., 2017)	KX658223 / KX657921 / KX658497 / KX658550 / KX658603	X		X		
990	*Podarcis muralis*	NHMC 80.3.53.549	Greece – Karditsa prefecture – Plastiras lake	Present Study	ddRADseq: TBP					X

Sample Code	Taxon Name	NHMC Voucher Numbers (or isolate codes of NCBI sequences)	Country – Region – Locality	Study	Sanger / ddRADseq Sequences Accession Numbers (16S rRNA/cyt *b*/MC1R/Pod15b/Pod55)	I. Phylogeny (Sanger data) by Psonis et al. 2017	II. Demography and mtDNA haplotype networks (Sanger data)	III. Molecular Dating (Sanger data)	IV. Microsatellites data	V. ddRADseq data
992	*Podarcis muralis*	NHMC 80.3.53.562	Greece – Florina prefecture – Gavros to Prespa lakes	Present Study	ddRADseq: TBP					X
INDATE	*Podarcis muralis*	MTA1	Spain – Asturias – Tanes	(Pinho *et al.* 2006)	DQ081106 / DQ081150 / - / - / -	X		X		
INDATE	*Podarcis muralis*	DB8970	Spain – Asturias – Tanes	(Salvi *et al.* 2013)	- / - / KF372123 / - / -	X		X		
INDATE	*Podarcis muralis*	Tan11	Spain – Asturias – Tanes	(Pereira *et al.* 2013)	- / - / - / KC681277 / KC681728	X		X		
1000	*Podarcis peloponnesiacus*	NHMC 80.3.54.119	Greece – Korinthia prefecture – Epidavros	Present Study	ddRADseq: TBP					X
396	*Podarcis peloponnesiacus*	NHMC 80.3.54.114	Greece – Achaia – Erymanthos Mt.	(Psonis et al., 2017)	KX658224 / KX657922 / KX658498 / KX658551 / KX658604	X		X		
397	*Podarcis peloponnesiacus*	NHMC 80.3.54.117	Greece – Messinia – Aigaleo Mt.	(Psonis et al., 2017)	KX658225 / KX657923 / KX658499 / KX658552 / KX658605	X		X		
999	*Podarcis peloponnesiacus*	NHMC 80.3.54.118	Greece – Korinthia prefecture – Epidavros	Present Study	ddRADseq: TBP					X
641	*Podarcis pityusensis*	NHMC 80.3.176.1	Spain – Mallorca Isl. – Palma (introduced)	(Kapli *et al.* 2013) (isolate Ppit1; cyt *b*) / (Psonis et al., 2017) (16S rRNA & nDNA markers)	KX658226 / KF003363 / KX658500 / KX658553 / KX658606	X		X		
642	*Podarcis pityusensis*	NHMC 80.3.176.2	Spain – Mallorca Isl. – Palma (introduced)	(Kapli *et al.* 2013) (isolate Ppit2; cyt *b*) / (Psonis et al., 2017) (16S rRNA & nDNA markers)	KX658227 / KF003364 / KX658501 / KX658554 / KX658607	X		X		
894	*Podarcis siculus*	NHMC 80.3.55.17	Slovenia – Dragonje	(Psonis et al., 2017)	KX658228 / KX657924 / KX658502 / KX658555 / KX658608	X		X		

Sample Code	Taxon Name	NHMC Voucher Numbers (or isolate codes of NCBI sequences)	Country – Region – Locality	Study	Sanger / ddRADseq Sequences Accession Numbers (16S rRNA/cyt *b*/MC1R/Pod15b/Pod55)	I. Phylogeny (Sanger data) by Psonis et al. 2017	II. Demography and mtDNA haplotype networks (Sanger data)	III. Molecular Dating (Sanger data)	IV. Microsatellites data	V. ddRADseq data
170	*Podarcis tauricus*	NHMC 80.3.50.28	Greece – Fthiotida – Spercheios river	(Psonis et al., 2017)	KX658229 / KX657925 / - / - / -	X	X		X	
171	*Podarcis tauricus*	NHMC 80.3.50.16	Greece – Aliakmonas river	Present Study					Discarded	
172	*Podarcis tauricus*	NHMC 80.3.50.19	Greece – Pieria, Olympos Mt.	Present Study					Discarded	
176	*Podarcis tauricus*	NHMC 80.3.50.35	Greece – Florina, Niki	(Poulakakis *et al.* 2005c) (16S rRNA) / (Poulakakis *et al.* 2005b) (cyt *b*)	AY768711 / AY768747 / - / - / -	X	X		X	
180	*Podarcis tauricus*	NHMC 80.3.50.34	Greece – Evros, Feres	(Poulakakis *et al.* 2005c) (16S rRNA) / (Poulakakis *et al.* 2005b) (cyt *b*) / (Psonis et al., 2017) (nDNA markers)	AY768710 / AY768746 / KX658503 / KX658556 / KX658609	X	X	X	X	
198	*Podarcis tauricus*	NHMC 80.3.50.27	Greece – Kozani	Present Study					Discarded	
208	*Podarcis tauricus*	NHMC 80.3.50.2	Greece – Ioannina, Theriakisi	Present Study					Discarded	
224	*Podarcis tauricus*	NHMC 80.3.50.33	Greece – Kavala, Thasos Isl. – Thasopoula islet	(Poulakakis *et al.* 2005c) (16S rRNA) / (Poulakakis *et al.* 2005b) (cyt *b*)	AY768723 / AY768759 / - / - / -	X	X			
225	*Podarcis tauricus*	NHMC 80.3.50.36	Greece – Kavala, Thasos Isl. – Thasopoula islet	(Poulakakis *et al.* 2005c) (16S rRNA) / (Poulakakis *et al.* 2005b) (cyt *b*)	AY768724 / AY768760 / - / - / -	X	X		X	
227	*Podarcis tauricus*	NHMC 80.3.50.32	Greece – Kavala, Thasos Isl. – Thasopoula islet	(Poulakakis *et al.* 2005c) (16S rRNA) / (Poulakakis *et al.* 2005b) (cyt b)	AY768725 / AY768761 / - / - / -	X	X			
432	*Podarcis tauricus*	NHMC 80.3.50.66	Crimea – western part of Main range of the Crimean Mts. – near village	(Psonis et al., 2017)	KX658230 / KX657926 / - / - / -	X	X		X	

Sample Code	Taxon Name	NHMC Voucher Numbers (or isolate codes of NCBI sequences)	Country – Region – Locality	Study	Sanger / ddRADseq Sequences Accession Numbers (16S rRNA/cyt *b*/MC1R/Pod15b/Pod55)	I. Phylogeny (Sanger data) by Psonis et al. 2017	II. Demography and mtDNA haplotype networks (Sanger data)	III. Molecular Dating (Sanger data)	IV. Microsatellites data	V. ddRADseq data
433	*Podarcis tauricus*	NHMC 80.3.50.67	Uzundzha, western slope of Mt. Chuvash–Koyi (Range Trapan–Bair); Sevastopol territory Crimea – western part of Main range of the Crimean Mts. – near village Uzundzha, western slope of Mt. Chuvash–Koyi (Range Trapan–Bair); Sevastopol territory Crimea – Southern Coast – between settlements Parthenit and Gurzuf, Cape Ayu-Dagh; Alushta territory Crimea – Southern Coast – between settlements Parthenit and Gurzuf, Cape Ayu-Dagh; Alushta territory Crimea – Southern Coast – near Cape Sarych, locality of Choban-Tash;	Present Study					X	
434	*Podarcis tauricus*	NHMC 80.3.50.68		(Psonis et al., 2017)	KX658231 / KX657927 / - / - / -	X	X		X	
435	*Podarcis tauricus*	NHMC 80.3.50.69		Present Study					X	
436	*Podarcis tauricus*	NHMC 80.3.50.70		(Psonis et al., 2017)	KX658232 / KX657928 / - / - / -	X	X			

Sample Code	Taxon Name	NHMC Voucher Numbers (or isolate codes of NCBI sequences)	Country – Region – Locality	Study	Sanger / ddRADseq Sequences Accession Numbers (16S rRNA/cyt *b*/MC1R/Pod15b/Pod55)	I. Phylogeny (Sanger data) by Psonis et al. 2017	II. Demography and mtDNA haplotype networks (Sanger data)	III. Molecular Dating (Sanger data)	IV. Microsatellites data	V. ddRADseq data
437	*Podarcis tauricus*	NHMC 80.3.50.71	Sevastopol territory Crimea – Southern Coast – near Cape Sarych, locality of Choban-Tash; Sevastopol territory Crimea – western border between Main range of the Crimean Mts. and Southern Coast – near town of Balaclava,Range Spilia; Sevastopol territory Crimea – western border between Main range of the Crimean Mts. and western Foothills – between villages of Rodnoe and Ternovka; Sevastopol territory Crimea – western border between Main range of the Crimean Mts. and western Foothills – between villages	Present Study					X	
438	*Podarcis tauricus*	NHMC 80.3.50.72		(Psonis et al., 2017)	KX658233 / KX657929 / - / - / -	X	X		X	X
439	*Podarcis tauricus*	NHMC 80.3.50.73		(Psonis et al., 2017)	KX658234 / KX657930 / - / - / -	X	X		X	X
440	*Podarcis tauricus*	NHMC 80.3.50.74		(Psonis et al., 2017)	KX658235 / KX657931 / - / - / -	X	X		X	X

Sample Code	Taxon Name	NHMC Voucher Numbers (or isolate codes of NCBI sequences)	Country – Region – Locality	Study	Sanger / ddRADseq Sequences Accession Numbers (16S rRNA/cyt *b*/MC1R/Pod15b/Pod55)	I. Phylogeny (Sanger data) by Psonis et al. 2017	II. Demography and mtDNA haplotype networks (Sanger data)	III. Molecular Dating (Sanger data)	IV. Microsatellites data	V. ddRADseq data
441	*Podarcis tauricus*	NHMC 80.3.50.75	of Rodnoe and Ternovka; Sevastopol territory Crimea – western border between Main range of the Crimean Mts. and western Foothills – between villages of Rodnoe and Ternovka; Sevastopol territory	Present Study					X	
442	*Podarcis tauricus*	NHMC 80.3.50.76	Crimea – western border between Main range of the Crimean Mts. and western Foothills – between villages of Rodnoe and Ternovka; Sevastopol territory	Present Study					X	
443	*Podarcis tauricus*	NHMC 80.3.50.77	Crimea – extreme eastern maritime plot of Main Range of the Crimean Mts. – Dvuyakornaya Valley, between village of Yuzhnoe and settlement Ordzhonikidze;	Present Study					Discarded	

Sample Code	Taxon Name	NHMC Voucher Numbers (or isolate codes of NCBI sequences)	Country – Region – Locality	Study	Sanger / ddRADseq Sequences Accession Numbers (16S rRNA/cyt *b*/MC1R/Pod15b/Pod55)	I. Phylogeny (Sanger data) by Psonis et al. 2017	II. Demography and mtDNA haplotype networks (Sanger data)	III. Molecular Dating (Sanger data)	IV. Microsatellites data	V. ddRADseq data
444	*Podarcis tauricus*	NHMC 80.3.50.78	Theodosia territory Crimea – extreme eastern maritime plot of Main Range of the Crimean Mts. – Dvuyakornaya Valley, between village of Yuzhnoe and settlement Ordzhonikidze;	Present Study					Discarded	
445	*Podarcis tauricus*	NHMC 80.3.50.79	Theodosia territory Crimea – extreme eastern maritime plot of Main Range of the Crimean Mts. – Dvuyakornaya Valley, between village of Yuzhnoe and settlement Ordzhonikidze;	(Psonis et al., 2017)	KX658236 / KX657932 / - / - / -	X	X		X	
446	*Podarcis tauricus*	NHMC 80.3.50.80	Theodosia territory Crimea – extreme eastern maritime plot of Main Range of the Crimean Mts. – Dvuyakornaya Valley, between village of Yuzhnoe and settlement	(Psonis et al., 2017)	KX658237 / KX657933 / - / - / -	X	X		X	

Sample Code	Taxon Name	NHMC Voucher Numbers (or isolate codes of NCBI sequences)	Country – Region – Locality	Study	Sanger / ddRADseq Sequences Accession Numbers (16S rRNA/cyt *b*/MC1R/Pod15b/Pod55)	I. Phylogeny (Sanger data) by Psonis et al. 2017	II. Demography and mtDNA haplotype networks (Sanger data)	III. Molecular Dating (Sanger data)	IV. Microsatellites data	V. ddRADseq data
447	*Podarcis tauricus*	NHMC 80.3.50.81	Ordzhonikidze; Theodosia territory Crimea – eastern Foothills – Mt. Ak–Kaya, Belogorsk Distr.	(Psonis et al., 2017)	KX658238 / KX657934 / - / - / -	X	X		X	
448	*Podarcis tauricus*	NHMC 80.3.50.82	Crimea – eastern Foothills – Mt. Ak–Kaya, Belogorsk Distr.	(Psonis et al., 2017)	KX658239 / KX657935 / - / - / -	X	X		X	
449	*Podarcis tauricus*	NHMC 80.3.50.83	Crimea – eastern Foothills – Mt. Ak–Kaya, Belogorsk Distr.	Present Study					X	
450	*Podarcis tauricus*	NHMC 80.3.50.84	Romania - Muntii Macinului	(Psonis et al., 2017)	KX658240 / KX657936 / - / - / -	X	X		X	
451	*Podarcis tauricus*	NHMC 80.3.50.85	Romania - Muntii Macinului	(Psonis et al., 2017)	KX658241 / KX657937 / - / - / -	X	X		X	
452	*Podarcis tauricus*	NHMC 80.3.50.86	Crimea – Black Sea coast of Kerch Peninsula – Mt. Opuk, Lenin's Distr.	Present Study					X	
453	*Podarcis tauricus*	NHMC 80.3.50.87	Crimea – Black Sea coast of Kerch Peninsula – Mt. Opuk, Lenin's Distr.	(Psonis et al., 2017)	KX658242 / KX657938 / - / - / -	X	X		X	
454	*Podarcis tauricus*	NHMC 80.3.50.88	Crimea – Azov Sea, coast of Kerch Penisula – Karalarskaya Steppe, between Cape Chagany (near village Zolotoe) and salt Lake	(Psonis et al., 2017)	KX658243 / KX657939 / KX658505 / KX658558 / KX658611	X	X	X	X	

Sample Code	Taxon Name	NHMC Voucher Numbers (or isolate codes of NCBI sequences)	Country – Region – Locality	Study	Sanger / ddRADseq Sequences Accession Numbers (16S rRNA/cyt *b*/MC1R/Pod15b/Pod55)	I. Phylogeny (Sanger data) by Psonis et al. 2017	II. Demography and mtDNA haplotype networks (Sanger data)	III. Molecular Dating (Sanger data)	IV. Microsatellites data	V. ddRADseq data
455	*Podarcis tauricus*	NHMC 80.3.50.89	Chokrak, Lenino Distr. Crimea – Azov Sea coast of Kerch Penisula – Karalarskaya Steppe, valley of sulfatar spring Suurtash, Lenino Distr.	Present Study					X	
456	*Podarcis tauricus*	NHMC 80.3.50.90	Crimea – Azov Sea coast of Kerch Penisula – Karalarskaya Steppe, valley of sulfatar spring Suurtash, Lenino Distr.	Present Study					X	
457	*Podarcis tauricus*	NHMC 80.3.50.91	Crimea – Azov Sea coast of Kerch Penisula – Karalarskaya Steppe, valley of sulfatar spring Suurtash, Lenino Distr.	Present Study					X	
458	*Podarcis tauricus*	NHMC 80.3.50.92	Crimea – Azov Sea coast of Kerch Penisula – Karalarskaya Steppe, valley of sulfatar spring Suurtash, Lenino Distr.	(Psonis et al., 2017)	KX658244 / KX657940 / - / - / -	X	X		X	
459	*Podarcis tauricus*	NHMC 80.3.50.93	Crimea – Azov Sea coast of Kerch Peninsula – Karalarskaya Steppe, valley of river Sernaya, Lenino Distr.	(Psonis et al., 2017)	KX658245 / KX657941 / - / - / -	X	X		X	

Sample Code	Taxon Name	NHMC Voucher Numbers (or isolate codes of NCBI sequences)	Country – Region – Locality	Study	Sanger / ddRADseq Sequences Accession Numbers (16S rRNA/cyt *b*/MC1R/Pod15b/Pod55)	I. Phylogeny (Sanger data) by Psonis et al. 2017	II. Demography and mtDNA haplotype networks (Sanger data)	III. Molecular Dating (Sanger data)	IV. Microsatellites data	V. ddRADseq data
462	*Podarcis tauricus*	NHMC 80.3.50.96	Crimea – near the border of the western Foothills and Main Range – sanatorium Adzhi–Su, environs of village Polyana, Bakhchisarayi Distr.	(Psonis et al., 2017)	KX658246 / KX657942 / - / - / -	X	X		X	
463	*Podarcis tauricus*	NHMC 80.3.50.97	Crimea – eastern part of the Kerch Peninsula – ruins of ancient town Ilurat near village Ivanovka, Lenino Distr.	(Psonis et al., 2017)	KX658247 / KX657943 / - / - / -	X	X		X	
464	*Podarcis tauricus*	NHMC 80.3.50.98	Crimea – extreme eastern , part of Black Sea coast of Kerch Peninsula – environs of the village Yakovenkovo, Cape Ak–Burun, Lenino Distr.	(Psonis et al., 2017)	KX658248 / KX657944 / - / - / -	X	X		X	
465	*Podarcis tauricus*	NHMC 80.3.50.99	Serbia environs of the village Šumarak	(Psonis et al., 2017)	KX658249 / KX657945 / - / - / -	X	X		X	
466	*Podarcis tauricus*	NHMC 80.3.50.100	Turkey - suburbs of Adapazary	Present Study					Discarded	
467	*Podarcis tauricus*	NHMC 80.3.50.101	eastern coast of the lake Sapanca Romania – ancient colony	(Psonis et al., 2017)	KX658250 / KX657946 / - / - / -	X	X		X	

Sample Code	Taxon Name	NHMC Voucher Numbers (or isolate codes of NCBI sequences)	Country – Region – Locality	Study	Sanger / ddRADseq Sequences Accession Numbers (16S rRNA/cyt *b*/MC1R/Pod15b/Pod55)	I. Phylogeny (Sanger data) by Psonis et al. 2017	II. Demography and mtDNA haplotype networks (Sanger data)	III. Molecular Dating (Sanger data)	IV. Microsatellites data	V. ddRADseq data
468	*Podarcis tauricus*	NHMC 80.3.50.102	Histria near Tulcea Romania – ancient colony	(Psonis et al., 2017)	KX658251 / KX657947 / - / - / -	X	X		X	
469	*Podarcis tauricus*	NHMC 80.3.50.103	Histria near Tulcea Romania – ancient colony	(Psonis et al., 2017)	KX658252 / KX657948 / - / - / -	X	X		X	
470	*Podarcis tauricus*	NHMC 80.3.50.104	Histria near Tulcea Romania – ancient colony	(Psonis et al., 2017)	KX658253 / KX657949 / - / - / -	X	X			
471	*Podarcis tauricus*	NHMC 80.3.50.105	Histria near Tulcea Romania – ancient colony	(Psonis et al., 2017)	KX658254 / KX657950 / - / - / -	X	X		X	
472	*Podarcis tauricus*	NHMC 80.3.50.106	Ukraine – northern border of Stentsovsko–Zhebriyanskie marshy areas – environs of the village Desantnoe, Killia Distr., Odessa Province	(Psonis et al., 2017)	KX658255 / KX657951 / - / - / -	X	X		X	
473	*Podarcis tauricus*	NHMC 80.3.50.107	Ukraine – northern border of Stentsovsko–Zhebriyanskie marshy areas – environs of the village Desantnoe, Killia Distr., Odessa Province	Present Study					Discarded	
474	*Podarcis tauricus*	NHMC 80.3.50.108	Crimea – SE part of Main Range, upper	(Psonis et al., 2017)	KX658256 / KX657952 / - / - / -	X	X		X	

Sample Code	Taxon Name	NHMC Voucher Numbers (or isolate codes of NCBI sequences)	Country – Region – Locality	Study	Sanger / ddRADseq Sequences Accession Numbers (16S rRNA/cyt *b*/MC1R/Pod15b/Pod55)	I. Phylogeny (Sanger data) by Psonis et al. 2017	II. Demography and mtDNA haplotype networks (Sanger data)	III. Molecular Dating (Sanger data)	IV. Microsatellites data	V. ddRADseq data
475	*Podarcis tauricus*	NHMC 80.3.50.109	belt of southern macroslope – SW spur of Ridge Papas–Tepe between the settlement Krasnokamenka and village Lesnoe, Sudak territory. Crimea – SW part of Main Range – area of the Pass Bechku between the Valleys Baidarskaya and Belbekskaya environs of village Peredovoe, border of Sevastopol territory and Bakhshisarayi Distr. Crimea – SE part of Main Range, upper belt of southern macroslope – southern slopes of Upland Karabi–Yaila, valley of river Mikropotamo and foot of Mt. Likon, environs of the village Generalskoe; Alushta territory	(Psonis et al., 2017)	KX658257 / KX657953 / - / - / -	X	X		X	
476	*Podarcis tauricus*	NHMC 80.3.50.110		(Psonis et al., 2017)	KX658258 / KX657954 / - / - / -	X	X		X	

Sample Code	Taxon Name	NHMC Voucher Numbers (or isolate codes of NCBI sequences)	Country – Region – Locality	Study	Sanger / ddRADseq Sequences Accession Numbers (16S rRNA/cyt *b*/MC1R/Pod15b/Pod55)	I. Phylogeny (Sanger data) by Psonis et al. 2017	II. Demography and mtDNA haplotype networks (Sanger data)	III. Molecular Dating (Sanger data)	IV. Microsatellites data	V. ddRADseq data
477	*Podarcis tauricus*	NHMC 80.3.50.111	Crimea – NW Crimean height plain – between the settlement Chernomorskyi and the village Olenevka, northern coast of Tarkhankutskyi Penisula, Chernomorskoe Distr.	(Psonis et al., 2017)	KX658259 / KX657955 / - / - / -	X	X		X	
479	*Podarcis tauricus*	NHMC 80.3.50.113	Crimea – NW Crimean height plain – between the settlement Chernomorskyi and the village Olenevka, northern coast of Tarkhankutskyi Penisula, Chernomorskoe Distr	(Psonis et al., 2017)	KX658260 / KX657956 / - / - / -	X	X		X	
480	*Podarcis tauricus*	NHMC 80.3.50.114	Crimea – Southern Coast – environs of s. Parthenit, Cape Ayu-Dagh, Alushta Territory	(Psonis et al., 2017)	KX658261 / KX657957 / - / - / -	X	X			
481	*Podarcis tauricus*	NHMC 80.3.50.115	Crimea – Southern Coast – s. Vinogradnyi, Alushta territory	(Psonis et al., 2017)	KX658262 / KX657958 / - / - / -	X	X			
482	*Podarcis tauricus*	NHMC 80.3.50.116	Crimea – western Foothills –	(Psonis et al., 2017)	KX658263 / KX657959 / - / - / -	X	X		Discarded	

Sample Code	Taxon Name	NHMC Voucher Numbers (or isolate codes of NCBI sequences)	Country – Region – Locality	Study	Sanger / ddRADseq Sequences Accession Numbers (16S rRNA/cyt *b*/MC1R/Pod15b/Pod55)	I. Phylogeny (Sanger data) by Psonis et al. 2017	II. Demography and mtDNA haplotype networks (Sanger data)	III. Molecular Dating (Sanger data)	IV. Microsatellites data	V. ddRADseq data
483	*Podarcis tauricus*	NHMC 80.3.50.117	village Kuibyshevo Bahshisarayi Distr. Crimea – Suburbs of Balaclava, Kanrobers Hill, Valley of death, Sevastopol territory	Present Study					Discarded	
484	*Podarcis tauricus*	NHMC 80.3.50.118	Crimea – western Foothills – v. Priyatnoe Svidanie, Mt. Bakla, Bakhshisarayi Distr.	(Psonis et al., 2017)	KX658264 / KX657960 / - / - / -	X	X		X	
485	*Podarcis tauricus*	NHMC 80.3.50.119	Crimea – central Foothills – suburbs of Simferopol, coast of Simferopol reservoire, Simferopol Distr.	(Psonis et al., 2017)	KX658265 / KX657961 / - / - / -	X	X		X	
486	*Podarcis tauricus*	NHMC 80.3.50.120	Crimea – western plain – v. Skvortsovo, Simferopol Distr.	(Psonis et al., 2017)	KX658266 / KX657962 / - / - / -	X	X		X	
489	*Podarcis tauricus*	NHMC 80.3.50.123	Crimea – western Foothills – v. Preduschelnoe, Mt Kachi–Kal'on, Bakhchisarayi Distr.	(Psonis et al., 2017)	KX658267 / KX657963 / - / - / -	X	X		X	

Sample Code	Taxon Name	NHMC Voucher Numbers (or isolate codes of NCBI sequences)	Country – Region – Locality	Study	Sanger / ddRADseq Sequences Accession Numbers (16S rRNA/cyt *b*/MC1R/Pod15b/Pod55)	I. Phylogeny (Sanger data) by Psonis et al. 2017	II. Demography and mtDNA haplotype networks (Sanger data)	III. Molecular Dating (Sanger data)	IV. Microsatellites data	V. ddRADseq data
490	*Podarcis tauricus*	NHMC 80.3.50.124	Crimea – extreme eastern plot of Main Range – stm. Solnechnyi, foot of Mt. Pasha Oba, Theodosia Distr.	(Psonis et al., 2017)	KX658268 / KX657964 / - / - / -	X	X		X	
491	*Podarcis tauricus*	NHMC 80.3.50.125	Crimea – SE coast – stm. Schebetovka, northern clope of Mt. Echki-Dagh, Theodosia territory	(Psonis et al., 2017)	KX658269 / KX657965 / - / - / -	X	X		X	
492	*Podarcis tauricus*	NHMC 80.3.50.126	Crimea – SE coast – Karadagh Reserve, SE slope of Mt. Karadagh, Theodosia territory	(Psonis et al., 2017)	KX658270 / KX657966 / - / - / -	X	X		X	
493	*Podarcis tauricus*	NHMC 80.3.50.127	Crimea – SE coast – Karadagh Reserve, Southern slope of Ridge Kara-Agach, Theodosia territory	(Psonis et al., 2017)	KX658271 / KX657967 / - / - / -	X	X		X	
494	*Podarcis tauricus*	NHMC 80.3.50.128	Crimea – SE coast – Karadagh Reserve, Karadagh Valley, Theodosia territory	(Psonis et al., 2017)	KX658272 / KX657968 / - / - / -	X	X		X	

Sample Code	Taxon Name	NHMC Voucher Numbers (or isolate codes of NCBI sequences)	Country – Region – Locality	Study	Sanger / ddRADseq Sequences Accession Numbers (16S rRNA/cyt *b*/MC1R/Pod15b/Pod55)	I. Phylogeny (Sanger data) by Psonis et al. 2017	II. Demography and mtDNA haplotype networks (Sanger data)	III. Molecular Dating (Sanger data)	IV. Microsatellites data	V. ddRADseq data
495	*Podarcis tauricus*	NHMC 80.3.50.129	Crimea – SE coast – stm. Krasnokamenka, Mt. Frenk Mezer, Sudak territory.	(Psonis et al., 2017)	KX658273 / KX657969 / - / - / -	X	X		X	
496	*Podarcis tauricus*	NHMC 80.3.50.130	Crimea – SE coast – Karadagh Reserve, S slope of Ridge Kara-Agach, Theodosia territory	(Psonis et al., 2017)	KX658274 / KX657970 / - / - / -	X	X		X	
497	*Podarcis tauricus*	NHMC 80.3.50.131	Crimea – SE coast – stm. Krasnokamenka, Mt. Gondarly-Kaya, Sudak territory	(Psonis et al., 2017)	KX658275 / KX657971 / - / - / -	X	X		X	
498	*Podarcis tauricus*	NHMC 80.3.50.132	Crimea – SE coast – Karadagh Reserve, SE slope of Mt. Karadagh, Theodosia territory	(Psonis et al., 2017)	KX658276 / KX657972 / - / - / -	X	X		X	
499	*Podarcis tauricus*	NHMC 80.3.50.133	Crimea – SE coast – Karadagh Reserve, NW slope of Mt. Legener Theodosia territory	(Psonis et al., 2017)	KX658277 / KX657973 / - / - / -	X	X		X	
500	*Podarcis tauricus*	NHMC 80.3.50.134	Crimea – SE coast – Karadagh Reserve, Biological	(Psonis et al., 2017)	KX658278 / KX657974 / - / - / -	X	X		X	

Sample Code	Taxon Name	NHMC Voucher Numbers (or isolate codes of NCBI sequences)	Country – Region – Locality	Study	Sanger / ddRADseq Sequences Accession Numbers (16S rRNA/cyt *b*/MC1R/Pod15b/Pod55)	I. Phylogeny (Sanger data) by Psonis et al. 2017	II. Demography and mtDNA haplotype networks (Sanger data)	III. Molecular Dating (Sanger data)	IV. Microsatellites data	V. ddRADseq data
501	*Podarcis tauricus*	NHMC 80.3.50.135	station, Theodosia territory Crimea – central part of Kerch Peninsula – between village Doroshenkovo and reservoir Yuzmak, Lenino Distr.	(Psonis et al., 2017)	KX658279 / KX657975 / - / - / -	X	X		X	
502	*Podarcis tauricus*	NHMC 80.3.50.136	Crimea – eastern part of Kerch Peninsula – village Ivanovka, Churbashskaya ravine, near ancient town Ilurat, Lenino Distr.	(Psonis et al., 2017)	KX658280 / KX657976 / - / - / -	X	X		X	
503	*Podarcis tauricus*	NHMC 80.3.50.137	Crimea – central part of Kerch Peninsula – village Leninskoe, southern slope of Ridge Parpachskyi, Lenino Distr.	(Psonis et al., 2017)	KX658281 / KX657977 / - / - / -	X	X		X	
504	*Podarcis tauricus*	NHMC 80.3.50.138	Crimea – SE part of Kerch Peninsula – village Zavetnoe, Lenino Distr.	(Psonis et al., 2017)	KX658282 / KX657978 / - / - / -	X	X		X	
505	*Podarcis tauricus*	NHMC 80.3.50.8	Greece – Florina – Prespes lakes	Present SAtudy					Discarded	
510	*Podarcis tauricus*	NHMC 80.3.50.48	Greece – Larisa – Kalyvia, 3.5km NE	(Psonis et al., 2017)	KX658286 / KX657982 / KX658506 / KX658559 / KX658612	X	X	X	X	

Sample Code	Taxon Name	NHMC Voucher Numbers (or isolate codes of NCBI sequences)	Country – Region – Locality	Study	Sanger / ddRADseq Sequences Accession Numbers (16S rRNA/cyt *b*/MC1R/Pod15b/Pod55)	I. Phylogeny (Sanger data) by Psonis et al. 2017	II. Demography and mtDNA haplotype networks (Sanger data)	III. Molecular Dating (Sanger data)	IV. Microsatellites data	V. ddRADseq data
512	*Podarcis tauricus*	NHMC 80.3.50.302	Greece – Florina – Prespes lakes	(Psonis et al., 2017)	KX658288 / KX657984 / - / - / -	X	X		X	
514	*Podarcis tauricus*	NHMC 80.3.50.139	Greece – Grevena – Voio Mt., Aidona	(Psonis et al., 2017)	KX658290 / KX657986 / - / - / -	X	X		X	
515	*Podarcis tauricus*	NHMC 80.3.50.140	Greece – Grevena – Voio Mt., Aidona	(Psonis et al., 2017)	- / KX657987 / - / - / -	X			X	
516	*Podarcis tauricus*	NHMC 80.3.50.141	Greece – Grevena – Voio Mt., Aidona	(Psonis et al., 2017)	KX658291 / KX657988/ KX658507 / KX658560 / KX658613	X	X	X	X	
517	*Podarcis tauricus*	NHMC 80.3.50.142	Greece – Grevena – Voio Mt., Aidona	(Psonis et al., 2017)	KX658292 / KX657989 / - / - / -	X	X		X	
518	*Podarcis tauricus*	NHMC 80.3.50.143	Greece – Kozani – Voio Mt., Agios Sotiras	(Psonis et al., 2017)	- / KX657990 / - / - / -	X			X	
519	*Podarcis tauricus*	NHMC 80.3.50.144	Greece – Kozani – Voio Mt., Agios Sotiras	Present Study					Discarded	
520	*Podarcis tauricus*	NHMC 80.3.50.145	Greece – Kozani – Voio Mt., Vouxorina	(Psonis et al., 2017)	KX658293 / KX657991 / - / - / -	X	X		X	
521	*Podarcis tauricus*	NHMC 80.3.50.146	Greece – Kozani – Voio Mt., Agioi Anargyroi	(Psonis et al., 2017)	KX658294 / KX657992 / - / - / -	X	X		X	
522	*Podarcis tauricus*	NHMC 80.3.50.147	Greece – Trikala – Antichasia Mt., Korydalos	(Psonis et al., 2017)	KX658295 / KX657993 / - / - / -	X	X		X	
523	*Podarcis tauricus*	NHMC 80.3.50.148	Greece – Trikala – Antichasia Mt., Korydalos	(Psonis et al., 2017)	KX658296 / KX657994 / KX658508 / KX658561 / KX658614	X	X	X	X	
524	*Podarcis tauricus*	NHMC 80.3.50.149	Serbia – Brvenica	(Psonis et al., 2017)	KX658297 / KX657995 / - / - / -	X	X		X	
525	*Podarcis tauricus*	NHMC 80.3.50.150	Serbia – road to Studenica	(Psonis et al., 2017)	KX658298 / KX657996 / - / - / -	X	X		X	
526	*Podarcis tauricus*	NHMC 80.3.50.151	Serbia – Maglič	(Psonis et al., 2017)	KX658299 / KX657997 / - / - / -	X	X		X	
527	*Podarcis tauricus*	NHMC 80.3.50.152	Ukraine – eastern environs of the villages	(Psonis et al., 2017)	KX658300 / KX657998 / - / - / -	X	X		X	

Sample Code	Taxon Name	NHMC Voucher Numbers (or isolate codes of NCBI sequences)	Country – Region – Locality	Study	Sanger / ddRADseq Sequences Accession Numbers (16S rRNA/cyt *b*/MC1R/Pod15b/Pod55)	I. Phylogeny (Sanger data) by Psonis et al. 2017	II. Demography and mtDNA haplotype networks (Sanger data)	III. Molecular Dating (Sanger data)	IV. Microsatellites data	V. ddRADseq data
535	*Podarcis tauricus*	NHMC 80.3.50.160	Tabaki and Zaliznichne, Odessa Province, Bolgradskyi Distr. Ukraine – Ukrainian-Moldavian state border along the river Bol'shoyi Yalpug, Odessa Province, Bolgradskyi Distr., Ukraine – right bank of Dnieper river – suburbs of town of Nikolaev, settlement Shirokaya Balka, Nikolaev Province Ukraine – right bank of Dnieper river – suburbs of town of Nikolaev, settlement Shirokaya Balka, Nikolaev Province Ukraine – right bank of Dnieper river – suburbs of town of Nikolaev, settlement	Present Study				X	
536	*Podarcis tauricus*	NHMC 80.3.50.161		(Psonis et al., 2017)	KX658301 / KX657999 / - / - / -	X	X		X	
537	*Podarcis tauricus*	NHMC 80.3.50.162		Present Study					X	
538	*Podarcis tauricus*	NHMC 80.3.50.163		(Psonis et al., 2017)	KX658302 / KX658000 / - / - / -	X	X		X	

Sample Code	Taxon Name	NHMC Voucher Numbers (or isolate codes of NCBI sequences)	Country – Region – Locality	Study	Sanger / ddRADseq Sequences Accession Numbers (16S rRNA/cyt *b*/MC1R/Pod15b/Pod55)	I. Phylogeny (Sanger data) by Psonis et al. 2017	II. Demography and mtDNA haplotype networks (Sanger data)	III. Molecular Dating (Sanger data)	IV. Microsatellites data	V. ddRADseq data
539	*Podarcis tauricus*	NHMC 80.3.50.164	Ukraine – right bank of Dnieper river – suburbs of town of Nikolaev, settlement Shirokaya Balka, Nikolaev Province	Present Study					X	
540	*Podarcis tauricus*	NHMC 80.3.50.165	Ukraine – right bank of Dnieper river – suburbs of town of Nikolaev, settlement Shirokaya Balka, Nikolaev Province	Present Study					X	
541	*Podarcis tauricus*	NHMC 80.3.50.166	Moldova – on the river Yalpug, suburbs of town of Comrat, autonomous region of Gagauzia	(Psonis et al., 2017)	KX658303 / KX658001 / - / - / -	X	X		X	
542	*Podarcis tauricus*	NHMC 80.3.50.167	Moldova – on the river Yalpug, suburbs of town of Comrat, autonomous region of Gagauzia	(Psonis et al., 2017)	KX658304 / KX658002 / - / - / -	X	X		X	
543	*Podarcis tauricus*	NHMC 80.3.50.168	Moldova – on the river Yalpug, suburbs of town of	(Psonis et al., 2017)	KX658305 / KX658003 / - / - / -	X	X		X	

Sample Code	Taxon Name	NHMC Voucher Numbers (or isolate codes of NCBI sequences)	Country – Region – Locality	Study	Sanger / ddRADseq Sequences Accession Numbers (16S rRNA/cyt *b*/MC1R/Pod15b/Pod55)	I. Phylogeny (Sanger data) by Psonis et al. 2017	II. Demography and mtDNA haplotype networks (Sanger data)	III. Molecular Dating (Sanger data)	IV. Microsatellites data	V. ddRADseq data
544	*Podarcis tauricus*	NHMC 80.3.50.169	Comrat, autonomous region of Gagauzia Moldova – on the river Yalpug, suburbs of town of Comrat, autonomous region of Gagauzia	(Psonis et al., 2017)	KX658306 / KX658004 / - / - / -	X	X		X	
556	*Podarcis tauricus*	NHMC 80.3.50.190	Romania – Tulcea – Macin	(Psonis et al., 2017)	KX658307 / KX658005 / - / - / -	X	X		X	
557	*Podarcis tauricus*	NHMC 80.3.50.191	Romania – Tulcea – Babadag	(Psonis et al., 2017)	KX658308 / KX658006 / - / - / -	X	X		X	
558	*Podarcis tauricus*	NHMC 80.3.50.192	Romania – Constanta county – Canaraua Feti	(Psonis et al., 2017)	KX658309 / KX658007 / - / - / -	X	X		X	
559	*Podarcis tauricus*	NHMC 80.3.50.193	Romania – Constanta county – Gura Dobrogei	(Psonis et al., 2017)	KX658310 / KX658008 / - / - / -	X	X		X	
561	*Podarcis tauricus*	NHMC 80.3.50.196	Bulgaria – Golyamo Bukovo, Distr. Sredets	(Psonis et al., 2017)	KX658311 / KX658009 / - / - / -	X	X		X	
562	*Podarcis tauricus*	NHMC 80.3.50.197	Bulgaria – Petrelik, Distr. Gotse Delchev	(Psonis et al., 2017)	KX658312 / KX658010 / - / - / -	X	X		X	
563	*Podarcis tauricus*	NHMC 80.3.50.198	Bulgaria – Krapchene, Distr. Montana	(Psonis et al., 2017)	KX658313 / KX658011 / - / - / -	X	X		X	
564	*Podarcis tauricus*	NHMC 80.3.50.199	Bulgaria – Ognyanovo, Distr. Pazardzhik	(Psonis et al., 2017)	KX658314 / KX658012 / - / - / -	X	X		X	
565	*Podarcis tauricus*	NHMC 80.3.50.200	Bulgaria – Sredna Gora	(Psonis et al., 2017)	KX658315 / KX658013 / - / - / -	X	X		X	

Sample Code	Taxon Name	NHMC Voucher Numbers (or isolate codes of NCBI sequences)	Country – Region – Locality	Study	Sanger / ddRADseq Sequences Accession Numbers (16S rRNA/cyt *b*/MC1R/Pod15b/Pod55)	I. Phylogeny (Sanger data) by Psonis et al. 2017	II. Demography and mtDNA haplotype networks (Sanger data)	III. Molecular Dating (Sanger data)	IV. Microsatellites data	V. ddRADseq data
566	*Podarcis tauricus*	NHMC 80.3.50.178	Mt., near Panagyurishte Serbia – Gaj village	(Psonis et al., 2017)	KX658316 / KX658014 / - / - / -	X	X		X	
568	*Podarcis tauricus*	NHMC 80.3.50.180	Serbia – surroundings of Banatska Palanka	(Psonis et al., 2017)	KX658317 / KX658015 / - / - / -	X	X		X	
570	*Podarcis tauricus*	NHMC 80.3.50.182	Serbia – environs of Donji Milanovac	(Psonis et al., 2017)	KX658318 / KX658016 / - / - / -	X	X		X	
571	*Podarcis tauricus*	NHMC 80.3.50.183	Serbia – Diana Karataš	(Psonis et al., 2017)	KX658319 / KX658017 / - / - / -	X	X		X	
574	*Podarcis tauricus*	NHMC 80.3.50.187	Serbia – environs of Trgovište	(Psonis et al., 2017)	KX658320 / KX658018 / - / - / -	X	X		X	
576	*Podarcis tauricus*	NHMC 80.3.50.201	Ukraine – eastern environs of the villages Tabaki and Zaliznichne, Odessa Province, Bolgradskyi Distr.	(Psonis et al., 2017)	KX658321 / KX658019 / - / - / -	X	X		X	
582	*Podarcis tauricus*	NHMC 80.3.50.207	Ukraine – Ukrainian-Moldavian state border along the river Bol'shoyi Yalpug, Odessa Province, Bolgradskyi Distr.,	(Psonis et al., 2017)	KX658322 / KX658020 / - / - / -	X	X		X	
583	*Podarcis tauricus*	NHMC 80.3.50.208	Ukraine – Odessa Province, Bolgradskyi Distr.	(Psonis et al., 2017)	KX658323 / KX658021 / - / - / -	X	X		X	

Sample Code	Taxon Name	NHMC Voucher Numbers (or isolate codes of NCBI sequences)	Country – Region – Locality	Study	Sanger / ddRADseq Sequences Accession Numbers (16S rRNA/cyt *b*/MC1R/Pod15b/Pod55)	I. Phylogeny (Sanger data) by Psonis et al. 2017	II. Demography and mtDNA haplotype networks (Sanger data)	III. Molecular Dating (Sanger data)	IV. Microsatellites data	V. ddRADseq data
584	*Podarcis tauricus*	NHMC 80.3.50.209	Ukraine – right bank of Dnieper river – suburbs of town of Nikolaev, settlement Shirokaya Balka, Nikolaev Province	(Psonis et al., 2017)	KX658324 / KX658022 / - / - / -	X	X		X	
588	*Podarcis tauricus*	NHMC 80.3.50.213	Moldova – on the river Yalpug, suburbs of town of Comrat, autonomous region of Gagauzia	(Psonis et al., 2017)	KX658325 / KX658023 / - / - / -	X	X		X	
592	*Podarcis tauricus*	NHMC 80.3.50.217	Crimea – SE coast, Karadagh Reserve, Mt. Malyi Karadagh, Theodosia territory	(Psonis et al., 2017)	KX658326 / KX658024 / - / - / -	X	X		X	
593	*Podarcis tauricus*	NHMC 80.3.50.218	Crimea – Tarkhankutskyi Peninsula, 5,5km to N-NW from village Olenevka, locality Dzhanghul', Chernomorskoe Distr..	(Psonis et al., 2017)	KX658327 / KX658025 / - / - / -	X	X		X	
594	*Podarcis tauricus*	NHMC 80.3.50.220	Crimea – extreme western part of Southern Coast, 1,5 km to SE from town of Balaclava, loc. Micro–Yalo,	(Psonis et al., 2017)	KX658328 / KX658026 / - / - / -	X	X		X	

Sample Code	Taxon Name	NHMC Voucher Numbers (or isolate codes of NCBI sequences)	Country – Region – Locality	Study	Sanger / ddRADseq Sequences Accession Numbers (16S rRNA/cyt *b*/MC1R/Pod15b/Pod55)	I. Phylogeny (Sanger data) by Psonis et al. 2017	II. Demography and mtDNA haplotype networks (Sanger data)	III. Molecular Dating (Sanger data)	IV. Microsatellites data	V. ddRADseq data
611	*Podarcis tauricus*	NHMC 80.3.50.9	Sevastopol territory. Greece – Florina – Prespes lakes	Present Study					Discarded	
612	*Podarcis tauricus*	NHMC 80.3.50.189	Greece – Thessaloniki – Mavrouda	(Psonis et al., 2017)	KX658329 / KX658027 / - / - / -	X	X		X	
628	*Podarcis tauricus*	NHMC 80.3.50.225	FYROM – Vitachevo, S of Kavadarci	(Psonis et al., 2017)	KX658332 / KX658030 / - / - / -	X	X		X	
629	*Podarcis tauricus*	NHMC 80.3.50.226	Bulgaria – Gotse Delchev	(Psonis et al., 2017)	KX658333 / KX658031 / - / - / -	X	X		X	
630	*Podarcis tauricus*	NHMC 80.3.50.227	Bulgaria – Damyanica	(Psonis et al., 2017)	KX658334 / KX658032 / - / - / -	X	X		X	
631	*Podarcis tauricus*	NHMC 80.3.50.228	Bulgaria – Arkutino, sand dunes	(Psonis et al., 2017)	KX658335 / KX658033 / - / - / -	X	X		X	
632	*Podarcis tauricus*	NHMC 80.3.50.229	Bulgaria – Balgari	(Psonis et al., 2017)	KX658336 / KX658034 / - / - / -	X	X		X	
633	*Podarcis tauricus*	NHMC 80.3.50.230	Bulgaria – Malko Tarnovo	(Psonis et al., 2017)	KX658337 / KX658035 / - / - / -	X	X		X	
634	*Podarcis tauricus*	NHMC 80.3.50.231	FYROM – Vitachevo, S of Kavadarci	(Psonis et al., 2017)	KX658338 / KX658036 / - / - / -	X	X		X	
637	*Podarcis tauricus*	NHMC 80.3.50.234	Hungary – Kunpeszér	(Psonis et al., 2017)	KX658339 / KX658037 / - / - / -	X	X		X	
651	*Podarcis tauricus*	NHMC 80.3.50.243	Hungary – Bugac	(Psonis et al., 2017)	KX658348 / KX658046 / - / - / -	X	X		X	
652	*Podarcis tauricus*	NHMC 80.3.50.244	Hungary – Bugac	(Psonis et al., 2017)	KX658349 / KX658047 / - / - / -	X	X		X	
653	*Podarcis tauricus*	NHMC 80.3.50.245	Hungary – Bugac	(Psonis et al., 2017)	KX658350 / KX658048 / - / - / -	X	X		X	
659	*Podarcis tauricus*	NHMC 80.3.50.248	Serbia – Crnovska River	(Psonis et al., 2017)	KX658352 / KX658050 / - / - / -	X	X		X	
660	*Podarcis tauricus*	NHMC 80.3.50.249	Turkey – Keşan	(Psonis et al., 2017)	KX658353 / KX658051 / - / - / -	X	X		X	
661	*Podarcis tauricus*	NHMC 80.3.50.250	Turkey – paragem II pedras berma estrada	(Psonis et al., 2017)	KX658354 / KX658052 / - / - / -	X	X		X	

Sample Code	Taxon Name	NHMC Voucher Numbers (or isolate codes of NCBI sequences)	Country – Region – Locality	Study	Sanger / ddRADseq Sequences Accession Numbers (16S rRNA/cyt *b*/MC1R/Pod15b/Pod55)	I. Phylogeny (Sanger data) by Psonis et al. 2017	II. Demography and mtDNA haplotype networks (Sanger data)	III. Molecular Dating (Sanger data)	IV. Microsatellites data	V. ddRADseq data
662	*Podarcis tauricus*	NHMC 80.3.50.251	Crimea – Mt. Yuzhnaya Demerdżhi, Alushta territory	(Psonis et al., 2017)	KX658355 / KX658053 / - / - / -	X	X		X	
663	*Podarcis tauricus*	NHMC 80.3.50.232 (HNHM-HER_2014.2.1)**	Hungary – Kiskunság – Kunpeszér	(Psonis et al., 2017)	KX658356 / KX658054 / - / - / -	X	X			
664	*Podarcis tauricus*	NHMC 80.3.50.233 (HNHM-HER_2010.68.1)**	Hungary – Kiskunság – Kunpeszér	(Psonis et al., 2017)	KX658357 / KX658055 / - / - / -	X	X		X	
719	*Podarcis tauricus*	NHMC 80.3.50.259	Bulgaria – Ladarevo	(Psonis et al., 2017)	KX658365 / KX658063 / - / - / -	X	X		X	
720	*Podarcis tauricus*	NHMC 80.3.50.260	Bulgaria – Sozopol	(Psonis et al., 2017)	KX658366 / KX658064 / - / - / -	X	X		X	
721	*Podarcis tauricus*	NHMC 80.3.50.261	Serbia – Prohor Pčinjski	(Psonis et al., 2017)	KX658367 / KX658065 / - / - / -	X	X		X	
722	*Podarcis tauricus*	NHMC 80.3.50.262	FYROM – Pretor, Lake Prespa	Present Study					Discarded	
724	*Podarcis tauricus*	NHMC 80.3.50.264	FYROM – Pretor, Lake Prespa	Present Study					Discarded	
725	*Podarcis tauricus*	NHMC 80.3.50.265	FYROM – Pretor, Lake Prespa	Present Study					Discarded	
726	*Podarcis tauricus*	NHMC 80.3.50.266	FYROM – Pretor, Lake Prespa	(Psonis et al., 2017)	KX658368 / KX658066 / - / - / -	X	X		X	
727	*Podarcis tauricus*	NHMC 80.3.50.267	FYROM – Stenje, Lake Prespa	(Psonis et al., 2017)	KX658369 / KX658067 / - / - / -	X	X		X	
728	*Podarcis tauricus*	NHMC 80.3.50.268	FYROM – Stenje, Lake Prespa	(Psonis et al., 2017)	KX658370 / KX658068 / - / - / -	X	X		X	
729	*Podarcis tauricus*	NHMC 80.3.50.269	FYROM – Stenje, Lake Prespa	Present Study					Discarded	
730	*Podarcis tauricus*	NHMC 80.3.50.270	FYROM – Stenje, Lake Prespa	(Psonis et al., 2017)	KX658371 / KX658069 / - / - / -	X	X		X	

Sample Code	Taxon Name	NHMC Voucher Numbers (or isolate codes of NCBI sequences)	Country – Region – Locality	Study	Sanger / ddRADseq Sequences Accession Numbers (16S rRNA/cyt *b*/MC1R/Pod15b/Pod55)	I. Phylogeny (Sanger data) by Psonis et al. 2017	II. Demography and mtDNA haplotype networks (Sanger data)	III. Molecular Dating (Sanger data)	IV. Microsatellites data	V. ddRADseq data
731	*Podarcis tauricus*	NHMC 80.3.50.271	Albania – Lin	Present Study					Discarded	
732	*Podarcis tauricus*	NHMC 80.3.50.272	Albania – Lin	(Psonis et al., 2017)	KX658372 / KX658070 / - / - / -	X	X		X	
733	*Podarcis tauricus*	NHMC 80.3.50.273	Albania – Lin	(Psonis et al., 2017)	KX658373 / KX658071 / - / - / -	X	X		X	
734	*Podarcis tauricus*	NHMC 80.3.50.274	Greece – Florina prefecture – Prespa lakes	Present Study	ddRADseq: TBP					X
735	*Podarcis tauricus*	NHMC 80.3.50.275	Greece – Florina prefecture – Prespa lakes	Present Study	ddRADseq: TBP					X
736	*Podarcis tauricus*	NHMC 80.3.50.276	Greece – Florina prefecture – Prespa lakes	Present Study	ddRADseq: TBP					X
738	*Podarcis tauricus*	NHMC 80.3.50.278	Greece – Florina – Prespes lakes	(Psonis et al., 2017) (Sanger data) / Present Study (ddRADseq)	KX658374 / KX658072 / - / - / - ddRADseq: TBP	X	X		X	X
739	*Podarcis tauricus*	NHMC 80.3.50.279	Greece – Florina – Prespes lakes	(Psonis et al., 2017)	KX658375 / KX658073 / - / - / -	X	X		X	
740	*Podarcis tauricus*	NHMC 80.3.50.280	Greece – Florina – Prespes lakes	(Psonis et al., 2017)	KX658376 / KX658074 / - / - / -	X	X		X	
741	*Podarcis tauricus*	NHMC 80.3.50.281	Greece – Florina – Prespes lakes	(Psonis et al., 2017)	KX658377 / KX658075 / - / - / -	X	X		X	
742	*Podarcis tauricus*	NHMC 80.3.50.282	Greece – Florina – Prespes lakes	(Psonis et al., 2017)	KX658378 / KX658076 / - / - / -	X	X		X	
743	*Podarcis tauricus*	NHMC 80.3.50.283	Greece – Florina – Prespes lakes	(Psonis et al., 2017)	KX658379 / KX658077 / - / - / -	X	X		X	
744	*Podarcis tauricus*	NHMC 80.3.50.284	Greece – Florina – Prespes lakes	(Psonis et al., 2017)	KX658380 / KX658078 / - / - / -	X	X		X	
745	*Podarcis tauricus*	NHMC 80.3.50.285	Greece – Florina – Prespes lakes	(Psonis et al., 2017)	KX658381 / KX658079 / - / - / -	X	X		X	
746	*Podarcis tauricus*	NHMC 80.3.50.286	Greece – Florina – Prespes lakes	(Psonis et al., 2017)	KX658382 / KX658080 / - / - / -	X	X		X	
747	*Podarcis tauricus*	NHMC 80.3.50.287	Greece – Florina – Prespes lakes	(Psonis et al., 2017)	KX658383 / KX658081 / KX658513 / KX658566 / KX658619	X	X	X	X	

Sample Code	Taxon Name	NHMC Voucher Numbers (or isolate codes of NCBI sequences)	Country – Region – Locality	Study	Sanger / ddRADseq Sequences Accession Numbers (16S rRNA/cyt *b*/MC1R/Pod15b/Pod55)	I. Phylogeny (Sanger data) by Psonis et al. 2017	II. Demography and mtDNA haplotype networks (Sanger data)	III. Molecular Dating (Sanger data)	IV. Microsatellites data	V. ddRADseq data
748	*Podarcis tauricus*	NHMC 80.3.50.288	Greece – Florina – Prespes lakes	(Psonis et al., 2017)	KX658384 / KX658082 / - / - / -	X	X		X	
749	*Podarcis tauricus*	NHMC 80.3.50.289	Greece – Florina – Prespes lakes	(Psonis et al., 2017)	KX658385 / KX658083 / - / - / -	X	X		X	
750	*Podarcis tauricus*	NHMC 80.3.50.290	Greece – Florina – Prespes lakes	(Psonis et al., 2017)	KX658386 / KX658084 / - / - / -	X	X		X	
751	*Podarcis tauricus*	NHMC 80.3.50.291	Greece – Florina – Prespes lakes	(Psonis et al., 2017)	KX658387 / KX658085 / - / - / -	X	X		X	
752	*Podarcis tauricus*	NHMC 80.3.50.247	Greece – Florina – Prespes lakes, Agios Germanos	(Psonis et al., 2017)	KX658388 / KX658086 / - / - / -	X	X		X	
776	*Podarcis tauricus*	NHMC 80.3.50.303	Greece – Florina – Prespes lakes	(Psonis et al., 2017)	KX658403 / KX658103 / - / - / -	X	X		X	
777	*Podarcis tauricus*	NHMC 80.3.50.304	Greece – Florina – Prespes lakes	(Psonis et al., 2017)	KX658404 / KX658104 / - / - / -	X	X		X	
797	*Podarcis tauricus*	NHMC 80.3.50.292	FYROM – Stenje, Prespansko jezero	(Psonis et al., 2017)	KX658406 / KX658106 / - / - / -	X	X		X	
798	*Podarcis tauricus*	NHMC 80.3.50.293	FYROM – Stenje, Prespansko jezero	Present Study					Discarded	
799	*Podarcis tauricus*	NHMC 80.3.50.294	FYROM – Stenje, Prespansko jezero	Present Study					Discarded	
800	*Podarcis tauricus*	NHMC 80.3.50.295	Albania – Schendli Mts.	Present Study					Discarded	
815	*Podarcis tauricus*	NHMC 80.3.50.305	Greece – Kavala, Thasos Isl. – Thasopoula islet	(Psonis et al., 2017)	KX658410 / KX658110 / - / - / - ddRADseq: TBP	X	X		X	X
854	*Podarcis tauricus*	NHMC 80.3.50.306	Greece – Kavala, Thasos Isl. – Thasopoula islet	(Psonis et al., 2017) (Sanger data) / Present Study (ddRADseq)	KX658411 / KX658111 / - / - / - ddRADseq: TBP	X	X		X	X
855	*Podarcis tauricus*	NHMC 80.3.50.307	Greece – Kavala, Thasos Isl. – Thasopoula islet	(Psonis et al., 2017) (Sanger data) / Present Study (ddRADseq)	KX658412 / KX658112 / - / - / - ddRADseq: TBP	X	X		X	X

Sample Code	Taxon Name	NHMC Voucher Numbers (or isolate codes of NCBI sequences)	Country – Region – Locality	Study	Sanger / ddRADseq Sequences Accession Numbers (16S rRNA/cyt *b*/MC1R/Pod15b/Pod55)	I. Phylogeny (Sanger data) by Psonis et al. 2017	II. Demography and mtDNA haplotype networks (Sanger data)	III. Molecular Dating (Sanger data)	IV. Microsatellites data	V. ddRADseq data
856	*Podarcis tauricus*	NHMC 80.3.50.308	Greece – Kavala, Thasos Isl. – Thasopoula islet	(Psonis et al., 2017) (Sanger data) / Present Study (ddRADseq)	KX658413 / KX658113 / - / - / - ddRADseq: TBP	X	X		X	X
857	*Podarcis tauricus*	NHMC 80.3.50.309	Greece – Kavala, Thasos Isl. – Thasopoula islet	(Psonis et al., 2017) (Sanger data) / Present Study (ddRADseq)	KX658414 / KX658114 / KX658518 / KX658571 / KX658624 ddRADseq: TBP	X	X	X	X	X
858	*Podarcis tauricus*	NHMC 80.3.50.310	Greece – Kavala, Thasos Isl. – Thasopoula islet	(Psonis et al., 2017)	KX658415 / KX658115 / KX658519 / KX658572 / KX658625	X	X	X	X	
859	*Podarcis tauricus*	NHMC 80.3.50.311	Greece – Kavala, Thasos Isl. – Thasopoula islet	(Psonis et al., 2017)	- / KX658116 / - / - / -	X			X	
860	*Podarcis tauricus*	NHMC 80.3.50.312	Greece – Kavala, Thasos Isl. – Thasopoula islet	(Psonis et al., 2017)	KX658416 / KX658117 / - / - / -	X	X		X	
861	*Podarcis tauricus*	NHMC 80.3.50.313	Greece – Kavala, Thasos Isl. – Thasopoula islet	(Psonis et al., 2017)	KX658417 / KX658118 / - / - / -	X	X		X	
862	*Podarcis tauricus*	NHMC 80.3.50.314	Greece – Kavala, Thasos Isl. – Thasopoula islet	(Psonis et al., 2017)	KX658418 / KX658119 / - / - / -	X	X		X	
863	*Podarcis tauricus*	NHMC 80.3.50.315	Greece – Kavala, Thasos Isl. – Thasopoula islet	(Psonis et al., 2017)	KX658419 / KX658120 / - / - / -	X	X		X	
864	*Podarcis tauricus*	NHMC 80.3.50.316	Greece – Nestos – Keramoti	(Psonis et al., 2017)	KX658420 / KX658121 / - / - / - ddRADseq: TBP	X	X		X	X
865	*Podarcis tauricus*	NHMC 80.3.50.317	Greece – Nestos – Keramoti	(Psonis et al., 2017) (Sanger data) / Present Study (ddRADseq)	KX658421 / KX658122 / KX658520 / KX658573 / KX658626 ddRADseq: TBP	X	X	X	X	X
866	*Podarcis tauricus*	NHMC 80.3.50.318	Greece – Kavala, Thasos	(Psonis et al., 2017) (Sanger data) / Present Study (ddRADseq)	KX658422 / KX658123 / - / - / -	X	X		X	

Sample Code	Taxon Name	NHMC Voucher Numbers (or isolate codes of NCBI sequences)	Country – Region – Locality	Study	Sanger / ddRADseq Sequences Accession Numbers (16S rRNA/cyt *b*/MC1R/Pod15b/Pod55)	I. Phylogeny (Sanger data) by Psonis et al. 2017	II. Demography and mtDNA haplotype networks (Sanger data)	III. Molecular Dating (Sanger data)	IV. Microsatellites data	V. ddRADseq data
867	*Podarcis tauricus*	NHMC 80.3.50.319	Isl. – Thasopoula islet Greece – Kavala, Thasos Isl. – Thasopoula islet	(Psonis et al., 2017)	KX658423 / KX658124 / - / - / -	X	X		X	
869	*Podarcis tauricus*	NHMC 80.3.50.333	Greece – Florina prefecture – Petron lake	Present Study					X	
870	*Podarcis tauricus*	NHMC 80.3.50.334	Greece – Florina – Petron lake	(Psonis et al., 2017)	KX658424 / KX658125 / - / - / -	X	X		X	
871	*Podarcis tauricus*	NHMC 80.3.50.335	Greece – Florina – Cheimaditida lake to Zazari lake	(Psonis et al., 2017)	KX658425 / KX658126 / - / - / -	X	X		X	
872	*Podarcis tauricus*	NHMC 80.3.50.336	Greece – Pella – Agra lake	(Psonis et al., 2017)	KX658426 / KX658127 / KX658521 / KX658574 / KX658627	X	X	X	X	
881	*Podarcis tauricus*	NHMC 80.3.50.345	Greece – Evros – Feres, 5km SE	(Psonis et al., 2017)	KX658435 / KX658136 / - / - / -	X	X		X	
882	*Podarcis tauricus*	NHMC 80.3.50.346	Greece – Evros – Treis Vryses	(Psonis et al., 2017)	KX658436 / KX658137 / - / - / -	X	X		X	
895	*Podarcis tauricus*	NHMC 80.3.50.330	Romania – Muntii Macinului	Present Study					X	
896	*Podarcis tauricus*	NHMC 80.3.50.331	Romania – Muntii Macinului	Present Study					X	
927	*Podarcis tauricus*	NHMC 80.3.50.195	Greece – Evros – Doriskos, 2.18km S.	(Psonis et al., 2017)	KX658449 / KX658150 / - / - / -	X	X			
936	*Podarcis tauricus*	NHMC 80.3.50.355	Greece – Karditsa – Mouzaki, 3km E.	(Psonis et al., 2017) (Sanger data) / Present Study (ddRADseq)	KX658458 / KX658159 / - / - / - ddRADseq: TBP	X	X			X
937	*Podarcis tauricus*	NHMC 80.3.50.356	Serbia – Šipačina	(Psonis et al., 2017)	KX658459 / KX658160 / - / - / -	X	X			
938	*Podarcis tauricus*	NHMC 80.3.50.357	Serbia – Šipačina	(Psonis et al., 2017)	KX658460 / KX658161 / - / - / -	X	X			

Sample Code	Taxon Name	NHMC Voucher Numbers (or isolate codes of NCBI sequences)	Country – Region – Locality	Study	Sanger / ddRADseq Sequences Accession Numbers (16S rRNA/cyt *b*/MC1R/Pod15b/Pod55)	I. Phylogeny (Sanger data) by Psonis et al. 2017	II. Demography and mtDNA haplotype networks (Sanger data)	III. Molecular Dating (Sanger data)	IV. Microsatellites data	V. ddRADseq data
939	*Podarcis tauricus*	NHMC 80.3.50.358	Kosovo – Cerajë	(Psonis et al., 2017)	KX658461 / KX658162 / - / - / -	X	X			
940	*Podarcis tauricus*	NHMC 80.3.50.359	Kosovo – Gjonaj	(Psonis et al., 2017)	KX658462 / KX658163 / - / - / -	X	X			
941	*Podarcis tauricus*	NHMC 80.3.50.360	Kosovo – Gjonaj	(Psonis et al., 2017)	KX658463 / KX658164 / - / - / -	X	X			
942	*Podarcis tauricus*	NHMC 80.3.50.361	Albania – Përbreg	(Psonis et al., 2017)	KX658464 / KX658165 / - / - / -	X	X			
943	*Podarcis tauricus*	NHMC 80.3.50.362	Albania – Lume	(Psonis et al., 2017)	KX658465 / KX658166 / - / - / -	X	X			
951	*Podarcis tauricus*	NHMC 80.3.50.173	Albania – Maliq	(Psonis et al., 2017)	KX658472 / KX658173 / - / - / -	X	X			
952	*Podarcis tauricus*	NHMC 80.3.50.174	Albania – Maliq	(Psonis et al., 2017)	KX658473 / KX658174 / - / - / -	X	X			
INDATE	*Podarcis tiliguerta*	Til01	France – Corsica – Padodell	(Buades *et al.* 2013)	- / JX852113 / - / - / -	X		X		
INDATE	*Podarcis tiliguerta*	Tp1	France – Corsica – Padodell	(Buades *et al.* 2013)	- / - / JX126692 / - / -	X		X		
INDATE	*Podarcis tiliguerta*	PT6	France – North Corsica	(Pereira *et al.* 2013)	- / - / - / KC681281 / KC681736	X		X		
INDATE	*Podarcis tiliguerta*	Til02	France – Corsica – Padodell	(Buades *et al.* 2013)	- / JX852114 / - / - / -	X		X		
INDATE	*Podarcis tiliguerta*	Tf2	France – Corsica – Padodell	(Buades *et al.* 2013)	- / - / JX126691 / - / -	X		X		
INDATE	*Podarcis tiliguerta*	PT5	France – Corsica – Solenzarea	(Pereira *et al.* 2013)	- / - / - / KC681283 / KC681735	X		X		
625	*Podarcis waglerianus*	NHMC 80.3.150.1	Italy – Sicilia – castle dona fiorata	(Psonis et al., 2017)	KX658475 / KX658176 / KX658528 / KX658581 / KX658634	X		X		
CALIB	*Timon lepidus*	ET-4	Spain - Alicante	(Pavlicev & Mayer 2009)	GQ142094 / GQ142119 / -			X		
CALIB	*Timon lepidus*	Nev418	Spain - Almeria	(Nunes *et al.* 2011)	- / - / JF732968			X		
CALIB	*Timon pater*	-	Tunisia - Tabarka	(Paulo *et al.* 2008)	AF378958 / - / -			X		
CALIB	*Timon pater*	-	Tunisia - Tabarka	(Paulo *et al.* 2008)	- / AF378964 / -			X		

Sample Code	Taxon Name	NHMC Voucher Numbers (or isolate codes of NCBI sequences)	Country – Region – Locality	Study	Sanger / ddRADseq Sequences Accession Numbers (16S rRNA/cyt *b*/MC1R/Pod15b/Pod55)	I. Phylogeny (Sanger data) by Psonis et al. 2017	II. Demography and mtDNA haplotype networks (Sanger data)	III. Molecular Dating (Sanger data)	IV. Microsatellites data	V. ddRADseq data
CALIB	*Timon pater*	Tun3	Tunisia - Tabarka	(Nunes *et al*. 2011)	- / - / JF732957			X		
CALIB	*Timon princeps*	-	Non available	(Harris *et al*. 1998)	AF080384 / AF080383 / -			X		
CALIB	*Timon tangitana*	-	Tunisia - Azrou	(Paulo *et al*. 2008)	AF378957 / - /			X		
CALIB	*Timon tangitana*	-	Tunisia - Azrou	(Paulo *et al*. 2008)	- / AF378959 /			X		
CALIB	*Timon tangitana*	Azr2	Tunisia - Azrou	(Nunes *et al*. 2011)	- / - / JF732953			X		

8 * Deposited also in the National Museum of Prague (NMP)

9 ** Deposited also in the Hungarian Natural History Museum (HNHM)

Table S2. Primers and amplification conditions of PCR[a] concerning the microsatellite data.

Loci name	Primers (Dye)	Sequence (5′ – 3′)	Multiplex	Annealing Temperature (°C)[b]	$MgCl_2$ Concentration (mM)	Study
B6	B6-F (ROX)	CTGCTGCTTCAATCACACTC	M5	50	1.5	(Nembrini & Oppliger 2003)
	B6-R	GCCTTGCCTCTCCAGAAC				
C9	C9-F (TAMRA)	CATTGCTGGTTCTGGAGAAAG	M1	57.4	1.5	(Nembrini & Oppliger 2003)
	C9-R	CCTGATGAAGGGAAGTGGTG				
Lv3-19	Lv3-19-F (TAMRA)	CTGTTGCTATTTTGTATGCTTAC	M3	47	1.5	(Boudjemadi *et al.* 1999)
	Lv3-19-R	CCTGTGACTGTCCTCAGAGG				
Lv4-72	Lv4-72-F (ROX)	CCCTACTTGAGTTGCCGTC	M3	47	1.5	(Boudjemadi *et al.* 1999)
	Lv4-72-R	CTTTGCAGGTAACAGAGTAG				
Pb10	Pb10-F (ROX)	AGTGGAATCGGCTGCAATAC	M1	50	1.5	(Pinho *et al.* 2004)
	Pb10-R	ACCAGTCCCAGGAATTTAGG				
Pb47	Pb47-F (FAM)	CTTGGTGGTTAACAATGTTGGC	M4	48	3	(Pinho *et al.* 2004)
	Pb47-R	GTGAGCTAATACAACTCTCCAC				
Pb50	Pb50-F (TET)	GGATGTTTCAGCATGCTTGG	M3	58	1.5	(Pinho *et al.* 2004)
	Pb50-R	AGACCTCACTGGGCCATTAC				
Pli4	Pli4-F (FAM)	TCAGTTCATGCATAAGGTCCA	M2	57.4	1.5	(Bloor *et al.* 2011)
	Pli4-R	TTCGGCATTTTTCTTCAGGT				
Pm16	Pm16- (TAMRA)	GGGATGGAGAAAGATGGCG	M4	57.4	1.5	(Richard *et al.* 2012)
	Pm16-R	GCACTTGCCTACTGGTCATAC				
Pm27	Pm27-F (HEX)	TCCATGAGCTCCACACACG	M4	57.4	1.5	(Richard *et al.* 2012)
	Pm27-R	TCCACAGCCACTTACGGAC				
Pmeli02	Pmeli02-F (TAMRA)	AGTGGAATCGGCTGCAATAC	M5	47	1.5	(Huyghe *et al.* 2009)
	Pmeli02-R	ACCAGTCCCAGGAATTTAGG				
Pmeli19	Pmeli19-F (FAM)	TTCCAAGTCTGATTCACTCCAA	M5	57.4	1.5	(Huyghe *et al.* 2009)
	Pmeli19-R	AGCTGCAAGCACCTAGCAAT				
Pod1A	Pod1A-F (FAM)	TGAGAAGCACATCTGCACAC	M1	47	1.5	(Poulakakis *et al.* 2005a)
	Pod1A-R	TGAACGCATAATGGCTGAAGG				
Pod1B	Pod1B-F (FAM)	CCTTCAGCCATTATGCGTTCATC	M3	50	1.5	(Poulakakis *et al.* 2005a)
	Pod1B-R	AGGATGGGGATAACCCCAGT				
Pod3	Pod3-F (TET)	TTATCAGACGTTGGGGAAAG	M2	45	3	(Poulakakis *et al.* 2005a)
	Pod3-R	GCACTTCAACCCGAGGTCTG				
Pod2	Pod2-F (FAM)	GGCAATGTTCCTGCATGACG	M2	55	1.5	(Poulakakis *et al.* 2005a)
	Pod2-R	TGGGACAAAAAGGCAGAACG				
Pod8	Pod8-F (TET)	CCTCTAACTATCTGTTGCTGCTG	M5	57.4	1.5	(Poulakakis *et al.* 2005a)
	Pod8-R	CACAAAGGGTATCGAAGGAGG				

[a] using *Taq* DNA Polymerase (KAPA BIOSYSTEMS®)

[b] Program: 94ºC/1min, 45 – 58ºC/1min, 72ºC/1min x35 cycles

Table S3. Results of the mean relative RF distances within the four different min_taxa filters for the three clustering threshold datasets regarding the ddRADseq data.

Clustering Threshold Dataset	min_taxa Filter	N_{res}	RF_{res}	RF_{score} (all)
0.85	4	1	0.000	0.073
	7	1	0.000	
	9	1	0.000	
	11	1	0.000	
0.90	4	2	0.015	0.085
	7	3	0.031	
	9	2	0.033	
	11	1	0.000	
0.95	4	1	0.000	0.151
	7	2	0.007	
	9	2	0.025	
	11	5	0.036	

N_{res}: number of unique trees from 100 ExaML tree searches
RF_{res}: mean relative RF distance among the 100 ExaML resulting trees
RF_{score}: mean relative RF distance across all four best scoring ExaML trees

Table S4. Results of the pairwise mean relative RF distances between the best scoring ExaML trees inferred from the 12 different datasets as defined by the three clustering thresholds and the four min_taxa filters regarding the ddRADseq data.

Clustering threshold		0.85				0.90				0.95			
min_taxa filtering		4	7	9	11	4	7	9	11	4	7	9	11
0.85	4	-											
	7	0.046	-										
	9	0.046	0.093	-									
	11	0.163	0.116	0.116	-								
0.90	4	0.163				-							
	7		0.116			0.093	-						
	9			0.186		0.046	0.046	-					
	11				0.163	0.116	0.093	0.116	-				
0.95	4	0.186				0.256				-			
	7		0.279				0.279			0.093	-		
	9			0.302				0.372		0.139	0.070	-	
	11				0.372				0.349	0.232	0.186	0.186	-

Table S5. Microsatellites summary statistics of the *P. tauricus* species subgroup for five of the final clusters of the hierarchical STRUCTURE analysis. Bolded values indicate heterozygote deficit according to MICROCHECKER ('ionicus_2' had insufficient number of samples to perform the analysis).

Locus	'tauricus 1'			'tauricus 2'			'tauricus 3'			'ionicus_1'			'ionicus_2'		
	H_o	H_e	F_{IS}	H_o	H_e	F_{IS}	H_o	H_e	F_{IS}	H_o	H_e	F_{IS}	H_o	H_e	F_{IS}
B6	0.461	0.735	0.382	0.523	0.587	0.111	0.781	0.898	0.132	0.809	0.912	0.115	0.800	0.929	0.142
C9	0.538	0.471	-0.151	0.067	0.066	-0.015	**0.364**	**0.663**	**0.456**	**0.091**	**0.922**	**0.906**	0.611	0.913	0.337
Lv3-19	0.538	0.452	-0.200	**0.717**	**0.869**	**0.176**	**0.697**	**0.905**	**0.232**	0.238	0.226	-0.053	0.684	0.796	0.144
Lv4-72	0.385	0.415	0.077	0.289	0.335	0.139	0.75	0.873	0.143	**0.454**	**0.831**	**0.459**	0.889	0.873	-0.0187
Pb10	0.667	0.783	0.154	**0.714**	**0.900**	**0.208**	0.800	0.907	0.120	**0.235**	**0.902**	**0.745**	0.454	0.385	-0.190
Pb50	**0.308**	**0.674**	**0.553**	0.089	0.874	-0.017	**0.212**	**0.402**	**0.477**	**0.000**	**0.241**	**1.000**	0.368	0.698	0.479
Pli4	**0.538**	**0.898**	**0.410**	**0.703**	**0.880**	**0.204**	0.833	0.934	0.109	**0.524**	**0.835**	**0.378**	0.789	0.872	0.097
Pm16	0.615	0.689	0.111	0.930	0.840	-0.109	0.788	0.824	0.045	0.818	0.871	0.062	0.600	0.867	0.333
Pm27	0.846	0.843	-0.004	0.75	0.804	0.068	**0.667**	**0.861**	**0.228**	0.364	0.738	0.513	0.500	0.782	0.367
Pmeli02	0.500	0.574	0.135	0.571	**0.941**	**0.396**	0.808	0.918	0.123	**0.583**	**0.909**	**0.369**	0.000	0.714	1.000
Pmeli19	0.846	0.791	-0.073	0.622	0.722	0.139	0.818	0.892	0.084	**0.619**	**0.920**	**0.332**	0.947	0.929	-0.020
Pod1A	0.000	0.000	*n.a.*	0.068	**0.382**	**0.823**	**0.069**	**0.222**	**0.693**	**0.071**	**0.204**	**0.658**	0.454	0.385	-0.190
Pod1B	0.077	0.077	0.000	0.109	0.142	0.237	**0.364**	**0.570**	**0.366**	0.454	0.626	0.278	0.000	0.097	1.000
Pod2	0.385	0.560	0.322	0.395	0.414	0.045	**0.4375**	**0.691**	**0.371**	**0.474**	**0.806**	**0.419**	0.778	0.9142	0.153
Average across all loci	0.479	0.569		0.468	0.414		0.599	0.754		0.410	0.710		0.562	0.725	

H_o: observed heterozygosity

H_e: estimated expected heterozygosity (Nei 1987)

F_{IS}: Inbreeding index based on Weir and Cockerham (1984)

n.a.: non accountable

Table S6. . Microsatellites summary statistics of *P. tauricus* species subgroup for four of the final clusters of the hierarchical STRUCTURE analysis. Bolded values indicate heterozygote deficit according to MICRO-CHECKER ('melisellensis' and 'gaigeae 2' had insufficient number of samples to perform the analysis).

Locus	'melisellensis'			'milensis'			'gaigeae 1'			'gaigeae 2'		
	H_o	H_e	F_{IS}	H_o	H_e	F_{IS}	H_o	H_e	F_{IS}	H_o	H_e	F_{IS}
B6	0.875	0.933	0.067	0.930	0.918	-0.014	0.900	0.888	-0.013	0.750	0.735	-0.021
C9	0.000	0.500	1.000	0.884	0.912	0.031	0.526	0.603	0.130	0.500	0.580	0.143
Lv3-19	0.875	0.833	-0.054	0.884	0.901	0.020	0.750	0.919	0.189	1.000	0.884	-0.139
Lv4-72	0.600	0.844	0.314	0.837	0.892	0.062	0.706	0.877	0.200	0.636	0.835	0.247
Pb10	0.167	0.924	0.833	**0.732**	**0.940**	**0.224**	0.842	0.866	0.029	0.583	0.496	-0.185
Pb50	0.500	0.442	-0.143	**0.186**	**0.588**	**0.686**	0.684	0.750	0.089	0.417	0.594	0.308
Pli4	0.500	0.833	0.500	0.775	0.887	0.128	**0.750**	**0.960**	**0.224**	0.571	0.736	0.238
Pm16	0.750	0.875	0.151	0.860	0.892	0.035	0.789	0.789	0.000	0.667	0.686	0.030
Pm27	0.500	0.883	0.451	**0.512**	**0.884**	**0.424**	**0.600**	**0.922**	**0.355**	0.750	0.670	-0.125
Pmeli02	0.600	0.822	0.294	**0.735**	**0.942**	**0.222**	0.800	0.940	0.154	0.500	0.816	0.400
Pmeli19	0.875	0.942	0.075	0.930	0.944	0.015	0.850	0.883	0.039	0.900	0.821	-0.102
Pod1A	0.500	0.608	0.188	0.461	0.525	0.1225	0.000	0.000	*n.a.*	0.454	0.498	0.091
Pod1B	0.429	0.681	0.390	**0.703**	**0.936**	**0.252**	**0.235**	**0.456**	**0.492**	0.083	0.083	0.000
Pod2	0.500	0.825	0.410	**0.732**	**0.928**	**0.213**	0.900	0.858	- 0.052	1.000	0.833	- 0.333
Average across all loci	0.548	0.782		0.726	0.863		0.667	0.765		0.629	0.833	

H_o: observed heterozygosity

H_e: estimated expected heterozygosity (Nei 1987)

F_{IS}: Inbreeding index based on Weirand Cockerham (1984)

n.a.: non accountable

Table S7. Pairwise estimated values of F*st* (Weir & Cockerham 1984) for the final clusters of the hierarchical STRUCTURE analysis of *P. tauricus* species subgroup using microsatellites. Asterisks indicate the statistical support (***P< 0.001, **P< 0.01) after 1,000 permutations.

Final cluster	**1**	**2**	**3**	**4**	**5**	**6**	**7**	**8**
1. 'gaigeae 2'								
2. 'gaigeae 1'	0.099***							
3. 'milensis'	0.154***	0.127***						
4. 'melisellensis'	0.244**	0.165**	0.125***					
5. 'ionicus 2'	0.165***	0.138***	0.130***	0.192**				
6. 'ionicus 1'	0.213**	0.146***	0.148***	0.154**	0.187***			
7. 'tauricus 1'	0.272**	0.194***	0.200***	0.257**	0.203***	0.254***		
8. 'tauricus 3'	0.273***	0.217***	0.223***	0.306***	0.226***	0.295***	0.202***	
9. 'tauricus 2'	0.148***	0.101***	0.118***	0.168***	0.116***	0.150***	0.116***	0.090***

Table S8. Estimates of recent migration rate between the final clusters of *P. tauricus* species subgroup as revealed by the hierarchical STRUCTURE analysis based on the microsatellite loci. Values greater than 0.1 are bolded and self-comparisons are italicized. Numbers in brackets show the standard deviation, whereas numbers in square brackets correspond to the following clusters: 0: 'tauricus 1', 1: 'tauricus 2', 2: 'tauricus 3', 3: 'melisellensis', 4: 'milensis', 5: 'gaigeae 1', 6: 'gaigeae 2', 7: 'ionicus 1', 8: 'ionicus 2'.

[0][0]: ***0.9187****(0.0231)*	[0][1]: 0.0250(0.0152)	[0][2]: 0.0089(0.0085)	[0][3]: 0.0079(0.0077)	[0][4]: 0.0078(0.0077)
[1][0]: 0.0064(0.0062)	*[1][1]:* ***0.9513****(0.0156)*	[1][2]: 0.0062(0.0061)	[1][3]: 0.0060(0.0059)	[1][4]: 0.0060(0.0059)
[2][0]: 0.0165(0.0156)	[2][1]: 0.0230(0.0184)	*[2][2]:* ***0.8833****(0.0326)*	[2][3]: 0.0129(0.0123)	[2][4]: 0.0129(0.0125)
[3][0]: 0.0195(0.0185)	[3][1]: 0.0193(0.0182)	[3][2]: **0.1764**(0.0392)	*[3][3]:* ***0.6865****(0.0185)*	[3][4]: 0.0199(0.0187)
[4][0]: 0.0059(0.0058)	[4][1]: 0.0059(0.0059)	[4][2]: 0.0059(0.0058)	[4][3]: 0.0060(0.0057)	*[4][4]:* ***0.9500****(0.0160)*
[5][0]: 0.0159(0.0151)	[5][1]: 0.0157(0.0149)	[5][2]: 0.0160(0.0153)	[5][3]: 0.0160(0.0154)	[5][4]: 0.0158(0.0149)
[6][0]: 0.0115(0.0112)	[6][1]: 0.0113(0.0110)	[6][2]: 0.0115(0.0112)	[6][3]: 0.0116(0.0114)	[6][4]: 0.0114(0.0110)
[7][0]: 0.0107(0.0104)	[7][1]: 0.0108(0.0105)	[7][2]: 0.0108(0.0105)	[7][3]: 0.0108(0.0106)	[7][4]: 0.0106(0.0104)
[8][0]: 0.0153(0.0137)	[8][1]: 0.0115(0.0111)	[8][2]: 0.0130(0.0126)	[8][3]: 0.0116(0.0112)	[8][4]: 0.0116(0.0112)
[0][5]: 0.0078(0.0076)	[0][6]: 0.0079(0.0077)	[0][7]: 0.0080(0.0078)	[0][8]: 0.0080(0.0078)	
[1][5]: 0.0060(0.0058)	[1][6]: 0.0061(0.0060)	[1][7]: 0.0061(0.0059)	[1][8]: 0.0059(0.0059)	
[2][5]: 0.0128(0.0122)	[2][6]: 0.0128(0.0124)	[2][7]: 0.0129(0.0124)	[2][8]: 0.0129(0.0124)	
[3][5]: 0.0198(0.0186)	[3][6]: 0.0197(0.0186)	[3][7]: 0.0195(0.0185)	[3][8]: 0.0194(0.0184)	
[4][5]: 0.0060(0.0058)	[4][6]: 0.0083(0.0074)	[4][7]: 0.0060(0.0060)	[4][8]: 0.0060(0.0059)	
[5][5]: ***0.6825****(0.0152)*	[5][6]: **0.2066**(0.0342)	[5][7]: 0.0157(0.0147)	[5][8]: 0.0157(0.0152)	
[6][5]: 0.0117(0.0111)	*[6][6]:* ***0.9077****(0.0275)*	[6][7]: 0.0116(0.0113)	[6][8]: 0.0117(0.0114)	
[7][5]: 0.0108(0.0105)	[7][6]: 0.0110(0.0106)	*[7][7]:* ***0.9138****(0.0257)*	[7][8]: 0.0107(0.0103)	
[8][5]: 0.0114(0.0110)	[8][6]: 0.0117(0.0113)	[8][7]: 0.0115(0.0111)	*[8][8]:* ***0.9024****(0.0283)*	

Table S9. Results (*p*-values) of bottleneck testing based on Wilcoxon test (probability of heterozygote excess) under three microsatellite mutation models: Infinite Allele Model (IAM), Two-Phase Model (TPM) and Stepwise Mutation Model (SMM) for the final clusters of the hierarchical STRUCTURE analysis of the *P. tauricus* species subgroup. Statistical significant values ($p<0.05$) are bolded.

Cluster	IAM	TPM	SMM
'tauricus 3'	**0.004**	0.903	0.241
'tauricus 1'	0.940	0.080	**0.025**
'tauricus 2'	0.583	**0.020**	**0.002**
'ionicus 2'	0.104	0.669	0.295
'ionicus 1'	0.146	1.00	**0.047**
'milensis'	**0.013**	0.172	0.669
'gaigeae_1'	0.375	0.375	0.167
'gaigeae_2'	**0.006**	0.094	0.273
'melisellensis'	0.635	0.587	0.541

Table S10. Tests of population expansion (k-test and g-test) using microsatellites for each final cluster of the hierarchical STRUCTURE analysis of the *P. tauricus* species subgroup.

Final cluster or species	Sample Number	Number of loci with negative k value (out of 14 used in total)	k-test value (intra-locus)[a]	g-test value (inter-loci)[b]
'gaigeae 2'	12	9	0.022*.	2.239 n.s.
'gaigeae 1'	20	11	0.180 n.s.	2.459 n.s.
'milensis'	43	10	0.073 n.s.	0.355 n.s.
'melisellensis'[c]	8	6	0.754 n.s.	4.170 n.s.
'ionicus 2'	20	9	0.111 n.s.	3.974 n.s.
'ionicus 1'	22	11	0.022*	1.388 n.s.
'tauricus 1'	13	8	0.352 n.s.	2.588 n.s.
'tauricus 3'	33	10	0.073 n.s.	1.950 n.s.
'tauricus 2'	46	12	0.005**	1.871 n.s.

[a] Indications of expansion are the statistically significant values (non-significance $P > 0.05$; * $P < 0.05$; ** $P < 0.01$; *** $P < 0.001$).

[b] The significance of the g statistic can be checked in Table 1 (p. 455) of Reich et al. (1999) based on the cut-off values for a particular number of samples and loci.

[c] The sample dataset of *P. melisellensis* is the same with the one of the final cluster 'melisellensis'.

Table S11. Summary of the genetic diversity indexes for each phylogenetic clade and subclade of the *P. tauricus* species subgroup based on the mtDNA sequencing data.

Phylogenetic clade or subclade	*n*	*h*	*S*	π	h_d	θ_w
P. gaigeae	18	9	10	0.003	0.895	0.004
P. ionicus	85	28	50	0.054	0.903	0.045
P. ionicus subclade *a*	9	7	12	0.005	0.917	0.005
P. ionicus subclade *b*	6	4	5	0.009	0.867	0.008
P. ionicus subclade *c*	20	5	4	0.002	0.505	0.004
P. ionicus subclade *d*	10	2	1	0.001	0.200	0.001
P. ionicus subclade *e*	43	18	64	0.007	0.884	0.026
P. melisellensis	18	10	28	0.029	0.915	0.026
P. milensis	33	11	11	0.015	0.886	0.015
P. tauricus	178	18	18	0.003	0.544	0.016

n: sample number
h: haplotype number
h_d: haplotype diversity
S: number of variable sites
π: nucleotide diversity
θ_w: Watterson's theta.

Table S12. Demographic indexes' values (Harpending's raggedness index *r*, Fu's *Fs*, Ramos-Onsins & Rozas' R_2, and Tajima's *D*) estimated for each phylogenetic clade and subclade of the *P. tauricus* species subgroup based on the mtDNA sequencing data.

Species and phylogenetic subclades	*n*	*r*	Fu's F_S	Tajima's *D*	R_2
P. gaigeae	18	$0.075^{n.s.}$	$-2.966^{n.s.}$	$-1.059^{n.s.}$	$0.099^{n.s.}$
P. melisellensis	18	$0.054^{n.s.}$	-6.110***	$0.403^{n.s.}$	$0.153^{n.s.}$
P. milensis	33	$0.022^{n.s.}$	-20.641***	$-0.221^{n.s.}$	$0.116^{n.s.}$
P. t. ionicus	85	$0.015^{n.s.}$	$-8.188^{n.s.}$	$0.689^{n.s.}$	$0.118^{n.s.}$
P. ionicus subclade *a*	9	$0.085^{n.s.}$	$-2.953^{n.s.}$	$-0.028^{n.s.}$	$0.144^{n.s.}$
P. ionicus subclade *b*	6	$0.169^{n.s.}$	-4.005*	$0.196^{n.s.}$	$0.186^{n.s.}$
P. ionicus subclade *c*	20	$0.150^{n.s.}$	-4.145***	$-1.43^{n.s.}$	$0.095^{n.s.}$
P. ionicus subclade *d*	10	$0.400^{n.s.}$	$-0.339^{n.s.}$	$-1.112^{n.s.}$	$0.300^{n.s.}$
P. ionicus subclade *e*	43	$0.106^{n.s.}$	-16.411***	-2.603***	$0.097^{n.s.}$
P. tauricus	178	$0.024^{n.s.}$	-27.179***	-2.176***	0.022*

n: sample number.

The statistically non-significant (*n.s.*) values of *r* (non-significance $P > 0.05$; * $P < 0.05$; ** $P < 0.01$; *** $P < 0.001$) and the significant negative values of Fu's F_S (significance limit: * $P < 0.02$, *** $P < 0.001$) are indications of sudden expansion. For small sample size equal indications are the statistically significant values of R_2 (non-significance $P > 0.05$; * $P < 0.05$; ** $P < 0.01$; *** $P < 0.001$). The statistically significant positive values of Tajima's *D* and Fu's F_S suggest bottleneck effect.

Table S13. Percent contribution and permutation importance of the factors* used in MaxEnt for each species of the *P. tauricus* species subgroup, as well as the entire subgroup.

Taxon / Taxa Group	Factor	Percent Contribution	Permutation Importance
Podarcis gaigeae	bio_7	49.3	33.4
	bio_15	23.1	12.2
	bio_14	14.1	11.2
	bio_12	8.9	42.9
	bio_6	4.3	0.0
	bio_1	0.2	0.1
	bio_5	0.0	0.1
Podarcis milensis	bio_7	49.7	19.6
	bio_15	18.6	4.7
	bio_12	14.3	41.7
	bio_14	13.4	30.6
	bio_6	4.0	3.0
	bio_5	0.0	0.4
	bio_1	0.0	0.0
Podarcis melisellensis	bio_6	42.1	35.7
	bio_14	29.1	47.4
	bio_7	11.4	2.5
	bio_1	10.2	6.7
	bio_12	3.8	1.5
	bio_15	3.3	5.8
	bio_5	0.2	0.5
Podarcis tauricus	bio_7	28.4	14.5
	bio_6	22.0	26.0
	bio_15	20.1	34.9
	bio_12	13.1	4.8
	bio_14	9.0	8.3
	bio_1	4.5	8.5
	bio_5	2.8	2.9
Podarcis ionicus	bio_15	43.8	29.1
	bio_12	35.5	41.3
	bio_7	13.7	16.6
	bio_6	4.1	5.1
	bio_14	2.5	5.7
	bio_1	0.3	2.0
	bio_5	0.1	0.1
Podarcis tauricus species subgroup	bio_6	34.9	44.9
	bio_7	22.5	7.6
	bio_14	17.1	18.7
	bio_12	10.5	5.1
	bio_15	9.3	9.6
	bio_5	3.6	5.6
	bio_1	2.2	8.5

*Factors' description: bio_1: Annual Mean Temperature, bio_5: Max Temperature of Warmest Month, bio_6: Min Temperature of Coldest Month, bio_7: Temperature Annual Range, bio_12: Annual Precipitation, bio_14: Precipitation of Driest Month, bio_15: Precipitation Seasonality (Coefficient of Variation).

Table S14. Schoener's *D* (upper right) and Hellinger's *I* (bottom left) indices for testing niche similarity between species pairs of the *P. tauricus* species subgroup.

Species	Niche Similarity				
	1.	**2.**	**3.**	**4.**	**5.**
1. Podarcis melisellensis	1	0.0029	0.0835	0.0323	0.1641
2. Podarcis milensis	0.0209	1	0.0075	0.2389	0.0255
3. Podarcis tauricus	0.2552	0.0526	1	0.0465	0.0904
4. Podarcis gaigeae	0.0941	0.5493	0.1632	1	0.0856
5. Podarcis ionicus	0.3650	0.0961	0.2682	0.2351	1

Bloor P, Rodríguez V, Terrasa B, *et al.* (2011) Polymorphic microsatellite loci for the Balearic Island Lizard *Podarcis lilfordi* (Squamata: Lacertidae). *Conservation Genet. Resour.* **3**, 323-325.

Boudjemadi K, Martin O, Simon JC, Estoup A (1999) Development and cross-species comparison of microsatellite markers in two lizard species, *Lacerta vivipara* and *Podarcis muralis*. *Mol. Ecol.* **8**, 518-520.

Brueckner M, Duering A (2001) PCR-RFLP a fast and inexpensive biochemical method for detecting species boundaries in the *Lacerta viridis/bilineata* species complex. *Mertensiella* **31**, 40-44.

Buades JM, Rodríguez V, Terrasa B, *et al.* (2013) Variability of the mc1r gene in melanic and non-melanic *Podarcis lilfordi* and *Podarcis pityusensis* from the Balearic archipelago. *PLoS ONE* **8**, e53088.

Carranza S, Arnold EN, Amat F (2004) DNA phylogeny of *Lacerta* (*Iberolacerta*) and other lacertine lizards (Reptilia: Lacertidae): did competition cause long-term mountain restriction? *Syst. Biodivers.* **2**, 57–77.

Carranza S, Harris DJ, Arnold EN, Batista V, Gonzalez de la Vega JP (2006) Phylogeography of the lacertid lizard, *Psammodromus algirus*, in Iberia and across the Strait of Gibraltar. *J. Biogeography* **33**, 1279-1288.

Godinho R, Crespo E, Ferrand N, Harris DJ (2005) Phylogeny and evolution of the green lizards, *Lacerta* spp. (Squamata: Lacertidae) based on mitochondrial and nuclear DNA sequences. *Amphibia-Reptilia* **26**, 271-285.

Harris DJ, Arnold EN, Thomas RH (1998) Relationships of lacertid lizards (Reptilia : Lacertidae) estimated from mitochondrial DNA sequences and morphology. *Proc. R. Soc. Lond. B* **265**, 1939-1948.

Harris DJ, Sá-Sousa P (2002) Molecular phylogenetics of Iberian wall lizards (*Podarcis*): is *Podarcis hispanica* a species complex? *Mol. Phylogenet. Evol.* **23**, 75-81.

Huyghe K, Breugelmans K, All M, *et al.* (2009) Characterization of polymorphic microsatellite markers in the Dalmatian wall lizard *Podarcis melisellensis* (Squamata: Lacertidae). *Mol. Ecol. Res.* **9**, 299-301.

Kapli P, Botoni D, Ilgaz Ç, *et al.* (2013) Molecular phylogeny and historical biogeography of the Anatolian lizard *Apathya* (Squamata, Lacertidae). *Mol. Phylogenet. Evol.* **66**, 992-1001.

Mayer W, Beyerlein P (2001) Genetic differentiation of the *Lacerta viridis/bilineata* complex and of *Lacerta trilineata* in Greece: mitochondrial DNA sequences. *Mertensiella* **13**, 52-59.

Nei M (1987) *Molecular Evolutionary Genetics* Columbia University Press, New York.

Nembrini M, Oppliger A (2003) Characterization of microsatellite loci in the wall lizard *Podarcis muralis* (Sauria: Lacertidae). *Mol. Ecol. Notes* **3**.

Nunes VL, Miraldo A, Beaumont MA, Butlin RK, Paulo OS (2011) Association of Mc1r variants with ecologically relevant phenotypes in the European ocellated lizard, *Lacerta lepida*. *J. Evol. Biol.* **24**, 2289-2298.

Paulo OS, Pinheiro J, Miraldo A, *et al.* (2008) The role of vicariance vs. dispersal in shaping genetic patterns in ocellated lizard species in the western Mediterranean. *Mol. Ecol.* **17**, 1535-1551.

Pavlicev M, Mayer W (2009) Fast radiation of the subfamily Lacertinae (Reptilia: Lacertidae): History or methodical artefact? *Mol. Phylogenet. Evol.* **52**, 727-734.

Pereira C, Couto A, Luís C, *et al.* (2013) Twenty-one new sequence markers for population genetics, species delimitation and phylogenetics in wall lizards (*Podarcis* spp.). *BMC Res. Notes* **6**, 299.

Pinho C, Ferrand N, Harris DJ (2006) Reexamination of the Iberian and North African *Podarcis* (Squamata: Lacertidae) phylogeny based on increased mitochondrial DNA sequencing. *Mol. Phylogenet. Evol.* **38**, 266-273.

Pinho C, Rocha S, Carvalho BM, *et al.* (2010) New primers for the amplification and sequencing of nuclear loci in a taxonomically wide set of reptiles and amphibians. *Conservation Genet. Resour.* **2**, 181-185.

Pinho C, Sequeira F, Godinho R, Harris DJ, Ferrand N (2004) Isolation and characterization of nine microsatellite loci in *Podarcis bocagei* (Squamata: Lacertidae). *Mol. Ecol. Notes* **4**, 268-288.

Podnar M, Madaric BB, Mayer W (2014) Non concordant phylogeographical patterns of three widely codistributed endemic Western Balkans lacertid lizards (Reptilia, Lacertidae) shaped by specific habitat requirements and different responses to Pleistocene climatic oscillations. *J. Zool. Syst. Evol. Res.* **52**, 119-129.

Podnar M, Mayer W, Tvrtkovic N (2005) Phylogeography of the Italian wall lizard, *Podarcis sicula*, as revealed by mitochondrial DNA sequences. *Mol. Ecol.* **14**, 575-588.

Podnar M, Mayer W, Tvrtković N (2004) Mitochondrial phylogeography of the Dalmatian wall lizard, (Lacertidae). *Org. Divers. Evol.* **4**, 307-317.

Poulakakis N, Goulielmos G, Antoniou A, Zouros E, Mylonas M (2005a) Isolation and characterization of polymorphic microsatellite markers in the wall lizard *Podarcis erhardii* (Squamata: Lacertidae). *Mol. Ecol. Notes* **5**, 549-551.

Poulakakis N, Lymberakis P, Antoniou A, *et al.* (2003) Molecular phylogeny and biogeography of the wall-lizard *Podarcis erhardii* (Squamata : Lacertidae). *Mol. Phyl. Evol.* **28**, 38-46.

Poulakakis N, Lymberakis P, Valakos E, *et al.* (2005b) Phylogeography of Balkan wall lizard (*Podarcis taurica*) and its relatives inferred from mitochondrial DNA sequences. *Mol. Ecol.* **14**, 2433-2443.

Poulakakis N, Lymberakis P, Valakos E, Zouros E, Mylonas M (2005c) Phylogenetic relationships and biogeography of *Podarcis* species from the Balkan Peninsula, by bayesian and maximum likelihood analyses of mitochondrial DNA sequences. *Mol. Phylogenet. Evol.* **37**, 845-857.

Richard M, Stevens AM, Le Henanff M, *et al.* (2012) Fourteen new polymorphic microsatellite loci for the wall lizard *Podarcis*

muralis (Sauria: Lacertidae). In : Abreu et al. (2012). Permanent Genetic Resources added to Molecular Ecology Resources Database 1 October 2011-30 November 2011. *Mol. Ecol. Res.* **12**, 374-376.

Rodríguez V, Brown RP, Terrasa B, *et al.* (2013) Genetic diversity and historical biogeography of the Maltese wall lizard, *Podarcis filfolensis* (Squamata: Lacertidae). *Conserv. Genet.* **15**, 295-304.

Sagonas K, Poulakakis N, Lymberakis P, *et al.* (2014) Molecular systematics and historical biogeography of the green lizards (*Lacerta*) in Greece: Insights from mitochondrial and nuclear DNA. *Mol. Phylogenet. Evol.* **76C**, 144-154.

Salvi D, Harris DJ, Kaliontzopoulou A, Carretero MA, Pinho C (2013) Persistence across Pleistocene ice ages in Mediterranean and extra-Mediterranean refugia: phylogeographic insights from the common wall lizard. *Bmc Evol. Biol.* **13**, 147.

Salvi D, Schembri PJ, Sciberras A, Harris JD (2014) Evolutionary history of the Maltese wall lizard *Podarcis filfolensis*: insights on the 'Expansion-Contraction' model of Pleistocene biogeography. *Mol. Ecol.*, 1167-1187.

Weir BS, Cockerham CC (1984) Estimating F-Statistics for the Analysis of Population-Structure. *Evolution* **38**, 1358-1370.

Text S1. Details on the procedure followed for ddRADseq library preparation and Illumina sequencing of the *P. tauricus* species subgroup.

The protocol described by Peterson et al. (2012) was followed for the ddRADseq library preparation. Specifically, 500ng of genomic DNA of each sample were simultaneously digested using two restriction enzymes, SbfI (restriction site 5'-CCTGCAGG-3') and MspI (restriction site 5'-CCGG-3') with CutSmart 10x Buffer (New England Biolabs) incubating at 37°C for 2 h. The success of the reaction was evaluated by agarose gel electrophoresis comparing, using a 100bp ladder, digested samples and their initial genomic DNA. The digestion fragments were purified with the Agencourt AMPure magnetic beads and adaptors were ligated after sample re-arrangement on the PCR plate based on sample concentration. The oligonucleotide sequences (oligos) used for barcoding and adding the Illumina indexes are provided by Peterson et al. (2012). Size selection was performed using Pippin® (Sage Science®, Beverly, MA, USA), under the range selection 415 -515 bp. Target fragments were amplified through 11 cycles of Polymerase Chain Reaction (PCR) using the Phusion® Polymerase kit (New England BioLabs®, Ipswich, MA, USA). The preliminary evaluation of the distribution of fragments and their concentration was made using the 2200 TapeStation® (Agilent Technologies®, Santa Clara, California, USA) and Qubit® 2.0 Fluorometer (Invitrogen®, Carlsbad, California, USA), respectively. The final evaluation of each pool (in terms of the quantity of target fragments for sequencing i.e. including the right adaptors) was achieved with a qPCR that was followed by multiplexing equimolar amounts of each pool to the final library. The sequencing of 46 samples was performed on an Illumina HiSeq 2000 lane (Illumina Inc., San Diego, California, USA) (100-bp, single end reads, pooled with 50 other samples) at the QB3 facility at the University of California, Berkeley (California, USA).

Text S2. Details on the bioinformatics pipeline followed for ddRADseq data filtering and dataset generation of the *P. tauricus* species subgroup.

Raw Illumina reads were processed using the pyRAD (Eaton, 2014) software. Samples were demultiplexed using their unique sequence barcodes and Illumina indexes. Nucleotide sites with Phred quality scores under 99% (Phred score = 20) were converted into undetermined characters (N). . Each locus was reduced by 11 bp after removing the 6-bp restriction site overhang and the 5-bp barcode. The filtered reads for each sample were clustered with VSEARCH v. 2.01 (https://github.com/torognes/vsearch) and were aligned using MUSCLE (Edgar, 2004) establishing homology among reads within samples. Three different clustering threshold values (Wclust equal to 0.85, 0.90, and 0.95) were tested as this parameter has been shown to affect phylogenetic relationships (Leaché et al., 2015). In each dataset reads with a number of N's above a specific threshold were discarded (NQual equal to 14, 9, and 5, respectively). In the filtering process, we used a minimum coverage (Mindepth) of 6 and the default values for the remaining parameters. These default values correspond to addition steps of filtering that remove consensus sequences that had either low coverage (<6), or excessive undetermined or heterozygous sites (>5), or too many haplotypes (>2). The clustering of the consensus sequences across samples was performed using the same three thresholds as above. At the per-locus alignment step of MUSCLE a paralog filter was used in order to allow a maximum of three species (MaxSH=3) to be heterozygous at a given site, discarding in that way loci with excessive shared heterozygosity among sites. The assemblage of the final ddRADseq loci was achieved using the variable "MinCov", which determines the minimum number of individuals that are required to have data present at a given locus in order to include that locus at the final

matrix. After applying several values the one of choice was MinCov=4, which accounts for 100% of the samples.

In addition to the pyRAD filtering, identical sequences were also grouped together in each locus to avoid incorrect inference, since the resulting topology of identical sequences will be completely random. Loci that contained less than four unique sequences (i.e., not counting exactly identical sequences) were also removed, since no topological relationships can be inferred with three or less unique sequences. Furthermore, in order to assist the impact of missing data on phylogenetic inference, as well as to determine the minimum amount of data that carry sufficient phylogenetic signal for resolving the topology, we constructed a set of supermatrices by selecting subsets of loci according to the minimum number of unique sequences per locus (min_taxa). The sets were selected such that they cover the subset that most closely contains 100% (min_taxa=4), 50%, 25%, and 12.5% of the loci, respectively. Finally, in each dataset two additional filters were applied, for the number of variable and/or informative sites, respectively. These filters in all cases took the value log2(n_tax) with n_tax being the number of taxa for each locus. This value was selected because it represents the minimum number of informative/variable sites that can resolve the topology. Overall, 12 datasets were assembled (three clustering thresholds × four min_taxa filters).

Text S3 Details on the evaluation of the phylogenetic signal and on the Maximum Likelihood and Bayesian Inference phylogenetic analyses using the selected concatenated dataset.

The stability of the phylogenetic signal for each dataset assembled was evaluated by performing a Maximum Likelihood tree inference using ExaML (Kozlov et al., 2015). Each dataset contained concatenated loci. The resulting topologies, both within each one of the 12 datasets and pairwise among them, were compared based on their RF distances (Robinson Foulds distances; Robinson and Foulds, 1981). To elaborate on this issue, for each one of the 12 datasets/settings (clustering threshold × min_taxa filtering), 100 ML inferences were performed each using a complete random starting tree and a GTR model. The 100 resulting trees were then concatenated into one file and the average pairwise RF distance was calculated using RAxML (Stamatakis, 2014) to evaluate the topological congruence within each dataset. Then, using the best scoring trees of each setting and calculating their average pairwise RF distance we tested for pairwise topological congruence between min_taxa filter / clustering threshold configuration (i.e. the 12 different settings). Bootstrap values were calculated in RAxML with the bootstopping option of autoMRE (Pattengale et al., 2010) enabled using the dataset with the minimum value of average pairwise RF distance among its 100 trees. Subsequently, the bootstrap support was drawn onto the best-scoring tree of the selected dataset. Bayesian Inference tree was constructed in ExaBayes (Aberer et al., 2014) using the selected dataset, too. The MCMC analysis ran for 500,000 generations using two independent runs with four chains each. The result was saved every 1,000 generations and the "burn in" period included the first 25% of samples. Convergence was evaluated using the standard deviation of split frequencies convergence option (sdsfConvergence; set at 5%), as well as by examining the effective sample sizes (ESSs) in Tracer (Rambaut et al., 2014).

Text S4. Details on the procedure followed for conducting historical demographic analyses using mtDNA of the *P. tauricus* species subgroup.

Mitochondrial DNA (cytochrome *b* and 16S rRNA) sequences of all previously revealed phylogenetic clades and subclades of the *P. tauricus* species subgroup (Podnar et al., 2004; Poulakakis et al., 2005a; Poulakakis et al., 2005b; Psonis et al., 2017) were retrieved from GenBank (**Table S1**). In total, 324 specimens (~77% of the total used in microsatellites analyses) were downloaded and used for demographic analyses, including 18 of *P. gaigeae* (17 in common with microsatellites), 15 of *P. melisellensis* (four in common with microsatellites), 30 of *P. milensis* (29 in common with microsatellites), 175 of *P. tauricus* (157 in common with microsatellites) and 86 of *P. ionicus* (70 in common with microsatellites).

The mtDNA sequences of the above specimens were aligned following the strategy of Psonis et al.(2017) using MAFFT (Katoh and Standley, 2013), whereas alignment sites with a high amount of missing data were discarded to avoid erroneous estimations (Joly et al., 2007). All the following analyses were performed for each species, as well as for each *P. ionicus* subclade, if applicable.

Haplotype networks (95% parsimony limit) were constructed in TCS (v.1.8.0_11, Clement et al., 2000). The estimation of genetic diversity was assessed using different indexes i.e., the number of haplotypes (h), the haplotype diversity (h_d), the number of variable nucleotide sites (S), the nucleotide diversity (π), and the Watterson's theta (θ_w), was performed using the DnaSP software (v.5.10.0.1, Librado and Rozas, 2009).

Historical demography was inferred by the distribution analysis of the number of site differences between pairs of sequences (mismatch distribution) using DnaSP. The observed values where calculated and plotted against expected values for a model of constant population

size. Unimodal distributions indicate a rapid demographic growth of the population in the recent past, whereas multimodal distributions indicate demographic equilibrium (Rogers and Harpending, 1992). Harpending's (1994) raggedness index (*r*) as implemented in ARLEQUIN (v.3.5.2.1; Excoffier and Lischer, 2010), was used to evaluate the Rogers' (1995) sudden expansion model that fits a unimodal mismatch distribution (Rogers and Harpending, 1992). To further test for population expansion, two other tests were performed: Fu's (1997) *Fs* test by using ARLEQUIN and Ramos-Onsins & Rozas' (Ramos-Onsins and Rozas, 2002) R_2 test as implemented in DnaSP. Tajima's (1989) *D* was also estimated by means of ARLEQUIN in order to detect bottlenecks. The statistical support of the above metrics and tests was assessed by 1,000 bootstrap replicates, except R_2 test for which 1,000 coalescent simulations were used instead.

Differences through time in non-parametric estimates of the effective population size (*Ne*) were assessed using Bayesian Skyline Plots (Drummond et al., 2005), which is implemented in BEAST 2. This method computes the *Ne* directly from the sequences without requiring any *a priori* demographic model. The nucleotide substitution models were also not given *a priori*, but selected via the BEAST Model Test. As for other priors, the category of Coalescent Bayesian Skyline was selected for speciation model and a strict molecular clock was applied. The evolutionary rate of each mtDNA gene was calculated based on the genetic distance and the divergence time (as estimated in the previous section) of each clade/subclade from its most closely related lineage. The MCMC analyses were run for 5×10^7 generations, saving the result every 1.000. The final results were evaluated in Tracer to check for convergence and to ensure that the effective sample sizes (ESSs) for all parameters exceeded the threshold of 200. The first 10% of the 20,000 saved generations was discarded as proposed by Tracer. Finally, the visualization of the Bayesian Skyline Plots was performed using the same software.

References

Aberer, A.J., Kobert, K., Stamatakis, A., 2014. ExaBayes: Massively Parallel Bayesian Tree Inference for the Whole-Genome Era. Mol. Biol. Evol. 31, 2553-2556.

Clement, M., Posada, D., Crandall, K.A., 2000. TCS: a computer program to estimate gene genealogies. Mol. Ecol. Notes 9, 1657-1659.

Drummond, A.J., Rambaut, A., Shapiro, B., Pybus, O.G., 2005. Bayesian Coalescent Inference of Past Population Dynamics from Molecular Sequences. Mol. Biol. Evol. 22, 1185-1192.

Eaton, D.A.R., 2014. PyRAD: assembly of de novo RADseq loci for phylogenetic analyses. Bioinformatics 30, 1844-1848.

Edgar, R.C., 2004. MUSCLE: multiple sequence alignment with high accuracy and high throughput. Nucleic Acids Res. 32, 1792-1797.

Excoffier, L., Lischer, H.E.L., 2010. Arlequin suite ver 3.5: A new series of programs to perform population genetics analyses under Linux and Windows. Mol. Ecol. Res. 10, 564-567.

Fu, Y., 1997. Statistical Tests of Neutrality of Mutations Against Population Growth, Hitchhiking and Background Selection. Genetics 147, 915-925.

Harpending, H.C., 1994. Signature of Ancient Population Growth in a Low-Resolution Mitochondrial DNA Mismatch Distribution. Hum. Biol. 66, 591-600.

Joly, S., Stevens, M.I., van Vuuren, B.J., 2007. Haplotype Networks Can Be Misleading in the Presence of Missing Data. Syst. Biol. 56, 857-862.

Katoh, K., Standley, D.M., 2013. MAFFT Multiple Sequence Alignment Software Version 7: Improvements in Performance and Usability. Mol. Biol. Evol. 30, 772-780.

Kozlov, A.M., Aberer, A.J., Stamatakis, A., 2015. ExaML Version 3: A Tool for Phylogenomic Analyses on Supercomputers. Bioinformatics.

Leaché, A.D., Chavez, A.S., Jones, L.N., Grummer, J.A., Gottscho, A.D., Linkem, C.W., 2015. Phylogenomics of Phrynosomatid Lizards: Conflicting Signals from Sequence Capture versus Restriction Site Associated DNA Sequencing. Genome Biol. Evol. 7, 706-719.

Librado, P., Rozas, J., 2009. DnaSP v5: a software for comprehensive analysis of DNA polymorphism data. Bioinformatics 25, 1451-1452.

Pattengale, N.D., Alipour, M., Bininda-Emonds, O.R., Moret, B.M., Stamatakis, A., 2010. How many bootstrap replicates are necessary? Journal of computational biology : a journal of computational molecular cell biology 17, 337-354.

Peterson, B.K., Weber, J.N., Kay, E.H., Fisher, H.S., Hoekstra, H.E., 2012. Double Digest RADseq: An Inexpensive Method for *De Novo* SNP Discovery and Genotyping in Model and Non-Model Species. PLoS ONE 7, e37135.

Podnar, M., Mayer, W., Tvrtković, N., 2004. Mitochondrial phylogeography of the Dalmatian wall lizard, (Lacertidae). Org. Divers. Evol. 4, 307-317.

Poulakakis, N., Lymberakis, P., Valakos, E., Pafilis, P., Zouros, E., Mylonas, M., 2005a. Phylogeography of Balkan wall lizard (*Podarcis taurica*) and its relatives inferred from mitochondrial DNA sequences. Mol Ecol 14, 2433-2443.

Poulakakis, N., Lymberakis, P., Valakos, E., Zouros, E., Mylonas, M., 2005b. Phylogenetic relationships and biogeography of *Podarcis* species from the Balkan Peninsula, by bayesian and maximum likelihood analyses of mitochondrial DNA sequences. Mol. Phylogenet. Evol. 37, 845-857.

Psonis, N., Antoniou, A., Kukushkin, O., Jablonski, D., Petrov, B., Crnobrnja-Isailović, J., Sotiropoulos, K., Gherghel, I., Lymberakis, P., Poulakakis, N., 2017. Hidden diversity in the *Podarcis tauricus* (Sauria, Lacertidae) species subgroup in the light of multilocus phylogeny and species delimitation. Mol. Phylogenet. Evol. 106, 6-17.

Rambaut, A., Suchard, M.A., Xie, D., Drummond, A.J., 2014. Tracer v1.6, Available from http://beast.bio.ed.ac.uk/Tracer.

Ramos-Onsins, S.E., Rozas, J., 2002. Statistical properties of new neutrality tests against population growth. Mol. Biol. Evol. 19, 2092-2100.

Robinson, D.F., Foulds, L.R., 1981. Comparison of phylogenetic trees. Math Biosci 53, 131-147.

Rogers, A.R., 1995. Genetic Evidence for a Pleistocene Population Explosion. Evolution 49, 608-615.

Rogers, A.R., Harpending, H., 1992. Population growth makes waves in the distribution of pairwise genetic differences. Mol. Biol. Evol. 9, 552-569.

Stamatakis, A., 2014. RAxML Version 8: A tool for Phylogenetic Analysis and Post-Analysis of Large Phylogenies. Bioinformatics 30, 1312-1313.

Tajima, F., 1989. Statistical Method for Testing the Neutral Mutation Hypothesis by DNA Polymorphism. Genetics 123, 585-595.